

CONFORMAL AND NEARLY CONFORMAL
THEORIES AT LARGE N

GRIGORY M. TARNOPOLSKIY

A DISSERTATION
PRESENTED TO THE FACULTY
OF PRINCETON UNIVERSITY
IN CANDIDACY FOR THE DEGREE
OF DOCTOR OF PHILOSOPHY

RECOMMENDED FOR ACCEPTANCE
BY THE DEPARTMENT OF
PHYSICS

ADVISERS: PROFESSORS IGOR R. KLEBANOV AND ALEXANDER M. POLYAKOV

SEPTEMBER 2017

© Copyright by Grigory M. Tarnopolskiy, 2017.

All rights reserved.

Abstract

In this thesis we present new results in conformal and nearly conformal field theories in various dimensions. In chapter two, we study different properties of the conformal Quantum Electrodynamics (QED) in continuous dimension d . At first we study conformal QED using large N_f methods, where N_f is the number of massless fermions. We compute its sphere free energy as a function of d , ignoring the terms of order $1/N_f$ and higher. For finite N_f we use the ϵ expansion. Next we use a large N_f diagrammatic approach to calculate the leading corrections to C_T , the coefficient of the two-point function of the stress-energy tensor, and C_J , the coefficient of the two-point function of the global symmetry current. We present explicit formulae as a function of d and check them versus the expectations in 2 and $4 - \epsilon$ dimensions.

In chapter three, we discuss vacuum stability in 1 + 1 dimensional conformal field theories with external background fields. We show that the vacuum decay rate is given by a non-local two-form. This two-form is a boundary term that must be added to the effective in/out Lagrangian. The two-form is expressed in terms of a Riemann-Hilbert decomposition for background gauge fields, and is given by its novel “functional” version in the gravitational case.

In chapter four, we explore Tensor models. Such models possess the large N limit dominated by the melon diagrams. The quantum mechanics of a real anti-commuting rank-3 tensor has a large N limit similar to the Sachdev-Ye-Kitaev (SYK) model. We also discuss the quantum mechanics of a complex 3-index anti-commuting tensor and argue that it is equivalent in the large N limit to a version of SYK model with complex fermions. Finally, we discuss models of a commuting tensor in dimension d . We study the spectrum of the large N quantum field theory of bosonic rank-3 tensors using the Schwinger-Dyson equations. We compare some of these results with the $4 - \epsilon$ expansion, finding perfect agreement. We also study the spectra of bosonic theories of rank $q - 1$ tensors with ϕ^q interactions.

Acknowledgements

I am deeply grateful to my advisers, Igor Klebanov and Alexander Polyakov.

For the past five years, I have had the privilege of collaborating with Igor Klebanov on various amazing projects in theoretical physics. I first met Igor in the Labyrinth Books store five years ago, when I was buying a book in preparation for taking his class on String Theory. In this class, I was impressed by Igor's outstanding ability to explain complicated concepts in a simple manner. His lectures always had a very clear structure and logic. His remarkable intuition in physics has always made our discussions both interesting and inspiring. Additionally, his deep knowledge of physics, history and literature, combined with his wonderful sense of humor, has made for many enjoyable hours of conversation. Igor has invested an extraordinary amount of time and care in my education. Without the steady guidance, constant encouragement and generous support he has provided throughout my time at Princeton, I would not be where I am today.

I am also very grateful to Alexander Markovich Polyakov for sharing his time and amazing ideas with me. In my second year I had the good fortune of taking his class on Quantum Field Theory. I was so impressed with this learning experience that I have since taken the same class every year; if I had more time at Princeton, I would have continued to do so. Each year this class is full of new striking ideas and topics in quantum field theory. Working with Alexander Markovich is an exciting experience; he can be relied upon to divine intuitively solutions to problems that normally require several pages of mathematical calculations to resolve. His physical perception and physical approach to theoretical problems in quantum field theory is nothing short of incredible.

I would also like to express my sincerest gratitude to Simone Giombi, with whom I have collaborated on many projects during my time at Princeton. I have extensively enjoyed doing physics with Simone, whose insight and deep knowledge of theoretical

physics have always motivated me. I am additionally very grateful to Simone for agreeing to be a reader of this thesis.

It also has been a wonderful experience collaborating with Ksenia Bulycheva, Shai Chester, Kenan Diab, Lin Fei, Luca Iliesiu, Mark Mezei, Alexey Milekhin, Silviu Pufu, Guilherme Pimentel and Benjamin Safdi.

I would like to thank Daniel Marlow and Herman Verlinde for serving on my thesis committee.

I am extremely grateful to my previous adviser, Alexander Belavin, for educating me in quantum field theory and theoretical physics at the Landau Institute for Theoretical Physics, Moscow.

I would also like to thank the Graduate School and Physics Department for awarding me with the Myhrvold-Havranek scholarship and Kusaka Memorial Prize in Physics.

I would like to thank my friends and colleagues in the Physics Department: Vasily Alba, Ilya Belopolski, Farzan Beroz, Ksenia Bulycheva, Shai Chester, Will Coulton, Kolya Dedushenko, Kenan Diab, Yale Fan, Lin Fei, Joshua Hardenbrook, Huan He, Po-Shen Hsin, Luca Iliesiu, Jiaqi Jiang, Vladimir Kirilin, Dima Krotov, Aitor Lewkowycz, Aaron Levy, Jeongseog Lee, Mark Mezei, Lauren McGough, Debayan Mitra, Alexey Milekhin, Victor Mikhaylov, Sarthak Parikh, Fedor Popov, Justin Ripley, Zach Sethna, Yu Shen, Siddharth Mishra Sharma, Joaquin Turiaci, Bin Xu, Zhenbin Yang and Sasha Zhiboedov.

Finally, I would like to express gratitude to my family for their love and support. I would especially like to express my heartfelt thanks to my cousin, Misha Gorokhovich, who supported me during all my time at Princeton. These years would have been much harder without his constant encouragement and help.

To my parents

Contents

Abstract	iii
Acknowledgements	iv
1 Introduction	1
1.1 Quantum Field Theory and Critical Phenomena	1
1.2 Landau theory	3
1.3 Wilson’s approach to the Renormalization Group	5
1.4 Wilson-Fisher critical point and ϵ expansion	9
1.5 Large N approximation	11
1.6 Conformal Quantum Electrodynamics	13
1.7 Tensor models	14
1.8 Overview of the thesis	17
2 Conformal QED	20
2.1 Introduction and Summary	20
2.1.1 Conformal Quantum Electrodynamics	20
2.1.2 Sphere free energy and the F -theorem in QED	22
2.1.3 Two point function of the stree-energy tensor in QED	24
2.2 Sphere free energy of Maxwell theory on S^d	28
2.3 Conformal QED at large N	34
2.4 Sphere free energy of the QED at large N	36

2.4.1	Comments on $d > 4$	41
2.5	Sphere free energy of the QED in the ϵ expansion	43
2.6	Padé approximation and the F -theorem	48
2.7	Calculation of C_{J_1} and C_{T_1}	53
2.8	C_J^{top} for the Topological Current in $d = 3$	59
2.9	$4 - \epsilon$ Expansion of C_J and C_T	60
2.10	Another Estimate for Symmetry Breaking in QED ₃	63
2.11	C_T for Large N_f QCD _{d}	64
2.12	Appendix A. Eigenvalues of the kernel $K_{\mu\nu}$	67
2.13	Appendix B. Zonal spherical harmonics in continuous dimesion	70
2.13.1	Rank 0 zonal harmonics	71
2.13.2	Rank 1 zonal harmonics	72
2.13.3	Computations in stereographical coordinates	73
2.13.4	Rank 1 kernel decomposition	77
2.14	Appendix C. Calculation of G_2 and G_4	78
2.15	Appendix D. Calculation of Z_T	82
2.16	Appendix E. Results for $\langle JJ \rangle$ and $\langle TT \rangle$ diagrams	87
3	Particle Production in 1 + 1 CFT	91
3.1	Introduction	91
3.2	Vacuum decay in an Abelian background	93
3.3	Vacuum decay in a non-Abelian background	97
3.4	Vacuum decay in the gravitational field	102
3.5	Appendix A. Boundary conditions on induced currents and alternative derivation of the boundary actions	106
3.6	Appendix B. Gauge-gravity duality in two dimensions	110
3.7	Appendix C. Non-Abelian and gravitational corrections to Caldeira- Leggett formula	112

4	Tensor Models	115
4.1	Introduction	115
4.2	Melonic Dominance in the $O(N)^3$ Symmetric Theories	121
4.3	$O(N)^3$ Quantum Mechanics and the SYK Model	125
4.3.1	Models with a Complex Fermion	132
4.4	$O(N)^3$ bosonic tensors	134
4.4.1	Spectrum of two-particle operators	136
4.4.2	Spectrum of higher-spin operators	139
4.4.3	Complex Large N Fixed Point in $d = 4 - \epsilon$	142
4.4.4	Generalization to Higher q	145
4.4.5	Higher spin operators	148
4.4.6	A Melonic ϕ^6 Theory in 2.99 Dimensions	149
4.5	Appendix A. Matrix model in $d = 4 - \epsilon$ dimension	151
	Bibliography	154

Chapter 1

Introduction

1.1 Quantum Field Theory and Critical Phenomena

Various physical systems containing large numbers of particles can be well described by Statistical Mechanics. In many cases it can be described by weakly interacting constituents which are called quasiparticles. Amazingly, this approximation often gives very good and precise results. Nevertheless, there are phenomena in Nature, which cannot be approximated by non-interacting or weakly-interacting particles. One well-known example of this kind is a phase transition. In this case, near the critical point where the transition occurs, the interactions become huge. And it does not even make sense to think about independent particles or excitations as a description of such a state.

In everyday life, we observe different phase transitions such as the melting of ice or evaporation of water. These are first order phase transitions, and they are characterized by a sharp change of physical parameters such as density. Less common are so-called second order phase transitions. Such a phase transition is near the critical point of the water phase diagram, depicted in Fig. 1.1.

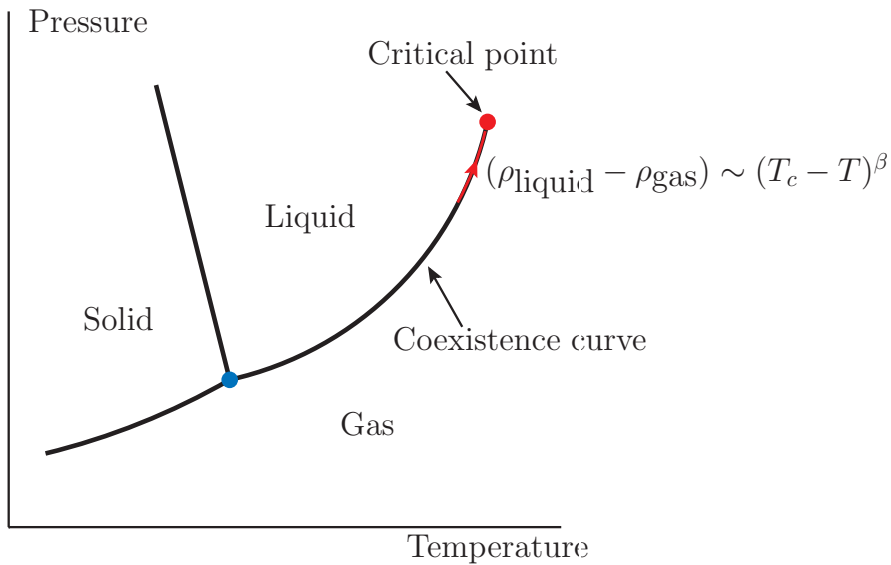


Figure 1.1: A schematic water phase diagram. The red dot denotes the critical point ($T_c \approx 374^\circ\text{C}$, $p_c \approx 22\text{MPa}$). When we approach the critical point along the coexistence curve, the difference between the liquid and vapor densities scales as $(\rho_{\text{liquid}} - \rho_{\text{gas}}) \sim (T_c - T)^\beta$, where the scaling exponent is $\beta \approx 0.33$.

When we approach the critical point along the coexistence curve, the difference between the liquid and vapor densities scales as $(\rho_{\text{liquid}} - \rho_{\text{gas}}) \sim (T_c - T)^\beta$, where the scaling exponent is $\beta \approx 0.33$. The most striking fact is that this scaling exponent is universal. The same $\beta \approx 0.33$ can be found near the critical point of Xenon, Carbon dioxide, and many other substances. There are other physical parameters of water which also exhibit a scaling law with some different scaling exponents. The table of critical exponents and references to experimental measurements can be found in [1].

The other well-known example of the second order phase transition is the paramagnetic-ferromagnetic transition. This transition occurs at some critical temperature, which is called the Curie point. Amazingly, if we measure the magnetization of a ferromagnet near the Curie point, it obeys the scaling law

$$|\vec{M}| \sim (T_c - T)^\beta, \quad (1.1)$$

where again $\beta \approx 0.33$. This is a manifestation of the universality principle.

From a quantitative point of view, it is extremely difficult to obtain theoretical predictions for the scaling exponents. This problem in Statistical Mechanics is closely related to Quantum Field Theory, as we will see below. And this is still work in progress, though much progress has been made in this direction. From a qualitative point of view, second order phase transitions can be understood using the Landau theory.

1.2 Landau theory

In 1937, in the seminal paper "On the theory of phase transitions" [2], Landau formulated a theory which gives a very good qualitative description of the second order phase transition. Here we briefly repeat the main steps of this theory.

Consider the free energy $F(\vec{M}, T)$ of some magnetic material, where \vec{M} is the magnetization and T is the temperature. At high enough temperature, we expect the magnetization to be very small, and therefore we can expand the free energy in a Taylor series

$$F(\vec{M}, T) = F_0(T) + a(T)\vec{M}^2 + b(T)(\vec{M}^2)^2 + \dots \quad (1.2)$$

The equilibrium magnetization can be found from the equation

$$\frac{\partial F(\vec{M}, T)}{\partial \vec{M}} = 0. \quad (1.3)$$

Obviously, when $a(T) > 0$, the solution of this equation is $\vec{M} = 0$. On the other hand, if $a(T) < 0$, the solution is $|\vec{M}| = \sqrt{\frac{-a(T)}{2b(T)}}$. The Landau theory assumes that near the critical point T_c , one can write $a(T) \approx a_0(T - T_c)$ and $b(T) \approx b_0$. Thus it

gives for the magnetization

$$|\vec{M}| \sim (T_c - T)^{1/2}, \quad T < T_c \quad \text{and} \quad |\vec{M}| = 0, \quad T > T_c. \quad (1.4)$$

So we see that though the Landau theory captures some basic properties of the second order phase transition, it gives an incorrect prediction for the scaling exponent β , which is not 0.5, but ≈ 0.33 .

The Landau theory does not take into account fluctuations of the magnetization, which become very important near the critical point. To improve this theory, one has to assume that each configuration has its Boltzmann statistical weight

$$W(\vec{M}) = e^{-\frac{1}{k_B T} F(\vec{M}, T)}. \quad (1.5)$$

Also, we assume that the magnetization \vec{M} is not a constant and may depend on coordinates: $\vec{M}(x)$. Thus the free energy now can depend on derivatives of $\vec{M}(x)$ and we have to consider the functional

$$F[\vec{M}(x), T] = \int d^3x F(\vec{M}(x), \nabla \vec{M}(x), \dots, T). \quad (1.6)$$

The Taylor expansion of the free energy now takes the form

$$F[\vec{M}(x), T] = \int d^3x \left(F_0(T) + a(T) \vec{M}^2(x) + b(T) (\vec{M}^2(x))^2 + c(T) (\nabla \vec{M}(x))^2 + \dots \right). \quad (1.7)$$

Finally the partition function, which is the sum over all different configurations with the Boltzmann statistical weight, is

$$Z = \int D\vec{M}(x) e^{-\frac{1}{k_B T} F[\vec{M}(x), T]}. \quad (1.8)$$

After simple rescaling of the magnetization $\vec{M}(x) = z\vec{\phi}(x)$ with a specially chosen constant z , we arrive at the functional integral which describes the quantum field theory of the scalar field $\vec{\phi}$

$$Z = \int D\vec{\phi}(x) e^{-S[\vec{\phi}(x)]}, \quad (1.9)$$

with the Euclidean three-dimensional action

$$S[\vec{\phi}(x)] = \int d^3x \left(\frac{1}{2}(\nabla\vec{\phi})^2 + \frac{1}{2}m^2\vec{\phi}^2 + \frac{g}{4!}(\vec{\phi}^2)^2 + \dots \right). \quad (1.10)$$

In the case of a magnet, $\vec{\phi}$ is the vector with $N = 3$ components. For simplicity, we can consider a theory where we have only one component:

$$S[\phi(x)] = \int d^3x \left(\frac{1}{2}(\nabla\phi)^2 + \frac{1}{2}m^2\phi^2 + \frac{g}{4!}\phi^4 + \dots \right). \quad (1.11)$$

Theoretical analysis of this quantum field theory reveals the existence of the critical point. And gives an extremely precise estimate for the critical exponents. In particular, it predicts β to be equal to 0.326 ± 0.003 . The first quantitatively successful result was achieved only in 1971 in the famous work of Wilson and Fisher [3]. In their paper, they obtained $\beta \approx 0.306$, which is already close to up-to-date results [4, 5].

1.3 Wilson's approach to the Renormalization Group

In this section we briefly review Wilson's approach to the Renormalization Group (RG) [6]. We consider ϕ^4 theory in general d dimensions. The action of the theory reads

$$S[\phi(x)] = \int d^d x \left(\frac{1}{2}(\nabla\phi)^2 + \frac{1}{2}m^2\phi^2 + \frac{g}{4!}\phi^4 \right). \quad (1.12)$$

Assuming that the coupling constant g is small, we can expand the exponential of the interaction term in a Taylor series. Each order in perturbation theory can be graphically represented by Feynman diagrams. If we try to compute these diagrams, we find that they have divergences at short distances (UV divergences). Of course, in real materials we have to cut off our integrals at the scale of a lattice size a , which in the momentum representation, implies that all momenta are less than $\Lambda \sim 1/a$. Thus the Fourier transform of the field $\phi(x)$ is

$$\phi(x) = \int_{|k| < \Lambda} \frac{d^d k}{(2\pi)^d} \phi(k) e^{ikx}. \quad (1.13)$$

So the physically well-defined problem is to compute different correlation functions in the theory with the cutoff Λ and the action (1.12):

$$\langle \phi(x_1) \dots \phi(x_n) \rangle_{S_\Lambda, \Lambda} = \frac{1}{Z} \int [D\phi]_\Lambda \phi(x_1) \dots \phi(x_n) e^{-S_\Lambda[\phi(x)]}. \quad (1.14)$$

Now we are going to perform Wilson's renormalization procedure. Suppose now we would like to integrate over all high-frequency fields from the frequency Λ_1 to Λ , where $\Lambda_1 < \Lambda$. Namely, we can decompose the field $\phi(k)$ into a sum of two fields

$$\phi(x) = \phi_1(x) + \varphi(x), \quad (1.15)$$

where $\phi_1(x)$ and $\varphi(x)$ are “slow” and “fast” fields defined through their Fourier transforms

$$\phi(x) = \int_{|k| < \Lambda_1} \frac{d^d k}{(2\pi)^d} \phi(k) e^{ikx}, \quad \varphi(x) = \int_{\Lambda_1 < |k| < \Lambda} \frac{d^d k}{(2\pi)^d} \phi(k) e^{ikx}. \quad (1.16)$$

Next, we assume that the fields in the correlation function (1.14) have small Fourier momenta, so we can replace these fields by the “slow” fields. Therefore we get

$$\langle \phi(x_1) \dots \phi(x_n) \rangle_{S_\Lambda, \Lambda} = \frac{1}{Z} \int [D\phi_1]_{\Lambda_1} \phi_1(x_1) \dots \phi_1(x_n) \int [D\varphi] e^{-S_\Lambda[\phi_1 + \varphi]}. \quad (1.17)$$

The new effective action S_{Λ_1} is defined as

$$e^{-S_{\Lambda_1}[\phi_1]} = c \int [D\varphi] e^{-S_\Lambda[\phi_1 + \varphi]}, \quad (1.18)$$

where c is some unimportant constant, because we also have

$$Z = \int [D\phi_1]_{\Lambda_1} [D\varphi] e^{-S_\Lambda[\phi_1 + \varphi]} = c \int [D\phi_1]_{\Lambda_1} e^{-S_{\Lambda_1}[\phi_1]} = cZ_1. \quad (1.19)$$

Thus we finally obtain the following equality

$$\langle \phi(x_1) \dots \phi(x_n) \rangle_{S_\Lambda, \Lambda} = \langle \phi_1(x_1) \dots \phi_1(x_n) \rangle_{S_{\Lambda_1}, \Lambda_1}. \quad (1.20)$$

In other words, it means that if we are interested only in low-momenta correlation functions, the theory with the action S_Λ and the cutoff Λ is equivalent to the theory with the action S_{Λ_1} and the cutoff Λ_1 .

What does the new action $S_{\Lambda_1}[\phi_1]$ look like? To compute it, one has to evaluate a series of Feynman diagrams using the propagator of the “fast” field

$$\langle \varphi(k) \varphi(-k) \rangle = \frac{\Theta(k)}{k^2 + m^2}, \quad (1.21)$$

where $\Theta(k) = 1$ if $\Lambda_1 < |k| < \Lambda$ and $\Theta(k) = 0$ otherwise. It is not possible to compute all Feynman diagrams, but analysis of the first few diagrams shows that the new action $S_{\Lambda_1}[\phi_1]$ will contain infinitely many terms, which are powers of the field

ϕ_1 and its derivatives:

$$S_{\Lambda_1}[\phi_1] = \int d^d x \left(\frac{1}{2} f_0 (\nabla \phi_1)^2 + \frac{1}{2} g_2 \phi_1^2 + \sum_{n=2}^{\infty} \frac{g_{2n}}{(2n)!} \phi_1^{2n}(x) + \sum_{n=1}^{\infty} \frac{f_{2n}}{(2n)!} \phi_1^{2n} (\nabla \phi_1)^2 + \dots \right). \quad (1.22)$$

Notice that in the action (1.11) we have dots, which represent higher terms in the Taylor expansion of the functional (1.6). We omitted these higher terms in the action (1.12), which has only a single ϕ^4 interaction term. But after Wilson's renormalization procedure, we obtain the action (1.22), which again contains infinitely many terms.

The next step of Wilson's procedure is to rescale coordinates $x \rightarrow x/l$, where $l = \Lambda/\Lambda_1 > 1$. Namely, we make the variable transformation

$$\phi_1(x) = Z^{-1/2}(l) \phi'(x/l), \quad (1.23)$$

where $Z(l)$ is some factor, which in principle can be arbitrary. This transformation brings the cutoff parameter to its original value Λ and gives the new action

$$S'_{\Lambda}[\phi'(x)] = S_{\Lambda_1}[Z^{-1/2}(l) \phi'(x/l)]. \quad (1.24)$$

Therefore, after Wilson's full renormalization procedure, we obtain

$$\langle \phi(x_1) \dots \phi(x_n) \rangle_{S_{\Lambda}, \Lambda} = Z^{-n/2}(l) \langle \phi(x_1/l) \dots \phi(x_n/l) \rangle_{S'_{\Lambda}, \Lambda}. \quad (1.25)$$

Schematically, the RG transformation from the action S_{Λ} to the action S'_{Λ} can be written as

$$S' = RG_t(S), \quad (1.26)$$

where we defined the RG time $t = \log l$, which is a more convenient parameter. Obviously, $RG_0(S) = S$ and $RG_{t_1+t_2}(S) = RG_{t_2}(RG_{t_1}(S))$. If we consider infinitesimal RG transformations, we can write

$$RG_{dt}(S) = S + \beta(S)dt + \mathcal{O}(dt^2), \quad \text{where} \quad \beta(S) = \left. \frac{d}{dt}RG_t(S) \right|_{t=0}. \quad (1.27)$$

In terms of the parameters of the action (1.22), one gets

$$\begin{aligned} \frac{d}{dt}f_{2n}(t) &= \beta_{f_{2n}}(\{f_{2n}(t)\}, \{g_{2n}(t)\}, \dots), \\ \frac{d}{dt}g_{2n}(t) &= \beta_{g_{2n}}(\{f_{2n}(t)\}, \{g_{2n}(t)\}, \dots), \\ &\dots\dots\dots \end{aligned} \quad (1.28)$$

where $\beta_{f_{2n}}$ and $\beta_{g_{2n}}$ and similar functions for other couplings are called beta-functions. The critical point corresponds to a set of couplings $f_{2n}^*, g_{2n}^*, \dots$ for which $\beta_{f_{2n}} = \beta_{g_{2n}} = \dots = 0$, so that the action is invariant under the RG transformation

$$S^* = RG_t(S^*). \quad (1.29)$$

In general, it is impossible to find the exact RG equations (1.28). Nevertheless, there are some special limits in which one can obtain and analyze these equations. We are going to discuss these special limits in the next few sections.

1.4 Wilson-Fisher critical point and ϵ expansion

The breakthrough idea of Wilson and Fisher was to consider the ϕ^4 theory in a non-integer dimension close to 4. Namely we can set $d = 4 - \epsilon$, where ϵ is a very small number, for example $\epsilon = 0.01$ and $d = 3.99$. In this dimension, one can analyze and

where the anomalous dimensions are

$$\Delta_\phi = \left(1 - \frac{\epsilon}{2} + \frac{(g_4^*)^2}{12(4\pi)^4} + \mathcal{O}(\epsilon^3)\right), \quad \Delta_{m^2} = \left(2 - \frac{g_4^*}{(4\pi)^2} + \mathcal{O}(\epsilon^2)\right). \quad (1.34)$$

The equations (1.33) have a simple solution

$$\langle\phi(t)\rangle = \langle\phi_0\rangle e^{\Delta_\phi t}, \quad m^2(t) = \delta m^2 e^{\Delta_{m^2} t}. \quad (1.35)$$

Therefore we finally obtain

$$\langle\phi(t)\rangle \sim (m^2(t))^{\frac{\Delta_\phi}{\Delta_{m^2}}}. \quad (1.36)$$

In fact $\langle\phi\rangle$ is proportional to the magnetization, while m^2 is proportional to the deviation of the temperature from the critical value. Therefore, the formula (1.36) gives

$$|\vec{M}| \sim (T_c - T)^\beta, \quad \beta = \frac{\Delta_\phi}{\Delta_{m^2}} = \frac{1 - \frac{\epsilon}{2} + \frac{\epsilon^2}{108}}{2 - \frac{\epsilon}{3}}. \quad (1.37)$$

Now the magic trick is to set $\epsilon = 1$ and obtain the result for the three-dimensional theory: $\beta = 0.306$. The trick works because the ϵ - expansion converges very fast and higher powers of ϵ don't change the result considerably.

1.5 Large N approximation

The idea of the large N approximation is to replace a single scalar field ϕ by a vector ϕ^i , where $i = 1, \dots, N$. So the action for the vector field ϕ^i takes the form

$$S[\phi^i(x)] = \int d^d x \left(\frac{1}{2} (\nabla \phi^i)^2 + \frac{1}{2} m^2 \phi^i \phi^i + \frac{g}{4} (\phi^i \phi^i)^2 \right). \quad (1.38)$$

We notice that this action is invariant under global $O(N)$ transformations of the vector field $\phi^i \rightarrow M^{ij}\phi^j$, where M is an orthogonal matrix.

When N is large, it is possible to develop an expansion in $1/N$. At leading order, one needs to sum only diagrams which look like a chain of bubbles, see figure 1.2.



Figure 1.2: An example of a Feynman diagrams dominating at the large N limit.

Using this one can compute anomalous dimensions of the operators ϕ^i and $\phi^i\phi^i$ as series in $1/N$. In fact, it is possible to obtain the coefficients of this series for arbitrary dimension d . The results are

$$\begin{aligned}\Delta_\phi &= \frac{d-2}{2} + \frac{2 \sin\left(\frac{\pi d}{2}\right) \Gamma(d-2)}{\pi \Gamma\left(\frac{d}{2}-2\right) \Gamma\left(\frac{d}{2}+1\right)} \frac{1}{N} + \mathcal{O}(1/N^2), \\ \Delta_{\phi^2} &= 2 + \frac{4 \sin\left(\frac{\pi d}{2}\right) \Gamma(d)}{\pi \Gamma\left(\frac{d}{2}-1\right) \Gamma\left(\frac{d}{2}+1\right)} \frac{1}{N} + \mathcal{O}(1/N^2).\end{aligned}\tag{1.39}$$

In the case of $d=3$, these formulas give

$$\begin{aligned}\Delta_\phi &= \frac{1}{2} + \frac{4}{3\pi^2} \frac{1}{N} + \mathcal{O}(1/N^2), \\ \Delta_{\phi^2} &= 2 - \frac{32}{3\pi^2} \frac{1}{N} + \mathcal{O}(1/N^2).\end{aligned}\tag{1.40}$$

One also finds for the scaling exponent β :

$$\beta = \frac{\Delta_\phi}{3 - \Delta_{\phi^2}} = \frac{1 + \frac{8}{3\pi^2} \frac{1}{N}}{2\left(1 + \frac{32}{3\pi^2} \frac{1}{N}\right)},\tag{1.41}$$

where we used that $\Delta_{m^2} = d - \Delta_{\phi^2}$. Quite surprisingly, setting $N=1$, we obtain $\beta = 0.305$, which is not far from the correct result. In this case we should not expect

that setting $N = 1$ gives a precise result because the $1/N$ series converges slowly and subleading $1/N$ corrections become small only for big enough N .

We also note that today the most accurate method of finding anomalous dimensions of the $O(N)$ model for arbitrary N belongs to the Bootstrap approach [7, 8, 9, 10, 4]. By imposing crossing relations on the four-point functions of fields ϕ and ϕ^2 it is possible to determine an allowed region for Δ_ϕ and Δ_{ϕ^2} . The accuracy of this method is phenomenal and is equal to five digits after the decimal point! The bootstrap results are $\Delta_\phi = 0.51816$ and $\Delta_{\phi^2} = 1.41267$, which gives $\beta = 0.32643$.

1.6 Conformal Quantum Electrodynamics

The four-dimensional Quantum Electrodynamics coupled to N_f Dirac fermions is an original model of Quantum Field Theory; its predictions have been verified experimentally with high accuracy. If the fermions are massless, then the theory is conformally invariant for zero charge e , but the interaction effects are well known to break the conformal invariance. They produce a positive β function for e , which means that the theory becomes free at long distances.

The physics of QED is different in $d \neq 4$. Then the free Maxwell action $\frac{1}{4}F_{\mu\nu}F^{\mu\nu}$ is not conformally invariant [11], but the one loop fermion vacuum polarization diagram induces a scale invariant quadratic term proportional to

$$F_{\mu\nu}(-\nabla^2)^{\frac{d}{2}-2}F^{\mu\nu} , \quad (1.42)$$

which is in general non-local. For $d < 4$ this term dominates at long distances, and well-known examples of such “induced QED” are the Schwinger model [12] in $d = 2$ and the conformal phase of QED₃ [13, 14]. In $d = 4 - \epsilon$ the conformal QED _{d} theory

may be studied using the ϵ expansion, because the β function

$$\beta = -\frac{\epsilon}{2}e + \frac{4N_f}{3}\frac{e^3}{(4\pi)^2} + \mathcal{O}(e^5) \quad (1.43)$$

has a weakly coupled IR fixed point at $e_*^2 = 6\epsilon\pi^2/N_f + \mathcal{O}(\epsilon^2)$ [15]. The ϵ expansion of various operator dimensions in QED $_d$ was introduced in [16, 17].

Among the important physical applications of the conformal QED is the theory in $d = 3$ coupled to massless Dirac fermions and/or complex scalars. An early motivation to study QED $_3$ came from work on the high temperature behavior of four-dimensional gauge theory [13]. More recently, its various applications to condensed matter physics have been explored as well (see, for example, [18, 19, 20]). Work on QED $_3$ has uncovered a variety of interesting phenomena, which include chiral symmetry breaking and interacting conformal field theory [21, 22, 14]. Both of these phases of the theory are consistent with the Vafa-Witten theorem [23], which requires the presence of massless modes for $N_f > 3$. Yet, some questions remain about the infrared behavior of the theory.

1.7 Tensor models

In the section (1.5) we replaced a scalar field ϕ by a vector ϕ^i , where $i = 1, \dots, N$. Taking the large N limit we saw that only a special set of diagrams contributing. It is possible to compute all the diagrams in this set and obtain results as a series in $1/N$. The next logical step is to promote a vector field ϕ^i to a matrix ϕ^{ij} with $i, j = 1, \dots, N$. The action for such a matrix can take the form

$$S[\phi^{ij}(x)] = \int d^d x \left(\frac{1}{2}(\nabla\phi^{ij})^2 + \frac{1}{2}m^2\phi^{ij}\phi^{ij} + \frac{g_1}{4}(\phi^{ij}\phi^{ij})^2 + \frac{g_2}{4}(\phi^{i_1j_1}\phi^{i_1j_2}\phi^{i_2j_1}\phi^{i_2j_2}) \right). \quad (1.44)$$

If we set $g_2 = 0$ we essentially obtain the vector model, where N is replaced by N^2 . So in this case the leading large N diagrams are bubbles. But if we set $g_1 = 0$ the dominating Feynman diagrams are completely different from those in the vector case. Surprisingly they again form a specific set, namely each diagram must be planar or equivalently has the Euler characteristic $\chi = 2$ [24]. An example of such a diagram is depicted in figure 1.3.

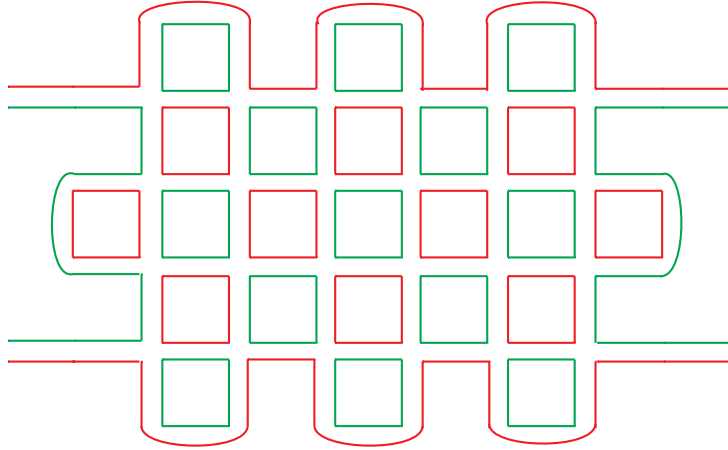


Figure 1.3: An example of a planar diagram contributing to the four-point function.

Because the field ϕ^{ij} has two indices we denote its propagator by a double line. The interaction term is represented by a vertex depicted in figure 1.4.

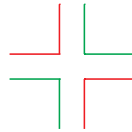


Figure 1.4: Graphical representation of the interaction term $V = \phi^{i_1 j_1} \phi^{i_1 j_2} \phi^{i_2 j_1} \phi^{i_2 j_2}$.

In order to obtain the $1/N$ expansion in the matrix case one has to compute all planar diagrams. The set of all planar diagrams is much larger than the set of the bubble diagrams and thus the computation of all planar diagrams is a hard problem. Nevertheless this problem is solved for theories living in dimensions $d = 0$ and $d = 1$ [25].

The next obvious step in our discussion is to add one more index to the matrix ϕ^{ij} promoting it to a tensor ϕ^{ijk} , where $i, j, k = 1, \dots, N$. In this case one can find a new fascinating large N limit for the interaction [26, 27, 28]

$$V = \phi^{i_1 j_1 k_1} \phi^{i_1 j_2 k_2} \phi^{i_2 j_1 k_2} \phi^{i_2 j_2 k_1}. \quad (1.45)$$

Its graphical representation is depicted in figure 1.5.

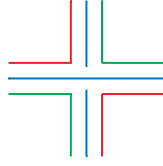


Figure 1.5: Graphical representation of the interaction term $V = \phi^{i_1 j_1 k_1} \phi^{i_1 j_2 k_2} \phi^{i_2 j_1 k_2} \phi^{i_2 j_2 k_1}$.

In this case the leading large N limit is dominated by a specific set of diagrams, which are called melonic diagrams [29, 30]. An example of a melonic diagram contributing to the four-point function is depicted in figure 1.6. Here we denote each propagator by a single line. One can also represent diagrams in stranded way, where propagators are triple lines and vertices look like in the matrix case, but with two additional crossing lines.

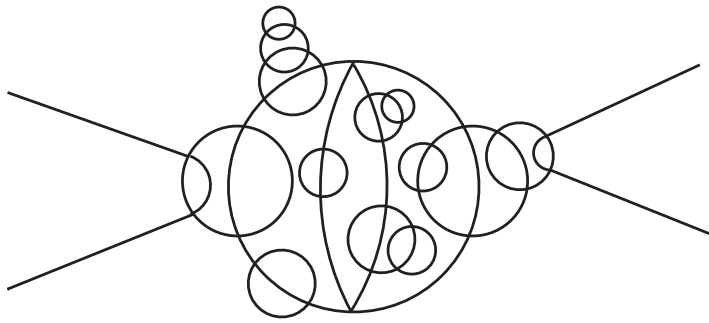


Figure 1.6: An example of a melonic diagram contributing to the four-point function.

Unfortunately the interaction (1.45) for bosonic fields is not bounded from below. This leads to instability of the theory. Nevertheless one can consider a quantum

mechanics of N^3 Majorana fermions ψ^{abc} with the action [31]

$$S = \int dt \left(\frac{i}{2} \psi^{abc} \partial_t \psi^{abc} + \frac{1}{4} g \psi^{a_1 b_1 c_1} \psi^{a_1 b_2 c_2} \psi^{a_2 b_1 c_2} \psi^{a_2 b_2 c_1} \right). \quad (1.46)$$

In this case the theory is well defined and one can exactly compute sum of all melonic Feynman diagrams. We discuss this theory and other similar models in chapter 4.

1.8 Overview of the thesis

The chapter 2 is devoted to conformal Quantum Electrodynamics. We calculate the free energies F for $U(1)$ gauge theories on the d dimensional sphere of radius R . For the theory with free Maxwell action we find the exact result as a function of d ; it contains the term $\frac{d-4}{2} \log R$ consistent with the lack of conformal invariance in dimensions other than 4. When the $U(1)$ gauge theory is coupled to a sufficient number N_f of massless 4-component fermions, it acquires an interacting conformal phase, which in $d < 4$ describes the long distance behavior of the model. The conformal phase can be studied using large N_f methods. We compute its sphere free energy as a function of d , ignoring the terms of order $1/N_f$ and higher. For finite N_f , we develop the $4 - \epsilon$ expansion for the sphere free energy of conformal QED $_d$. Its extrapolation to $d = 3$ shows very good agreement with the large N_f approximation for $N_f > 3$. For N_f at or below some critical value N_{crit} , the $SU(2N_f)$ symmetric conformal phase of QED $_3$ is expected to disappear or become unstable. By using the F -theorem and comparing the sphere free energies in the conformal and broken symmetry phases, we show that $N_{\text{crit}} \leq 4$. As another application of our results, we calculate the one loop beta function in conformal QED $_6$, where the gauge field has a 4-derivative kinetic term. We show that this theory coupled to N_f massless fermions is asymptotically free.

Next we use a large N_f diagrammatic approach to calculate the leading corrections to C_T , the coefficient of the two-point function of the stress-energy tensor, and C_J ,

the coefficient of the two-point function of the global symmetry current. We present explicit formulae as a function of d and check them versus the expectations in 2 and 4- ϵ dimensions. Using our results in higher even dimensions we find a concise formula for C_T of the conformal Maxwell theory with higher derivative action $F_{\mu\nu}(-\nabla^2)^{\frac{d}{2}-2}F^{\mu\nu}$. In $d = 3$, QED has a topological symmetry current, and we calculate the correction to its two-point function coefficient, C_J^{top} . We also show that some RG flows involving QED in $d = 3$ obey $C_T^{\text{UV}} > C_T^{\text{IR}}$ and discuss possible implications of this inequality for the symmetry breaking at small values of N .

In chapter 3 we study vacuum stability in 1 + 1 dimensional Conformal Field Theories with external background fields. We show that the vacuum decay rate is given by a non-local two-form. This two-form is a boundary term that must be added to the effective in/out Lagrangian. The two-form is expressed in terms of a Riemann-Hilbert decomposition for background gauge fields, and its novel “functional” version in the gravitational case.

In chapter 4 we study the tensor models. Certain tensor models with rank-3 tensor degrees of freedom possess a novel large N limit, where g^2N^3 is held fixed. In this limit the perturbative expansion in the quartic coupling constant, g , is dominated by a special class of “melon” diagrams. We study “uncolored” models of this type, which contain a single copy of real rank-3 tensor. Its three indices are distinguishable; therefore, the models possess $O(N)^3$ symmetry with the tensor field transforming in the tri-fundamental representation. Such uncolored models also possess the large N limit dominated by the melon diagrams. The quantum mechanics of a real anti-commuting tensor therefore has a similar large N limit to the Sachdev-Ye-Kitaev (SYK) model, but does not require disorder. Gauging the $O(N)^3$ symmetry in our quantum mechanical model removes the non-singlet states; therefore, one can search for its well-defined gravity dual. We point out, that the model possesses a vast number of gauge-invariant operators involving higher powers of the tensor field, suggesting that the complete

gravity dual will be intricate. We also discuss the quantum mechanics of a complex 3-index anti-commuting tensor, which has $U(N)^2 \times O(N)$ symmetry and argue that it is equivalent in the large N limit to a version of SYK model with complex fermions.

Finally, we study the spectrum of the large N quantum field theory of bosonic rank-3 tensors, whose quartic interactions are such that the perturbative expansion is dominated by the melonic diagrams. We use the Schwinger-Dyson equations to determine the scaling dimensions of the bilinear operators of arbitrary spin. Using the fact that the theory is renormalizable in $d = 4$, we compare some of these results with the $4 - \epsilon$ expansion, finding perfect agreement. This helps elucidate why the dimension of operator $\phi^{abc}\phi^{abc}$ is complex for $d < 4$: the large N fixed point in $d = 4 - \epsilon$ has complex values of the couplings for some of the $O(N)^3$ invariant operators. We show that a similar phenomenon holds in the $O(N)^2$ symmetric theory of a matrix field ϕ^{ab} , where the double-trace operator has a complex coupling in $4 - \epsilon$ dimensions. We also study the spectra of bosonic theories of rank $q - 1$ tensors with ϕ^q interactions. In dimensions $d > 1.93$ there is a critical value of q , above which we have not found any complex scaling dimensions. The critical value is a decreasing function of d , and it becomes 6 in $d \approx 2.97$. This raises a possibility that the large N theory of rank-5 tensors with sextic potential has an IR fixed point which is free of perturbative instabilities for $2.97 < d < 3$.

Chapter 2

Conformal QED

This chapter is an edited version of ref. [32] and [33] written in collaboration with Simone Giombi and Igor Klebanov. The first part of the chapter is devoted to computation of the sphere free energy in the conformal QED in d dimensions. In the second part we compute C_T and C_J in the conformal QED in d dimensions.

2.1 Introduction and Summary

2.1.1 Conformal Quantum Electrodynamics

In this chapter we study infrared behavior of QED using the relatively new tools provided by the F -theorem [34, 35, 36, 37]. Our analysis is similar in spirit to that of [38, 39], although some of our reasoning is different. We will work with the $U(1)$ gauge theory coupled to N_f massless 4-component Dirac fermions ψ^j . The lagrangian of this theory has $SU(2N_f)$ global symmetry, which is often referred to as the “chiral symmetry.” In QED₃ the fine structure constant $\alpha = \frac{e^2}{4\pi}$ has dimension of mass; this makes the theory super-renormalizable. At short distances we find a weakly interacting theory of massless fermions and photons, where the field strength $F_{\mu\nu}$ has scaling dimension $3/2$. The short distance limit of QED₃ is scale invariant, but not conformal.

mal. This is because the free Maxwell action $\frac{1}{4}F_{\mu\nu}F^{\mu\nu}$ is not conformally invariant in three dimensions [11]. The lack of conformal invariance of the free Maxwell theory translates into the fact that its three-sphere free energy F depends logarithmically on the sphere radius R [40]. In section 2.2 we will generalize this result to free Maxwell theory on S^d and show that its free energy contains the term $\frac{d-4}{2}\log R$. We will refer to the short distance limit of QED₃ as the UV theory. The fact that its F value, F_{UV} , diverges is important for consistency of the RG flows with the F -theorem.

As QED₃ flows to longer distances, the effective interaction strength grows and various interesting phenomena become possible. The one loop fermion vacuum polarization diagram induces a non-local quadratic term (1.42) for A_μ , which dominates in the IR over the Maxwell term [13]. Due to this effect, the theory flows to an interacting conformal field theory in the large N_f limit where e^2N_f is held fixed. In the CFT the scaling dimension of $F_{\mu\nu}$ is 2. The scaling dimensions of other operators can be calculated as series in $1/N_f$ (see, for example, [41, 42, 43]).

A different possibility is the spontaneous breaking of the $SU(2N_f)$ global symmetry due to generation of vacuum expectation value of the operator $\sum_{j=1}^{N_f}\bar{\psi}_j\psi^j$ (it is written using the 4-d notation for spinors ψ^i and gamma-matrices). This operator preserves the 3-d parity and time reversal symmetries, but it breaks the global symmetry to $SU(N_f)\times SU(N_f)\times U(1)$. This mechanism was proposed in [21], where it was argued using Schwinger-Dyson equations to be possible for any N_f ; however, for large N_f the scale of the VEV becomes exponentially small compared to α . Subsequently, modified treatments of the Schwinger-Dyson equations [14] suggested that the chiral symmetry breaking is possible only for $N_f \leq N_{\text{crit}}$. The estimates of N_{crit} typically range between 2 and 10 [44, 45, 46, 17].

It is widely believed that the QED₃ must be in the conformal phase for $N_f > N_{\text{crit}}$, but a nearly marginal operator may appear in the spectrum of the CFT as N_f is reduced towards N_{crit} . This operator must respect the $SU(2N_f)$ and parity

symmetries of the theory, and natural candidates are the operators quartic in the fermion fields [17] (see also [43, 46]).¹

When the quartic operator is slightly irrelevant, it should give rise to a nearby UV fixed point; there is a standard argument for this using conformal perturbation theory, which we present in section 2.6. We will call this additional fixed point QED_3^* . For $N_f = N_{\text{crit}}$ it merges with QED_3 , and for $N_f < N_{\text{crit}}$ both fixed points may become complex [44, 48, 49, 46]. In this “merger and annihilation of fixed points” scenario, for $N_f < N_{\text{crit}}$ the UV theory flows directly to the broken symmetry phase.

Alternatively, both fixed points may stay real and go through each other. Then the QED_3 fixed point continues to exist even after the appearance of a relevant operator; this relevant operator may create flow from QED_3 to the broken symmetry phase. If so, the edge of the conformal window may be associated with the dimension of some operator in QED_3 becoming so small that it violates the unitarity bound. This would be analogous to what happens at the lower edge of the conformal window in the $\mathcal{N} = 1$ supersymmetric gauge theory [50].

2.1.2 Sphere free energy and the F -theorem in QED

We will attempt to shed new light on the transition from the conformal to the symmetry breaking behavior by using the F -theorem and performing more precise calculations of F . Here $F = -\log Z_{S^3}$ is the 3-sphere free energy [34, 35] or, equivalently, the long-range Entanglement Entropy across a circle [36, 37]. The theorem states that for Renormalization Group (RG) flow from fixed point 1 to fixed point 2, $F_1 > F_2$. A proof of this inequality has been found using properties of the Renormalized Entanglement Entropy in relativistic field theories [51] (see also [52]).

¹ In the compact theory, monopole operators may also become relevant as one lowers N_f [47]; however, these operators transform in non-trivial representations of the $SU(2N_f)$ flavor symmetry, and so they are not expected to be generated along the RG flow if the UV theory has exact $SU(2N_f)$ symmetry. Monopoles may still condense, i.e. they may acquire expectation values in the spontaneously broken phase.

In order to apply the F -theorem to RG flows among different phases of QED₃, it is important to know their F -values. This is especially challenging for the interacting CFT phase of the theory. In [40] this calculation was performed using the $1/N_f$ expansion with the result

$$F_{\text{conf}} = N_f \left(\frac{\log(2)}{2} + \frac{3\zeta(3)}{4\pi^2} \right) + \frac{1}{2} \log \left(\frac{\pi N_f}{4} \right) + \mathcal{O}\left(\frac{1}{N_f}\right). \quad (2.1)$$

The first term on the RHS is the F -value of N_f free Dirac fermions, $N_f F_{\text{free-ferm}}$. Even though $F_{\text{conf}} - N_f F_{\text{free-ferm}}$ grows without bound for large N_f , the F -theorem inequality $F_{\text{UV}} > F_{\text{conf}}$ is satisfied. This is because F_{UV} is infinite due to the divergent contribution of the free Maxwell theory. In section 2.3 we review the large N description of conformal QED and generalize the result (2.1) by computing F_{conf} as a function of d .

Since we will be quite interested in F_{conf} for small N_f , in this paper we will apply a different approximation method [53, 54]. This method consists of developing the ϵ expansion of $\tilde{F} = -\sin(\pi d/2) F_{S^d}$ for $d = 4 - \epsilon$. It relies on the perturbative renormalization of the field theory on the sphere $S^{4-\epsilon}$ and requires inclusion of counter terms that involve the curvature tensor [55, 56, 57, 58, 59]. Applications of this method to the Wilson-Fisher $O(N)$ symmetric CFTs have produced high-quality estimates of $F_{O(N)}$ in $d = 3$; they are found to be only 2 – 3% below the F values for the corresponding free UV fixed points of these theories [53, 54].

In this chapter, we will perform a similar ϵ expansion for \tilde{F} of the conformal QED, building on earlier work which developed the perturbative renormalization of QED on $S^{4-\epsilon}$ [60, 61, 59, 62, 63]. This calculation is presented in section 2.5, and our main

result is

$$\begin{aligned} \tilde{F}_{\text{conf}} = & N_f \tilde{F}_{\text{free-ferm}} - \frac{1}{2} \sin\left(\frac{\pi d}{2}\right) \log\left(\frac{N_f}{\epsilon}\right) \\ & + \frac{31\pi}{90} - 1.2597\epsilon - 0.6493\epsilon^2 + 0.8429\epsilon^3 + \frac{0.4418\epsilon^2}{N_f} - \frac{0.6203\epsilon^3}{N_f} - \frac{0.5522\epsilon^3}{N_f^2} + \mathcal{O}(\epsilon^4). \end{aligned} \quad (2.2)$$

Extrapolating this to $d = 3$ using Padé approximants produces results very close to the large N_f formula (2.1) already for $N_f > 3$, see figure 2.4.

Applying the F -theorem, we find that RG flow from the conformal to the broken symmetry phase is impossible when $F_{\text{conf}} < F_{\text{SB}}$. This puts an upper bound on the value N_{crit} where the conformal phase can become unstable [38]. Using our resummed ϵ expansion results for \tilde{F}_{conf} , we find that the value of N_f where $F_{\text{conf}} = F_{\text{SB}}$ rather robustly lies between 4 and 5, and our best estimate is $N_f \approx 4.4$. If we restrict to integer values of N_f , this means that for $N_f \geq 5$ the QED₃ theory must be in the $SU(2N_f)$ symmetric conformal phase. Therefore, our results give the upper bound $N_{\text{crit}} \leq 4$. The same upper bound is obtained if we use the large N_f approximation (2.1) to F_{conf} , which was derived in [40]. The results obtained using the ϵ expansion of quartic operator dimensions [17], as well as computations in lattice gauge theory [64, 65], are consistent with our upper bound.

2.1.3 Two point function of the stress-energy tensor in QED

The other important observables in Conformal Field Theory (CFT) is C_T , the coefficient of the two-point function of the stress-energy tensor $T_{\mu\nu}$, defined via [66]

$$\langle T_{\mu\nu}(x_1) T_{\lambda\rho}(x_2) \rangle = C_T \frac{I_{\mu\nu,\lambda\rho}(x_{12})}{(x_{12}^2)^d}, \quad (2.3)$$

where

$$\begin{aligned}
I_{\mu\nu,\lambda\rho}(x) &\equiv \frac{1}{2}(I_{\mu\lambda}(x)I_{\nu\rho}(x) + I_{\mu\rho}(x)I_{\nu\lambda}(x)) - \frac{1}{d}\delta_{\mu\nu}\delta_{\lambda\rho}, \\
I_{\mu\nu}(x) &\equiv \delta_{\mu\nu} - 2\frac{x_\mu x_\nu}{x^2}.
\end{aligned}
\tag{2.4}$$

If the CFT has a global symmetry generated by conserved currents J_μ^a , then another interesting observable is C_J , the coefficient of their two-point functions:

$$\langle J_\mu^a(x_1) J_\nu^b(x_2) \rangle = C_J \frac{I_{\mu\nu}(x_{12})}{(x_{12}^2)^{d-1}} \delta^{ab}.
\tag{2.5}$$

In CFTs with a large number of degrees of freedom, N , these observables typically admit $1/N$ expansions of the form

$$\begin{aligned}
C_J &= C_{J_0} \left(1 + \frac{C_{J_1}}{N} + \frac{C_{J_2}}{N^2} + \mathcal{O}(1/N^3) \right), \\
C_T &= C_{T_0} \left(1 + \frac{C_{T_1}}{N} + \frac{C_{T_2}}{N^2} + \mathcal{O}(1/N^3) \right).
\end{aligned}
\tag{2.6}$$

The values of C_{J_1} and C_{T_1} have been calculated in a variety of models. Petkou [67] has used large N methods and operator products expansions to calculate them as a function of d in the scalar $O(N)$ model. Very recently, these results were reproduced using the large N diagrammatic approach in [68], where the same technique was also used to calculate C_{J_1} and C_{T_1} as a function of d in the conformal Gross-Neveu model. An important feature of the diagrammatic approach, which was uncovered in [68], is the necessity, in the commonly used regularization scheme [69, 70, 71, 72, 73], of a divergent multiplicative “renormalization” Z_T for the stress-energy tensor. This factor is required by the conformal Ward identities in the regularized theory.

In this chapter we extend the methods of [68] to calculate $C_{J_1}(d)$ and $C_{T_1}(d)$ in the conformal QED in d dimensions. This theory, which is reviewed in section 2.3, may be thought of as the Maxwell field coupled to N_f massless 4-component Dirac

fermions continued from 4 dimensions to a more general dimension d . The large N expansion in this model runs in powers of the total number of fermionic components, which is $N = 4N_f$. In the physically interesting dimension $d = 3$, this corresponds to an even number $2N_f$ of two-component Dirac fermions.

Our main results are

$$C_{J_1}(d) = \eta_{m_1} \left(\frac{3d(d-2)}{8(d-1)} \Theta(d) + \frac{d-2}{d} \right), \quad (2.7)$$

$$C_{T_1}(d) = \eta_{m_1} \left(\frac{3d(d-2)}{8(d-1)} \Theta(d) + \frac{d(d-2)}{(d-1)(d+2)} \Psi(d) - \frac{(d-2)(3d^2+3d-8)}{2(d-1)^2 d(d+2)} \right), \quad (2.8)$$

$$\Theta(d) \equiv \psi'(d/2) - \psi'(1), \quad \Psi(d) \equiv \psi(d-1) + \psi(2-d/2) - \psi(1) - \psi(d/2-1),$$

where $\psi(x) = \Gamma'(x)/\Gamma(x)$. Here $\eta_{m_1}(d)$ encodes the electron mass anomalous dimension; it is [74]²

$$\eta_{m_1}(d) = -\frac{2(d-1)\Gamma(d)}{\Gamma(\frac{d}{2})^2 \Gamma(\frac{d}{2}+1) \Gamma(2-\frac{d}{2})}. \quad (2.9)$$

In the physically interesting case of $d = 3$ we find

$$C_{J_1}(3) = \frac{736}{9\pi^2} - 8 \approx 0.285821,$$

$$C_{T_1}(3) = \frac{4192}{45\pi^2} - 8 \approx 1.43863. \quad (2.10)$$

A nontrivial check of our results (2.7) and (2.8) comes from comparing them with the known exact values in $d = 2$ and the $4 - \epsilon$ expansions, see sections 2.7 and 2.9. Had we not included Z_T , there would be no agreement with the $4 - \epsilon$ expansion. In higher even d , the conformal QED reduces to a free theory of N fermions and a

²We define the anomalous dimension of the electron mass operator $O_m = \bar{\psi}\psi$ as $\Delta_{O_m} = d-1+\eta_m$, where $\eta_m = \eta_{m_1}/N + \mathcal{O}(1/N^2)$.

conformal higher-derivative Maxwell theory with the action (see e.g. [33])

$$F_{\mu\nu}(-\nabla^2)^{\frac{d}{2}-2}F^{\mu\nu} . \quad (2.11)$$

Using the value of C_{T1} in general even dimensions, we extract the C_T of this conformal Maxwell theory

$$C_T^{\text{conf. Maxwell}}|_{\text{even } d} = (-1)^{\frac{d}{2}} \frac{d}{S_d^2} \binom{d}{\frac{d}{2}-1} , \quad (2.12)$$

where $S_d = \frac{2\pi^{d/2}}{\Gamma(d/2)}$.

In $d = 3$ the QED has a special ‘‘topological’’ $U(1)$ symmetry current $j^{\text{top}} = \frac{1}{2\pi} *F$. In section 2.8 we calculate its two-point function to order $1/N^2$, and obtain the associated C_J^{top} coefficient, in the normalization (2.5), to be

$$C_J^{\text{top}} = \frac{16}{\pi^4 N} \left(1 + \frac{1}{N} \left(8 - \frac{736}{9\pi^2} \right) + \mathcal{O}(1/N^2) \right) , \quad (2.13)$$

where $N = 4N_f$ is twice the number of two-components Dirac fermions. The leading order term is in agreement with [75, 76].

As we already mentioned above the QED₃ Lagrangian also has an enhanced $SU(2N_f)$ global symmetry, and for small N_f this symmetry may be broken spontaneously to $SU(N_f) \times SU(N_f) \times U(1)$. In section 2.10 we present a new estimate for the critical value of N_f above which the symmetry breaking cannot occur by using the RG inequality $C_T^{\text{UV}} > C_T^{\text{IR}}$. It implies that the chiral symmetry cannot be broken for $N_f > 1 + \sqrt{2}$. The status of this conclusion is uncertain, since there are known violations of the inequality in some supersymmetric RG flows [77]. Nevertheless, it is interesting that the critical value of N_f it yields is close to other available estimates [44, 45, 46, 17] and our estimate from the F -theorem and is consistent with the results available from lattice gauge theory [64, 65].

2.2 Sphere free energy of Maxwell theory on S^d

The action for Maxwell theory on a curved manifold is

$$S = \int d^d x \sqrt{g} \frac{1}{4e^2} F_{\mu\nu} F^{\mu\nu} = \frac{1}{2e^2} \int d^d x \sqrt{g} A^\nu \left(-\delta_\nu^\mu \nabla^2 + R_\nu^\mu + \nabla_\nu \nabla^\mu \right) A_\mu, \quad (2.14)$$

where we have used $F_{\mu\nu} = \nabla_\mu A_\nu - \nabla_\nu A_\mu$ and $[\nabla^\mu, \nabla_\nu] A_\mu = R_\nu^\mu A_\mu$. On a round S^d of radius R , we have $R_\nu^\mu = \frac{d-1}{R^2} \delta_\nu^\mu$ and so the action is

$$S = \int_{S^d} d^d x \sqrt{g} \frac{1}{2e^2} A^\nu \left(\delta_\nu^\mu (-\nabla^2 + \frac{d-1}{R^2}) + \nabla_\nu \nabla^\mu \right) A_\mu. \quad (2.15)$$

The partition function is given by

$$Z = \frac{1}{\text{vol}(G)} \int DA e^{-S(A)}, \quad (2.16)$$

where G is the volume of the group of gauge transformations. One way to proceed is to split the gauge field into transverse and pure gauge part³

$$A_\mu = B_\mu + \partial_\mu \phi, \quad \nabla^\mu B_\mu = 0. \quad (2.17)$$

Following [40], we have

$$\begin{aligned} DA &= DBD(d\phi) = DBD'\phi \sqrt{\det'(-\nabla^2)} \\ \text{vol}(G) &= 2\pi \sqrt{\text{vol}(S^d)} \int D'\phi, \quad \text{vol}(S^d) = \frac{2\pi^{\frac{d+1}{2}}}{\Gamma(\frac{d+1}{2})} R^d \equiv \Omega_d R^d, \end{aligned} \quad (2.18)$$

³Equivalently, one can use Feynman gauge by adding a gauge fixing term $L_{\text{fix}} = \frac{1}{2}(\nabla^\mu A_\mu)^2$. This gauge is more convenient for perturbative calculations when interactions with matter fields are included, and we will use it in Section 2.5.

where prime means that the constant mode is not included. Then, the partition function can be written as

$$\begin{aligned} Z &= \frac{\sqrt{\det'(-\nabla^2)}}{2\pi\sqrt{\text{vol}(S^d)}} \int DB e^{-\int_{S^d} d^d x \sqrt{g} \frac{1}{2e^2} B^\mu (-\nabla^2 + \frac{d-1}{R^2}) B_\mu} \\ &= \frac{1}{2\pi\sqrt{\text{vol}(S^d)}} \frac{\sqrt{\det'(-\nabla^2)}}{\sqrt{\det_T(-\nabla^2 + \frac{d-1}{R^2})}}, \end{aligned} \quad (2.19)$$

where the subscript ‘ T ’ indicates that the determinant is taken on the space of transverse vector fields.

The eigenvalues of the sphere Laplacian $-\nabla^2$ acting on a transverse vector and corresponding degeneracies are known to be (see e.g. [78, 79])

$$\lambda_\ell^{(1)} = \frac{1}{R^2}(\ell(\ell+d-1)-1), \quad g_\ell^{(1)} = \frac{\ell(\ell+d-1)(2\ell+d-1)\Gamma(\ell+d-2)}{\Gamma(\ell+2)\Gamma(d-1)}, \quad \ell \geq 1. \quad (2.20)$$

For a scalar field, one has

$$\lambda_\ell^{(0)} = \frac{1}{R^2}\ell(\ell+d-1), \quad g_\ell^{(0)} = \frac{(2\ell+d-1)\Gamma(\ell+d-1)}{\Gamma(\ell+1)\Gamma(d)}, \quad \ell \geq 0. \quad (2.21)$$

In the case of the scalar field, $\ell = 0$ corresponds to the constant mode which is to be excluded in our case. Using these results, the free energy of Maxwell theory on S^d , $F_{\text{Maxwell}} = -\log Z$, can be written as

$$\begin{aligned} F_{\text{Maxwell}} &= \frac{1}{2} \sum_{\ell=1}^{\infty} g_\ell^{(1)} \log\left(\frac{(\ell+1)(\ell+d-2)}{2\pi e^2 R^2}\right) \\ &\quad - \frac{1}{2} \sum_{\ell=1}^{\infty} g_\ell^{(0)} \log\left(\frac{\ell(\ell+d-1)}{R^2}\right) + \log(2\pi\sqrt{\text{vol}(S^d)}). \end{aligned} \quad (2.22)$$

In dimensional regularization, the following results for the sum over vector and scalar degeneracies hold

$$\sum_{\ell=1}^{\infty} g_{\ell}^{(1)} = 1, \quad \sum_{\ell=0}^{\infty} g_{\ell}^{(0)} = 0, \quad \rightarrow \quad \sum_{\ell=1}^{\infty} g_{\ell}^{(0)} = -1. \quad (2.23)$$

These can be obtained for example by evaluating the sums for sufficiently negative d where they converge, and analytically continuing to positive values of d . Using these regularized identities, one can readily extract the radius dependence of the Maxwell free energy (2.22) to be

$$F_{\text{Maxwell}} = -\frac{1}{2} \log(e^2 R^{4-d}) + F_{\text{Max.}}^{(0)}(d), \quad (2.24)$$

where $F_{\text{Max.}}^{(0)}(d)$ is a radius independent function of d (with simple poles at even d). In particular, we see that $F_{\text{Maxwell}} \rightarrow +\infty$ in the short distance limit for $d < 4$. The function $F_{\text{Max.}}^{(0)}(d)$ can be evaluated in continuous d by computing the non-trivial sums in (2.22), as we explain below.

We first find it convenient to rewrite the free energy in the following way

$$F_{\text{Maxwell}} = F_{\text{vector}} - 2F_{\text{min-sc}} + F_{\text{measure}}, \quad (2.25)$$

where we have defined

$$\begin{aligned} F_{\text{vector}} &= \frac{1}{2} \sum_{\ell=1}^{\infty} g_{\ell}^{(1)} \log\left(\frac{(\ell+1)(\ell+d-2)}{2\pi e^2 R^2}\right) + \frac{1}{2} \sum_{\ell=1}^{\infty} g_{\ell}^{(0)} \log\left(\frac{\ell(\ell+d-1)}{R^2}\right), \\ F_{\text{min-sc}} &= \frac{1}{2} \log \det'(-\nabla^2) = \frac{1}{2} \sum_{\ell=1}^{\infty} g_{\ell}^{(0)} \log\left(\frac{\ell(\ell+d-1)}{R^2}\right), \\ F_{\text{measure}} &= \log(2\pi \sqrt{\text{vol}(S^d)}). \end{aligned} \quad (2.26)$$

The grouping of terms in (2.25) is essentially equivalent to doing the calculation in Feynman gauge, where one has an unconstrained vector and a complex minimally

coupled scalar ghost. To proceed, we use the identity

$$\log(y) = \int_0^\infty \frac{dt}{t} (e^{-t} - e^{-yt}) . \quad (2.27)$$

Then, using the dimensionally regularized identities (2.23), one can rewrite the vector contribution as

$$\begin{aligned} F_{\text{vector}} = & -\frac{1}{2} \int_0^\infty \frac{dt}{t} \left[\sum_{\ell=1}^\infty g_\ell^{(1)} (e^{-(\ell+1)t} + e^{-(\ell+d-2)t}) + g_\ell^{(0)} (e^{-\ell t} + e^{-(\ell+d-1)t}) \right] \\ & - \frac{1}{2} \log(2\pi e^2) . \end{aligned} \quad (2.28)$$

Note that the radius dependence in F_{vector} , and the terms proportional to e^{-t} , have dropped out due to (2.23). The sum over ℓ can now be evaluated analytically, leading to elementary functions of e^{-t} . To perform the t -integral, it is convenient to use the identity

$$\frac{1}{t} = \frac{1}{1 - e^{-t}} \int_0^1 du e^{-ut} . \quad (2.29)$$

This allows for an analytical evaluation of the t integral, and after some algebra and using gamma function identities such as $\Gamma(x)\Gamma(1-x) = \pi \csc(\pi x)$, we arrive at the result

$$\begin{aligned} F_{\text{vector}} = & \int_0^1 du \left[(d^2 + 1 - 3d(1+u) + 2u(u+2)) \sin\left(\frac{\pi}{2}(d-2u)\right) \right. \\ & \left. \times \frac{\Gamma(d-2-u)\Gamma(1+u)}{2\sin(\frac{\pi d}{2})\Gamma(d)} - \frac{d-2}{(d-2)^2 - u^2} \right] - \frac{1}{2} \log(2\pi e^2) . \end{aligned} \quad (2.30)$$

To evaluate the ghost contribution $F_{\text{min-sc}}$ by similar methods, we can introduce a small regulator to deal with the zero mode, so that we can extend the sum over all modes and make use of (2.23)

$$F_{\text{min-sc}} = \lim_{\delta \rightarrow 0} \left[-\frac{1}{2} \int_0^\infty \frac{dt}{t} \sum_{\ell=0}^\infty g_\ell^{(0)} (e^{-(\ell+\delta)t} + e^{-(\ell+d-1)t}) - \frac{1}{2} \log\left(\frac{\delta(d-1)}{R^2}\right) \right] . \quad (2.31)$$

Performing first the sum over ℓ , using (2.29) and evaluating the t -integral, we obtain, after sending $\delta \rightarrow 0$ at the end⁴

$$F_{\text{min-sc}} = - \int_0^1 du \left[(d-2u) \sin\left(\frac{\pi}{2}(d-2u)\right) \frac{\Gamma(d-u)\Gamma(u)}{2 \sin\left(\frac{\pi d}{2}\right)\Gamma(d+1)} - \frac{1}{2u} \right] - \frac{1}{2} \log\left(\frac{(d-1)}{R^2}\right). \quad (2.32)$$

We can now put everything together in (2.25) and obtain the radius independent part of the Maxwell free energy (2.24). We find

$$F_{\text{Max.}}^{(0)}(d) = \frac{1}{2} \log(2\pi(d-1)^2\Omega_d) - \frac{1}{\sin\left(\frac{\pi d}{2}\right)} \int_0^1 du f_d(u), \quad (2.33)$$

where the form of $f_d(u)$ can be read off from the above results, and it is equal to

$$f_d(u) = -(d^2 + 1 - 3d(1+u) + 2u(u+2)) \sin\left(\frac{\pi}{2}(d-2u)\right) \frac{\Gamma(d-2-u)\Gamma(1+u)}{2\Gamma(d)} \\ + \frac{\sin\left(\frac{\pi d}{2}\right)(d-2)}{(d-2)^2 - u^2} - (d-2u) \sin\left(\frac{\pi}{2}(d-2u)\right) \frac{\Gamma(d-u)\Gamma(u)}{\Gamma(d+1)} + \frac{\sin\left(\frac{\pi d}{2}\right)}{u}. \quad (2.34)$$

Here the first line comes from the vector contribution (2.30), and the second line from the ghost contribution (2.32). Note that the UV divergences of the free energy are fully accounted for by the overall sine factor in front of the integral in (2.33).

Equivalently, in terms of \tilde{F} we have

$$\tilde{F}_{\text{Maxwell}} = \frac{1}{2} \sin\left(\frac{\pi d}{2}\right) \log(e^2 R^{4-d}) - \frac{1}{2} \sin\left(\frac{\pi d}{2}\right) \log(2\pi(d-1)^2\Omega_d) + \int_0^1 du f_d(u), \quad (2.35)$$

which is a finite smooth function of continuous d .

As a test of this result, we can check that in $d=4$ \tilde{F} reproduces the known value of the conformal anomaly a -coefficient for the Maxwell theory. From (2.35), we obtain

$$\tilde{F}_{\text{Maxwell}}^{d=4} = \frac{\pi}{12} \int_0^1 du (1-u)(u^3 - u^2 - 11u + 12) = \frac{\pi}{2} \cdot \frac{31}{45} \quad (2.36)$$

⁴We use $\log(\delta) = - \int_0^1 du \frac{1}{u+\delta} + \log(1+\delta)$.

corresponding to the correct a anomaly coefficient, $a = \frac{31}{45}$ (we use units where $a = \frac{1}{90}$ for a 4d conformal scalar field).

In other even values of d , the Maxwell theory is not conformal and \tilde{F} cannot be interpreted as an anomaly coefficient. Nevertheless, \tilde{F} still yields the coefficient of the $1/\epsilon$ pole in dimensional regularization, which fixes the coefficient of the curvature counterterm in the renormalized free energy. From (2.35), we find for instance

$$\tilde{F}_{\text{Maxwell}}^{d=6} = -\frac{\pi}{2} \cdot \frac{1271}{1890}, \quad \tilde{F}_{\text{Maxwell}}^{d=8} = \frac{\pi}{2} \cdot \frac{4021}{6300}, \quad \tilde{F}_{\text{Maxwell}}^{d=10} = -\frac{\pi}{2} \cdot \frac{456569}{748440}, \dots \quad (2.37)$$

The $d = 6$ result agrees with the value obtained in Appendix of [80]. For other even d values, we have checked that our results are in agreement with the coefficient of the logarithmic divergence for a massless spin 1 field obtained by zeta function methods on Euclidean AdS_{2n} [79].

As a further check, in $d = 3$ we obtain the result

$$\begin{aligned} F_{\text{Maxwell}}^{d=3} &= -\frac{1}{2} \log\left(\frac{e^2 R}{16\pi^3}\right) - \int_0^1 du \left[\frac{1}{1-u^2} + \frac{1}{u} - \frac{\pi}{12} (2u^3 + 3u^2 - 23u + 12) \cot(\pi u) \right] \\ &= -\frac{1}{2} \log(e^2 R) + \frac{\zeta(3)}{4\pi^2} \end{aligned} \quad (2.38)$$

in agreement with [40]. In $d = 3$, the Maxwell theory is Hodge dual to a compact minimally coupled scalar field. Note that from (2.32) we can read off the F -value for a (non-compact) minimal scalar in $d = 3$, with zero mode removed, to be

$$F_{\text{min-sc}}^{d=3} = \frac{1}{2} \log(\pi) + \frac{\zeta(3)}{4\pi^2} + \log(R). \quad (2.39)$$

This result agrees with the one obtained in [40, 81], and after carefully relating the radius of the compact scalar to the electric charge e , one can verify equality of the partition functions under Hodge duality.

In $d = 5$, we find for $\tilde{F} = -F$:

$$\begin{aligned}\tilde{F}_{\text{Maxwell}}^{d=5} &= \frac{1}{2} \log \left(\frac{e^2}{32\pi^4 R} \right) + \int_0^1 du \left[\frac{1}{u} - \frac{3}{u^2 - 9} - \frac{\pi}{240} (6u^5 - 35u^4 \right. \\ &\quad \left. + 275u^2 - 486u + 240) \cot(\pi u) \right] \\ &= \frac{1}{2} \log \left(\frac{e^2}{4\pi^2 R} \right) + \frac{5\zeta(3)}{16\pi^2} + \frac{3\zeta(5)}{16\pi^4}.\end{aligned}\tag{2.40}$$

It would be interesting to reproduce this result from a massless 2-form B_2 on S^5 , which is related by Hodge duality to the Maxwell theory.

2.3 Conformal QED at large N

The action for Maxwell theory coupled to N_f massless charged fermions in flat space is (in Euclidean signature)

$$S = \int d^d x \left(\frac{1}{4e^2} F^{\mu\nu} F_{\mu\nu} - \sum_{i=1}^{N_f} \bar{\psi}_i \gamma^\mu (\partial_\mu + iA_\mu) \psi^i \right).\tag{2.41}$$

Here the fermions ψ^i are assumed to be *four-component* complex spinors. These correspond to N_f usual Dirac fermions in $d = 4$, while in $d = 3$ they can be viewed as $2N_f$ 3d Dirac fermions. In particular, in $d = 3$ the model has the enhanced flavor symmetry $SU(2N_f)$. We define the dimensional continuation of the theory by keeping the number of fermion components fixed. In other words, we take γ^μ to be 4×4 matrices satisfying $\{\gamma^\mu, \gamma^\nu\} = 2\delta^{\mu\nu} \mathbf{1}$, with $\text{tr} \mathbf{1} = 4$. All vector indices are formally continued to d dimensions, i.e. $g^{\mu\nu} g_{\mu\nu} = d$, $\gamma^\mu \gamma_\mu = d \cdot \mathbf{1}$, etc.

One may develop the $1/N$ expansion of the theory by integrating out the fermions. This produces an effective action for the gauge field of the form

$$S_{\text{eff}} = \int d^d x \frac{1}{4e^2} F^{\mu\nu} F_{\mu\nu} - \int d^d x d^d y \left(\frac{1}{2} A^\mu(x) A^\nu(y) \langle J_\mu(x) J_\nu(y) \rangle_0 + \mathcal{O}(A^3) \right),\tag{2.42}$$

where

$$J_\mu = i\bar{\psi}_i \gamma_\mu \psi^i \quad (2.43)$$

is the conserved $U(1)$ current. Using the fermion propagator

$$\langle \psi^i(x) \bar{\psi}_j(0) \rangle = -\delta_j^i \frac{\Gamma\left(\frac{d}{2}\right)}{2\pi^{\frac{d}{2}}} \frac{\gamma^\mu x_\mu}{(x^2)^{\frac{d}{2}}} = i\delta_j^i \int \frac{d^d p}{(2\pi)^d} \frac{\gamma^\mu p_\mu}{p^2} e^{ipx} \quad (2.44)$$

the current two-point function in the free fermion theory is found to be

$$\langle J_\mu(x) J_\nu(0) \rangle_0 = C_J \frac{g_{\mu\nu} - 2\frac{x_\mu x_\nu}{x^2}}{x^{2(d-1)}}, \quad C_J = N_f \text{Tr} \mathbf{1} \left(\frac{\Gamma\left(\frac{d}{2}\right)}{2\pi^{\frac{d}{2}}} \right)^2. \quad (2.45)$$

In momentum space, one finds⁵

$$\begin{aligned} \langle J_\mu(p) J_\nu(-p) \rangle_0 &= \int d^d x e^{-ipx} \langle J_\mu(x) J_\nu(0) \rangle_0 \\ &= -C_J \frac{2^{3-d} \pi^{d/2} \Gamma\left(2 - \frac{d}{2}\right)}{\Gamma(d)} \left(g_{\mu\nu} - \frac{p_\mu p_\nu}{p^2} \right) (p^2)^{\frac{d}{2}-1}. \end{aligned} \quad (2.46)$$

Thus, when $d < 4$, one sees that the non-local kinetic term in (2.42) is dominant in the low momentum (IR) limit compared to the two-derivative Maxwell term. Hence, the latter can be dropped at low energies, and one may develop the $1/N$ expansion of the critical theory by using the induced quadratic term

$$S_{\text{crit QED}} = \int \frac{d^d p}{(2\pi)^d} \left(\frac{1}{2} A^\mu(p) \langle J_\mu(p) J_\nu(-p) \rangle_0 A^\nu(-p) - \bar{\psi}_i i \not{p} \psi^i - i \bar{\psi}_i \gamma^\mu A_\mu \psi^i \right). \quad (2.47)$$

Note that this effective action is gauge invariant as it should, due to conservation of the current.

The induced photon propagator is obtained by inverting the non-local kinetic term in (2.47). As usual, this requires gauge-fixing. Working in a generalized Feynman

⁵More generally, for a spin 1 primary operator of dimension Δ , one has $\langle J_\mu(x) J_\nu(0) \rangle = C_J \frac{g_{\mu\nu} - 2\frac{x_\mu x_\nu}{x^2}}{x^{2\Delta}}$ and $\langle J_\mu(p) J_\nu(-p) \rangle = C_J \frac{2^{d-2\Delta} \pi^{d/2} (\Delta-1) \Gamma\left(\frac{d}{2}-\Delta\right)}{\Gamma(\Delta+1)} \left(g_{\mu\nu} - \frac{2\Delta-d}{\Delta-1} \frac{p_\mu p_\nu}{p^2} \right) (p^2)^{\Delta-\frac{d}{2}}$.

gauge, the propagator is

$$D_{\mu\nu}(p) = \frac{C_A}{N(p^2)^{\frac{d}{2}-1+\Delta}} \left(\delta_{\mu\nu} - (1-\xi) \frac{p_\mu p_\nu}{p^2} \right), \quad (2.48)$$

where ξ is an arbitrary gauge parameter ($\xi = 0$ corresponds to Landau gauge $\partial_\mu A^\mu = 0$). The normalization constant C_A is given by

$$C_A = \frac{(4\pi)^{\frac{d}{2}} \Gamma(d)}{2\Gamma(\frac{d}{2})^2 \Gamma(2 - \frac{d}{2})} \quad (2.49)$$

and in (2.48) we have introduced, as in [68], a regulator Δ to handle divergences [69, 70, 71, 72, 73], which should be sent to zero at the end of the calculation. This makes the interaction vertex in (2.47) dimensionful, and one should introduce a renormalization scale μ so that $S_{\text{vertex}} = -i\mu^\Delta \int \bar{\psi}_i \gamma^\mu A_\mu \psi^i$.

The Feynman rules of the model are summarized in figure 2.1.

$$\begin{array}{ccc} \begin{array}{c} \mu \\ \text{~~~~~} \\ \text{~~~~~} \\ \nu \end{array} = D_{\mu\nu}(p) & \begin{array}{c} i \quad p \quad j \\ \longrightarrow \end{array} = \delta_j^i G(p) & \begin{array}{c} \nearrow \\ \text{~~~~~} \\ \searrow \end{array} = i\gamma^\mu \end{array}$$

Figure 2.1: Feynman rules for the Large N QED .

2.4 Sphere free energy of the QED at large N

To compute the sphere free energy, we need to conformally map to S^d and choose an appropriate gauge fixing. As in the previous section, we may gauge fix by splitting $A_\mu = B_\mu + \partial_\mu \phi$, where $\nabla_\mu B^\mu = 0$. Then, following the same steps as in (2.16), (2.19), the sphere free energy is given by

$$F = N_f F_{\text{free-ferm}}(d) + \frac{1}{2} \log \det_T \left(\frac{K_{\mu\nu}}{2\pi} \right) - \frac{1}{2} \log \det'(-\nabla^2) + \log \left(2\pi \sqrt{\text{vol}(S^d)} \right) + \mathcal{O}\left(\frac{1}{N_f}\right), \quad (2.50)$$

where $K_{\mu\nu} = -\langle J_\mu J_\nu \rangle$ is the non-local induced kinetic term, and $F_{\text{free-ferm}}$ is the contribution of a free four-component Dirac fermion [53]

$$F_{\text{free-ferm}}(d) = -\frac{4}{\sin(\frac{\pi d}{2})\Gamma(1+d)} \int_0^1 du \cos\left(\frac{\pi u}{2}\right) \Gamma\left(\frac{1+d+u}{2}\right) \Gamma\left(\frac{1+d-u}{2}\right). \quad (2.51)$$

The ghost contribution was already computed in the previous section, and is given in (2.32). To evaluate the contribution of the transverse vector, we first conformally map the current two-point function to the sphere of radius R , on which we choose the conformally flat metric

$$ds^2 = \frac{4R^2 dx^\mu dx^\mu}{(1+x^2)^2}. \quad (2.52)$$

Introducing the vielbein $e_\mu^m(x) = \frac{2R}{(1+x^2)}\delta_\mu^m$, the two-point function for a spin 1 primary operator of dimension Δ can be written as

$$\langle J_\mu(x) J_\nu(y) \rangle = C_J e_\mu^m(x) e_\nu^n(y) \frac{\left(\delta^{mn} - 2\frac{(x-y)^m(x-y)^n}{|x-y|^2}\right)}{s(x,y)^{2\Delta}}, \quad s(x,y) = \frac{2R|x-y|}{(1+x^2)^{1/2}(1+y^2)^{1/2}}, \quad (2.53)$$

where in our case $\Delta = d - 1$, corresponding to a conserved current. The spin 1 determinant in (2.50) may be computed by expanding in a basis of vector spherical harmonics [82, 40, 83]. Splitting the vector A_μ in transverse and longitudinal parts, the spin 1 and spin 0 eigenvalues of $K_{\mu\nu} = -\langle J_\mu J_\nu \rangle$ turn out to be, in the case of general conformal dimension Δ (see Appendix 2.12):

$$\begin{aligned} \lambda_\ell^{(1)} &= -C_J \frac{2^{d-2\Delta} \pi^{d/2} (\Delta-1) \Gamma\left(\frac{d}{2} - \Delta\right)}{\Gamma(\Delta+1)} \frac{\Gamma(\ell+\Delta)}{\Gamma(\ell+d-\Delta)} \frac{1}{R^{2\Delta-d}}, \\ \lambda_\ell^{(0)} &= \frac{d-1-\Delta}{\Delta-1} \lambda_\ell^{(1)}, \end{aligned} \quad (2.54)$$

with degeneracies given in (2.20) and (2.21). For $\Delta = d - 1$ the longitudinal eigenvalues vanish as expected, due to gauge invariance. The spin 1 contribution in (2.50)

is then

$$\frac{1}{2} \log \det_T \left(\frac{K^{\mu\nu}}{2\pi} \right) = \frac{1}{2} \log \left(N_f \frac{\Gamma(2 - \frac{d}{2}) \Gamma(\frac{d}{2})^2}{2^{d-2} \pi^{\frac{d}{2}+1} \Gamma(d) R^{d-2}} \right) + \frac{1}{2} \sum_{\ell=1}^{\infty} g_{\ell}^{(1)} \log \left(\frac{\Gamma(\ell + d - 1)}{\Gamma(\ell + 1)} \right), \quad (2.55)$$

where we have used the dimensionally regularized identity (2.23) to extract the constant prefactor in the eigenvalues, and used $C_J = 4N_f \left(\frac{\Gamma(\frac{d}{2})}{2\pi^{\frac{d}{2}}} \right)^2$. From this expression, we immediately see that the free energy contains a term $\frac{1}{2} \log(N_f)$, independently of dimension. This can be traced back to the trivial constant gauge transformations on the sphere, or equivalently to ghost zero modes [83]. Note also that the radius dependence cancels out against the ghost and measure contributions in (2.50), as expected by conformal invariance. The remaining non-trivial sum may be evaluated directly for instance by using the integral representation

$$\log \Gamma(z) = \int_0^{\infty} dt \left(z - 1 - \frac{1 - e^{-(z-1)t}}{1 - e^{-t}} \right) \frac{e^{-t}}{t} \quad (2.56)$$

and following similar steps as described in the previous section. A compact form of the final answer for the sum is suggested by the results of [83], where a formula for the change in F due to a deformation by the square of a spin s operator of dimension Δ was computed using higher spin fields in AdS_{d+1} with non-standard boundary conditions. For spin 1, that result implies:

$$\begin{aligned} & \frac{1}{2} \sum_{\ell=1}^{\infty} g_{\ell}^{(1)} \log \left(\frac{\Gamma(\ell + \Delta)}{\Gamma(\ell + d - \Delta)} \right) + \frac{1}{2} \sum_{\ell=1}^{\infty} g_{\ell}^{(0)} \log \left(\frac{d - 1 - \Delta}{\Delta - 1} \frac{\Gamma(\ell + \Delta)}{\Gamma(\ell + d - \Delta)} \right) \\ &= \frac{-1}{\sin\left(\frac{\pi d}{2}\right) \Gamma(d)} \int_0^{\Delta - \frac{d}{2}} du u (d^2 - 4u^2) \sin(\pi u) \Gamma\left(\frac{d}{2} - 1 + u\right) \Gamma\left(\frac{d}{2} - 1 - u\right) \end{aligned} \quad (2.57)$$

Taking carefully the limit of $\Delta = d - 1$, and using [84, 53] (note that the sum starts from $\ell = 0$ here):

$$\begin{aligned} \frac{1}{2} \sum_{\ell=0}^{\infty} g_{\ell}^{(0)} \log \left(\frac{\Gamma(\ell + \Delta)}{\Gamma(\ell + d - \Delta)} \right) &= \\ &= -\frac{1}{\sin\left(\frac{\pi d}{2}\right) \Gamma(d+1)} \int_0^{\Delta - \frac{d}{2}} du u \sin(\pi u) \Gamma\left(\frac{d}{2} + u\right) \Gamma\left(\frac{d}{2} - u\right) \end{aligned} \quad (2.58)$$

we finally obtain the result

$$\begin{aligned} \frac{1}{2} \sum_{\ell=1}^{\infty} g_{\ell}^{(1)} \log \left(\frac{\Gamma(\ell + d - 1)}{\Gamma(\ell + 1)} \right) &= \frac{1}{2} \log \left(\frac{\Gamma(d-1)}{2} \right) \\ &- \int_0^1 du \left[(d-2)^2 (d-1) u (4 + d^2 - (d-2)^2 u^2) \frac{\sin\left(\frac{\pi(d-2)u}{2}\right) \Gamma\left(\frac{(d-2)(1-u)}{2}\right) \Gamma\left(\frac{(d-2)(1+u)}{2}\right)}{16 \sin\left(\frac{\pi d}{2}\right) \Gamma(d+1)} \right. \\ &\quad \left. + \frac{1}{2(1-u)} \right]. \end{aligned} \quad (2.59)$$

We have explicitly verified that this agrees with a direct evaluation of the sum using (2.56).

Putting everything together, the final result for the sphere free energy F , or equivalently for $\tilde{F} = -\sin\left(\frac{\pi d}{2}\right)F$, takes the form⁶

$$\tilde{F} = N_f \tilde{F}_{\text{free-ferm}}(d) - \frac{1}{2} \sin\left(\frac{\pi d}{2}\right) \log \left(-\frac{N_f}{\sin\left(\frac{\pi d}{2}\right)} \right) + A_0(d) + \mathcal{O}\left(\frac{1}{N_f}\right), \quad (2.60)$$

where

$$\begin{aligned} A_0(d) &= -\sin\left(\frac{\pi d}{2}\right) \left[\frac{1}{2} \sum_{\ell=1}^{\infty} g_{\ell}^{(1)} \log \left(\frac{\Gamma(\ell + d - 1)}{\Gamma(\ell + 1)} \right) - \frac{1}{2} \sum_{\ell=1}^{\infty} g_{\ell}^{(0)} \log(\ell(\ell + d - 1)) \right. \\ &\quad \left. + \frac{1}{2} \log \left(\frac{2^{5-2d} \pi^3 (d-2)}{\Gamma\left(\frac{d+1}{2}\right)^2} \right) \right] \end{aligned} \quad (2.61)$$

⁶Note that, due to the factor $\log(-N_f/\sin(\frac{\pi d}{2}))$, the free energy is real for $2 \leq d \leq 4$, it has an imaginary part for $4 < d < 6$, then it is real again for $6 \leq d \leq 8$, etc. This is essentially due to the fact that the Maxwell term yields a contribution $-\frac{1}{2} \log(e^2 R^{4-d})$ to F , and at the RG fixed point e_*^2 is positive for $2 < d < 4$, negative for $4 < d < 6$, etc.

and the sums can be given the integral representations in (2.32) and (2.59). The resulting $A_0(d)$ is a smooth, finite function of d which is independent of R and N_f . In $d = 3$ it evaluates to

$$A_0(d = 3) = \frac{1}{2} \log \left(\frac{\pi}{4} \right) \quad (2.62)$$

and so we find agreement with (2.1). For comparison to the perturbative calculation in the ϵ expansion given in the next section, it is also useful to expand (2.61) in $d = 4 - \epsilon$. We find

$$A_0(d = 4 - \epsilon) = \frac{31\pi}{90} - 0.905\epsilon - 0.64931\epsilon^2 + 0.374025\epsilon^3 + \mathcal{O}(\epsilon^4). \quad (2.63)$$

The leading term correctly reproduces the a -anomaly coefficient of the $d = 4$ Maxwell field, as expected. In the next section we will reproduce the terms to order ϵ^3 from a perturbative calculation on $S^{4-\epsilon}$.

Let us also note that in $d = 2$ we find

$$A_0(d = 2) = -\frac{\pi}{6} \quad (2.64)$$

corresponding to a shift of the central charge by -1 . This is as expected, since in $d = 2$ we get the Schwinger model coupled to N_f massless fermions; via the non-abelian bosonization [85] one finds that at low energies it is a CFT with central charge $c = 2N_f - 1$ [86, 87]. This result is exact (all the $1/N_f$ corrections to \tilde{F} should vanish as $d \rightarrow 2$), and we will make use of it in Section 2.6 to impose a boundary condition on the Padé extrapolations of our ϵ expansion results. A plot of the function $A_0(d)$ is given in Fig. 2.2.

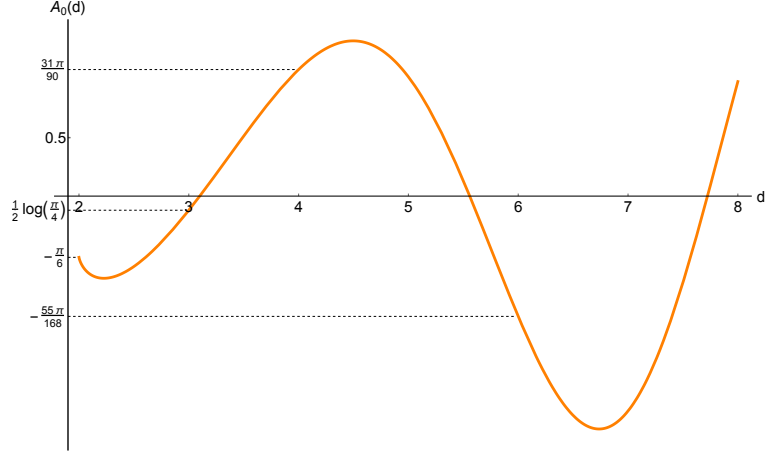


Figure 2.2: Plot of the smooth function $A_0(d)$ from eq. (2.60). It has values $\tilde{F} = -55\pi/168$ ($a = -55/84$) in $d = 6$, $\tilde{F} = 31\pi/90$ ($a = 31/45$) in $d = 4$, and $\tilde{F} = -\pi/6$ ($c = -1$) in $d = 2$.

2.4.1 Comments on $d > 4$

In $d > 4$, one still formally finds a conformal electrodynamics in the large momentum (UV) limit, see eq. (2.46), but the corresponding CFT's are non-unitary. For instance, in $d = 6$ the induced kinetic term (2.46) corresponds to the conformal spin 1 gauge field with Lagrangian $L \sim F_{\mu\nu} \partial^2 F^{\mu\nu}$ [88, 83, 89]. The a -anomaly coefficient for this conformal field can be extracted from our general result (2.60) setting $d = 6$, which yields

$$\begin{aligned}
 (\tilde{F} - N_f \tilde{F}_{\text{free-ferm}})|_{d=6} &= \\
 &= \frac{\pi}{240} \int_0^1 du (213u^6 + 6u^5 - 630u^4 + 160u^3 - 183u^2 + 314u - 120) \\
 &= -\frac{\pi}{2} \cdot \frac{55}{84}.
 \end{aligned} \tag{2.65}$$

corresponding to $a = -\frac{55}{84}$ (in units where $a = \frac{1}{756}$ for a 6d conformal scalar). This agrees with the result for the a -anomaly of the 6d conformal spin 1 field, which can be obtained from one-loop determinants in AdS_7 with non-standard boundary conditions [83, 90], or by a direct computation on S^6 [89]. Note that this is *not*

equal to the coefficient of the logarithmic divergence for a ordinary Maxwell field in $d = 6$, eq. (2.37). As recently observed in [80], this conformal spin 1 field is part of a non-unitary $\mathcal{N} = (1, 0)$ conformal multiplet including a Weyl fermion with 3-derivative kinetic term and 3 conformal scalar fields, whose total a anomaly coefficient is $a = -\frac{251}{360}$, which turns out to be the value assigned by definition in [91] to a $\mathcal{N} = (1, 0)$ vector multiplet in $d = 6$.

For finite N_f , one approach to the conformal QED in $d > 4$ is to use the $d = 4 + \epsilon$ expansion. From the one-loop beta function (1.43), one sees that there are UV fixed points at imaginary values of the coupling. The large N_f limit considerations discussed above strongly suggest that these UV fixed points have a UV completion in $d = 6 - \epsilon$ as the IR fixed points of the higher derivative renormalizable gauge theory

$$S = \int d^d x \left(\frac{1}{4e_0^2} F_{\mu\nu} (-\nabla^2) F^{\mu\nu} - \bar{\psi}_i \gamma^\mu (\partial_\mu + iA_\mu) \psi^i \right), \quad (2.66)$$

where ψ^i are N_f 6d Weyl fermions. To get an anomaly free theory, we may add N_f Weyl fermions of the opposite chirality, so that the model includes N_f 6d Dirac fermions. The one-loop beta function for this theory can be computed by evaluating the correction to the gauge field propagator due to the fermion loop, which is given by (2.46) for general d . Expanding in $d = 6 - \epsilon$, one finds a pole that fixes the charge renormalization, and for the theory with N_f Dirac fermions, we obtain the beta function

$$\beta_e = -\frac{\epsilon}{2} e - \frac{N_f}{120\pi^3} e^3 + \mathcal{O}(e^5). \quad (2.67)$$

Unlike the case of QED₄, this theory is asymptotically free in $d = 6$. It would be interesting to compute the beta function for the non-abelian version of this model. By analogy with $d = 4$, we expect that in this case the pure glue should give a *positive* contribution to the beta function, while matter gives negative contributions. The pure glue theory may then have IR fixed points for positive g^2 that could provide

a UV completion of the Yang-Mills theory in $d = 4 + \epsilon$. Also, in the theory with gauge group $SU(N_c)$ and N_f massless fermions, one may contemplate the existence of a conformal window directly in $d = 6$.

2.5 Sphere free energy of the QED in the ϵ expansion

The action for massless QED in $d = 4 - \epsilon$ on a general curved Euclidean manifold is

$$\begin{aligned}
S = \int d^d x \sqrt{g_x} & \left(\frac{1}{4e_0^2} F_{\mu\nu} F^{\mu\nu} + \frac{1}{2} (\nabla_\mu A^\mu)^2 - \sum_{i=1}^{N_f} \bar{\psi}_i \gamma^\mu (\nabla_\mu + iA_\mu) \psi^i \right. \\
& \left. + a_0 W^2 + b_0 E + c_0 \mathcal{R}^2 / (d-1)^2 \right), \tag{2.68}
\end{aligned}$$

where ψ^i are N_f four-component Dirac fermions, and we have added a Feynman gauge fixing term, which we find most convenient for the perturbative calculation below. Here ∇_μ is the curved space covariant derivative (when it acts on fermions, it includes the spin connection term as usual). Finally, \mathcal{R} denotes the Ricci scalar, W^2 is the square of the Weyl tensor and E is the Euler density:

$$\begin{aligned}
W^2 &= \mathcal{R}_{\mu\nu\lambda\rho} \mathcal{R}^{\mu\nu\lambda\rho} - \frac{4}{d-2} \mathcal{R}_{\mu\nu} \mathcal{R}^{\mu\nu} + \frac{2}{(d-2)(d-1)} \mathcal{R}^2, \\
E &= \mathcal{R}_{\mu\nu\lambda\rho} \mathcal{R}^{\mu\nu\lambda\rho} - 4 \mathcal{R}_{\mu\nu} \mathcal{R}^{\mu\nu} + \mathcal{R}^2. \tag{2.69}
\end{aligned}$$

The action includes all terms that are marginal in $d = 4$, and e_0, a_0, b_0, c_0 are the corresponding bare coupling parameters. Renormalizability of the theory on an arbitrary manifold implies that the divergencies of the free energy can be removed by a suitable renormalization of the bare parameters which is independent of the background metric. The renormalization of the electric charge is fixed by the flat space

theory and reads, in minimal subtraction scheme [15]:

$$e_0 = \mu^{\frac{\epsilon}{2}} \left(e + \frac{4N_f}{3\epsilon} \frac{e^3}{(4\pi)^2} + \left(\frac{8N_f^2}{3\epsilon^2} + \frac{2N_f}{\epsilon} \right) \frac{e^5}{(4\pi)^4} + \left(\frac{160N_f^3}{27\epsilon^3} + \frac{88N_f^2}{9\epsilon^2} - \frac{2N_f(22N_f + 9)}{27\epsilon} \right) \frac{e^7}{(4\pi)^6} + \dots \right), \quad (2.70)$$

where e is the renormalized coupling, and the corresponding beta function is⁷

$$\beta = -\frac{\epsilon}{2}e + \frac{4N_f}{3} \frac{e^3}{(4\pi)^2} + \frac{4N_f e^5}{(4\pi)^4} - \frac{2N_f(22N_f + 9)}{9} \frac{e^7}{(4\pi)^6} - \frac{2N_f(4N_f(154N_f + 2808\zeta(3) - 855) + 5589)e^9}{243(4\pi)^8}. \quad (2.71)$$

Then, one finds an IR stable perturbative fixed point at

$$e_* = \pi \sqrt{\frac{6\epsilon}{N_f}} \left(1 - \frac{9}{16N_f}\epsilon + \frac{3(44N_f + 207)}{512N_f^2}\epsilon^2 + \frac{(2464N_f^2 + 44928N_f\zeta(3) - 45756N_f - 62937)}{24576N_f^3}\epsilon^3 + \mathcal{O}(\epsilon^4) \right). \quad (2.72)$$

The first few terms in the renormalization of the curvature couplings have been obtained in [61] for $N_f = 1$, and in [59] for the general case. In our conventions, they read⁸

$$\begin{aligned} a_0 &= \mu^{-\epsilon} \left(a + \frac{N_f + 2}{20\epsilon(4\pi)^2} + \frac{7N_f}{72\epsilon} \frac{e^2}{(4\pi)^4} + \dots \right), \\ b_0 &= \mu^{-\epsilon} \left(b - \frac{11N_f + 62}{360\epsilon(4\pi)^2} + \frac{N_f}{6\epsilon} \frac{e^4}{(4\pi)^6} + \left(\frac{2N_f^2}{9\epsilon^2} - \frac{(16N_f + 9)N_f}{108\epsilon} \right) \frac{e^6}{(4\pi)^8} + \dots \right), \\ c_0 &= \mu^{-\epsilon} \left(c - \frac{N_f^2}{9\epsilon} \frac{e^6}{(4\pi)^8} + \dots \right). \end{aligned} \quad (2.73)$$

⁷The terms of order e^9 that we have omitted from (2.70) can be reconstructed from (2.71) if desired.

⁸The term of order e^6/ϵ in b_0 is scheme dependent in the sense that it depends on the definition of the Euler density E in $d = 4 - \epsilon$. Our conventions for E in (2.69) differ from [59] by an overall d -dependent factor. One can verify that the free energy at the fixed point is not affected by this convention dependence.

and the corresponding beta functions for the renormalized parameters a, b, c are

$$\begin{aligned}
\beta_a &= \epsilon a + \frac{N_f + 2}{20(4\pi)^2} + \frac{7N_f}{36} \frac{e^2}{(4\pi)^4} + \dots, \\
\beta_b &= \epsilon b - \frac{11N_f + 62}{360(4\pi)^2} + \frac{N_f}{2} \frac{e^4}{(4\pi)^6} - \frac{(16N_f + 9)N_f}{27} \frac{e^6}{(4\pi)^8} + \dots, \\
\beta_c &= \epsilon c - \frac{4N_f^2}{9} \frac{e^6}{(4\pi)^8} + \dots.
\end{aligned} \tag{2.74}$$

We are interested in computing the free energy of the theory on a round sphere S^d of radius R , for which one has $W^2 = 0$, $E = d(d-1)(d-2)(d-3)/R^4$, $\mathcal{R} = d(d-1)/R^2$. In particular, the renormalization of the Weyl square coupling a_0 will not play any role in this calculation. After renormalization, the sphere free energy $F(e, b, c, \mu R)$ is a finite function for any value of the renormalized couplings e, b, c . By standard arguments, it satisfies the Callan-Symanzik equation

$$\left(\mu \frac{\partial}{\partial \mu} + \beta_e \frac{\partial}{\partial e} + \beta_b \frac{\partial}{\partial b} + \beta_c \frac{\partial}{\partial c} \right) F(e, b, c, \mu R) = 0. \tag{2.75}$$

As explained in [54], it follows that to obtain the radius independent free energy at the IR fixed point we should set not only $\beta_e = 0$, but also the curvature beta functions $\beta_b = \beta_c = 0$. The corresponding fixed point values in $d = 4 - \epsilon$ are given by $e = e_*$ in eq. (2.72), and

$$\begin{aligned}
b_* &= \frac{1}{\epsilon} \left(\frac{11N_f + 62}{360(4\pi)^2} - \frac{N_f}{2} \frac{e_*^4}{(4\pi)^6} + \frac{(16N_f + 9)N_f}{27} \frac{e_*^6}{(4\pi)^8} \right) + \mathcal{O}(\epsilon^4), \\
c_* &= \frac{1}{\epsilon} \frac{4N_f^2}{9} \frac{e_*^6}{(4\pi)^8} + \mathcal{O}(\epsilon^4),
\end{aligned} \tag{2.76}$$

and the free energy at the fixed point is the radius independent quantity

$$F_{\text{conf}}(\epsilon) = F(e_*, b_*, c_*, \mu R). \tag{2.77}$$

Note that at the free field level, the effect of (2.76) is simply to remove the coupling independent part of the curvature terms. The fixed point free energy has then a pole due to the free field determinants, but $\tilde{F} = -\sin(\pi d/2)F$ is finite in the $d \rightarrow 4$ limit and reproduces the a anomaly of the 4d theory [53, 54].

To perform the explicit calculations, we find it convenient to follow [92, 93, 60, 94] and describe the sphere by flat embedding coordinates η^a , $a = 1, 2, \dots, d + 1$ satisfying $\sum_{a,b} \delta_{ab} \eta^a \eta^b = R^2$. In this approach, one also introduces Dirac matrices α_a of dimension $2^{d/2}$ satisfying the Clifford algebra in $d + 1$ dimensions $\{\alpha_a, \alpha_b\} = 2\delta_{ab}$, $a, b = 1, \dots, d + 1$. In this embedding formalism, the vertex in (2.68) is given by

$$\Gamma_a(\eta) = ie_0 Q_{ab}(\eta) \alpha_b, \quad Q_{ab}(\eta) = \delta_{ab} - \frac{\eta_a \eta_b}{R^2}, \quad (2.78)$$

where we have rescaled the gauge field to bring the coupling constant in the vertex. One advantage of using embedding coordinates is that the propagators take a relatively simple form [60]. The photon propagator in the Feynman gauge is

$$D_{ab}(\eta_1, \eta_2) = \delta_{ab} D(\eta_1, \eta_2) = \delta_{ab} \frac{\Gamma(d-2)}{(4\pi)^{\frac{d}{2}} R^{d-2} \Gamma(\frac{d}{2})} {}_2F_1\left(1, d-2, \frac{d}{2}, 1 - \frac{(\eta_1 - \eta_2)^2}{4R^2}\right) \quad (2.79)$$

and the fermion propagator is

$$S_j^i(\eta_1, \eta_2) = -\delta_j^i \frac{\Gamma(\frac{d}{2})}{2\pi^{\frac{d}{2}}} \frac{\alpha \cdot (\eta_1 - \eta_2)}{|\eta_1 - \eta_2|^d}. \quad (2.80)$$

Introducing the integrated n -point functions

$$G_n = \int \prod_{k=1}^n d^d \eta_k \langle \bar{\psi}_{i_1} \Gamma_{a_1} A^{a_1} \psi^{i_1}(\eta_1) \dots \bar{\psi}_{i_n} \Gamma_{a_n} A^{a_n} \psi^{i_n}(\eta_n) \rangle_0^{\text{conn}} \quad (2.81)$$

the free energy is given by

$$\begin{aligned}
F_{\text{QED}_d} = & N_f F_{\text{free-ferm}}(d) + F_{\text{Max.}}^{(0)}(d) - \frac{1}{2} \log(e_0^2 R^{4-d}) + \frac{1}{2!} e_0^2 G_2 - \frac{1}{4!} e_0^4 G_4 + \dots \\
& + \Omega_d R^{d-4} (d(d-1)(d-2)(d-3)b_0 + d^2 c_0),
\end{aligned} \tag{2.82}$$

where $\Omega_d = 2\pi^{\frac{d+1}{2}}/\Gamma(\frac{d+1}{2})$ is the volume of the unit sphere, the free fermion free energy is given in (2.51), and we have separated out the coupling dependent part $-\frac{1}{2} \log(e_0^2 R^{4-d})$ of the free Maxwell free energy, see eq. (2.24), (2.33). This term plays an important role in the renormalization procedure upon using (2.70), and its presence is necessary for cancellation of poles and to obtain a radius independent free energy at the fixed point.

The technical details of the calculation of G_2 and G_4 are given in Appendix 2.14. To the order needed here, we find that their ϵ expansion is given by

$$\begin{aligned}
G_2 = & N_f \left(\frac{1}{6\pi^2 \epsilon} + \frac{4(5 + 3(\log(4\pi R^2) + \gamma))}{12^2 \pi^2} \right. \\
& \left. + \frac{18\pi^2 + 124 + 4(5 + 3(\log(4\pi R^2) + \gamma))^2}{12^3 \pi^2} \epsilon + \mathcal{O}(\epsilon^2) \right),
\end{aligned} \tag{2.83}$$

and

$$\begin{aligned}
G_4 = & \frac{N_f^2}{6\pi^4 \epsilon^2} + \frac{N_f(8N_f(5 + 3(\log(4\pi R^2) + \gamma)) - 18)}{12^2 \pi^4 \epsilon} \\
& + \frac{1}{12^3 \pi^4} \left(16N_f^2(5 + 3(\log(4\pi R^2) + \gamma))^2 - 72N_f(5 + 3(\log(4\pi R^2) + \gamma)) \right. \\
& \left. + 4(77 + 9\pi^2)N_f^2 + 9N_f(72\zeta(3) - 47) \right) + \mathcal{O}(\epsilon).
\end{aligned} \tag{2.84}$$

Plugging these results into (2.82), as well as the coupling renormalization (2.70) and (2.73), we find that all poles indeed cancel for arbitrary e, b, c . In particular, our calculation provides an independent check on the curvature counterterms (2.73) to order e^4 .

We can now compute the free energy at the IR fixed point by plugging in the critical couplings (2.72), (2.76). Defining

$$F_{\text{conf}}(\epsilon) = F_{\text{QED}_d}(e_*, b_*, c_*, \mu R) \quad (2.85)$$

we find

$$\begin{aligned} F_{\text{conf}} &= N_f F_{\text{free-ferm}}(d) + F_{\text{Max.}}^{(0)}(d) + \frac{1}{2} \log\left(\frac{N_f}{6\pi^2\epsilon}\right) \\ &+ \left(40 + 24(\gamma + \log(4\pi)) + \frac{27}{N_f}\right) \frac{\epsilon}{96} + \left(\pi^2 + \frac{47}{9} - \frac{9(8N_f\zeta(3) - 4N_f + 5)}{4N_f^2}\right) \frac{\epsilon^2}{32} + \mathcal{O}(\epsilon^3). \end{aligned} \quad (2.86)$$

Note that the result is indeed independent of the radius R , consistently with conformal invariance and the Callan-Symanzik equation (2.75).

Using the explicit ϵ expansion of the free Maxwell contribution, which can be obtained from (2.33)

$$F_{\text{Max.}}^{(0)}(d) = -\frac{1}{\sin\left(\frac{\pi d}{2}\right)} \left(\frac{31\pi}{90} + 1.946\epsilon - 2.524\epsilon^2 - 1.216\epsilon^3 + \mathcal{O}(\epsilon^4)\right) \quad (2.87)$$

we then obtain our final result for $\tilde{F}_{\text{conf}} = -\sin\left(\frac{\pi d}{2}\right)F_{\text{conf}}$ given in eq. (2.2). As a test of this result, one can verify that to order N_f^0 it precisely agrees with the large N_f prediction, eq. (2.60) and (2.63).

2.6 Padé approximation and the F -theorem

A novel feature of the result (2.86) compared to the sphere free energy for the $O(N)$ Wilson-Fisher fixed points [54], is the appearance of the $\log(\epsilon)$ behavior in $d = 4 - \epsilon$. This makes it difficult to apply standard resummation techniques like Padé approximants. To circumvent this problem, we isolate the logarithmic term $\frac{1}{2} \log(N_f/\epsilon)$ in

F , which we treat exactly, and perform a Padé extrapolation on the function

$$\delta\tilde{F}_d(N_f) \equiv \tilde{F}_{\text{conf}} - N_f \tilde{F}_{\text{free-ferm}} + \frac{1}{2} \sin\left(\frac{\pi d}{2}\right) \log\left(\frac{N_f}{\epsilon}\right). \quad (2.88)$$

In $d = 2$, the IR fixed point of QED $_d$ is the Schwinger model with $2N_f$ massless two-component Dirac fermions. In the infrared it is described, via the non-abelian bosonization [85], by the level 1 $SU(2N_f)$ WZW model [86, 87]. This is a CFT with $c = 2N_f - 1$ corresponding to $\tilde{F} = \frac{\pi}{6}(2N_f - 1)$. Therefore, it is natural to use a two-sided Padé approximant subject to the constraints:

$$\delta\tilde{F}_d(N_f) = \begin{cases} -\frac{\pi}{6}, & d = 2, \\ \frac{31\pi}{90} - 1.26\epsilon - 0.65\epsilon^2 + 0.84\epsilon^3 + \frac{0.44\epsilon^2}{N_f} - \frac{0.62\epsilon^3}{N_f} - \frac{0.55\epsilon^3}{N_f^2}, & d = 4 - \epsilon. \end{cases} \quad (2.89)$$

This allows us to use Padé approximants $\text{Padé}_{[m,n]}$ of total order 4. The results for $d = 3$ using these two-sided approximants $\text{Padé}_{[2,2]}$ and $\text{Padé}_{[1,3]}$ are given in table 2.1. For comparison, we also present the results using one-sided approximant $\text{Padé}_{[1,2]}$ obtained without assuming the boundary condition at $d = 2$ (we see, however, that its agreement with the large N_f expansion is not as good as that of both two-sided Padé approximants). We also plot the $\text{Padé}_{[1,3]}$ approximant for different N_f in figure 2.3,

N_f	1	2	3	4	5	6	10
$\text{Padé}_{[2,2]}$	-	-0.1512	-0.1284	-0.1237	-0.1223	-0.1218	-0.1217
$\text{Padé}_{[1,3]}$	-0.2743	-0.1462	-0.1284	-0.1228	-0.1204	-0.1192	-0.1176
$\text{Padé}_{\text{average}}$	-	-0.1487	-0.1284	-0.1232	-0.1213	-0.1205	-0.1196
$\text{Padé}_{[1,2]}$	-	-0.1856	-0.1259	-0.1072	-0.0986	-0.0937	-0.0861
ϵ -expansion	-0.7148	-0.2113	-0.1049	-0.0632	-0.0418	-0.0291	-0.0074

Table 2.1: Various Padé approximations and the unresummed ϵ -expansion of $\delta\tilde{F}_d(N_f)$ at $d = 3$. The two-sided approximants $\text{Padé}_{[2,2]}$ and $\text{Padé}_{[1,3]}$ are obtained assuming the value $-\frac{\pi}{6}$ at $d = 2$, while $\text{Padé}_{[1,2]}$ does not use this assumption. Row 3 is the average of the two-sided approximants, i.e. of the first two rows. At large N_f we expect to find $\delta\tilde{F}_{d=3} = \frac{1}{2} \log\left(\frac{\pi}{4}\right) \approx -0.1208$.

as a function of $2 < d < 4$. In figure 2.4, we plot $F_{\text{conf-QED}_3} - N_f F_{\text{free-ferm}}$ comparing

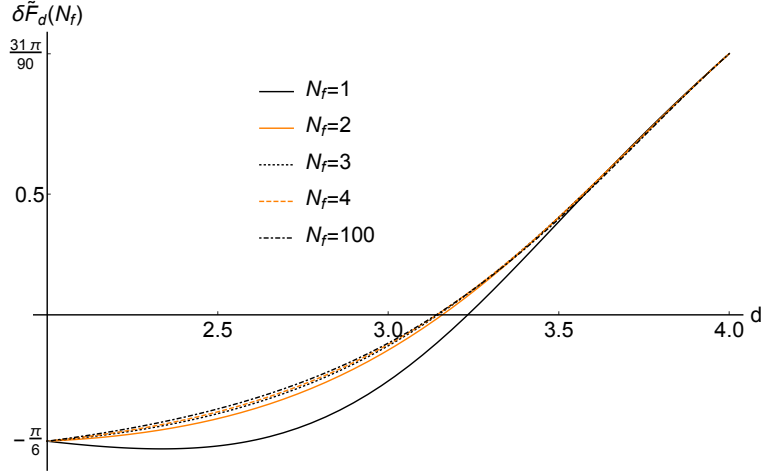


Figure 2.3: Padé_[1,3] on $\delta\tilde{F}_d(N_f)$ for various N_f

the result of the Padé approximation and the large N result (2.1).

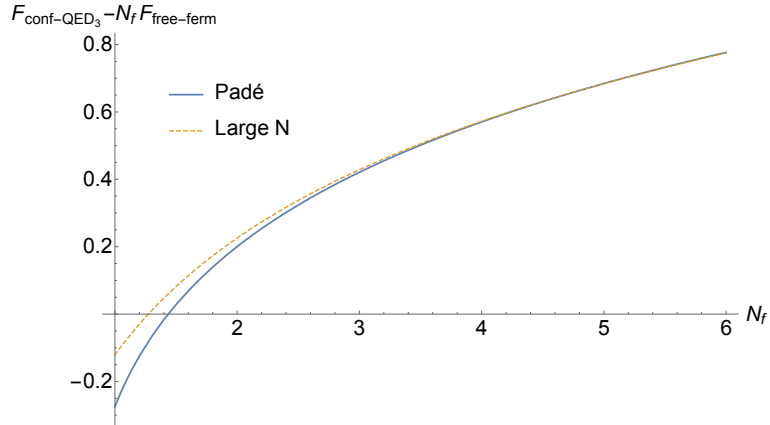


Figure 2.4: Comparison of the Padé resummation of the ϵ expansion, and the large N result (2.1) for the sphere free energy of conformal QED₃.

It is interesting to compare this result for the conformal phase of the theory with the F -value in the broken symmetry phase. The latter contains $2N_f^2$ Goldstone bosons and a free Maxwell field, which is dual to a scalar.⁹ At long distances, each of these fields is described by a conformally coupled scalar field. Therefore, after the chiral

⁹ In compact QED this scalar is compact [95], and it develops a vacuum expectation value. If there are no monopole operators in the action, then the topological $U(1)_T$ symmetry is spontaneously broken and there is a massless scalar degree of freedom in the IR, just as in the non-compact case.

symmetry breaking

$$F_{\text{SB}}(N_f) = (2N_f^2 + 1) \left(\frac{\log 2}{8} - \frac{3\zeta(3)}{16\pi^2} \right). \quad (2.90)$$

To study if the F -theorem allows flow from the conformal phase to the phase with global symmetry breaking, we define the function

$$\Delta(N_f) = F_{\text{conf}}(N_f) - (2N_f^2 + 1) \left(\frac{\log 2}{8} - \frac{3\zeta(3)}{16\pi^2} \right). \quad (2.91)$$

Its plot obtained using the $\text{Padé}_{[1,3]}$ with $d = 2$ boundary condition is shown in Fig. 2.5. One can also consider the corresponding function using the large N_f expression (2.1) for F_{conf} ; this gives results that are close to those shown in Fig. 2.5.

	$\text{Padé}_{[1,3]}$	$\text{Padé}_{[2,2]}$	$\text{Padé}_{[1,2]}$
$N_{f,c}$	4.4204	4.4180	4.4530

Table 2.2: Estimates of $N_{f,c}$, which is the solution of $F_{\text{conf}} = F_{\text{SB}}$, obtained from various Padé approximants. $\text{Padé}_{[1,3]}$ and $\text{Padé}_{[2,2]}$ use the $d = 2$ boundary condition in (2.89), while $\text{Padé}_{[1,2]}$ only uses data from the $d = 4 - \epsilon$ expansion.

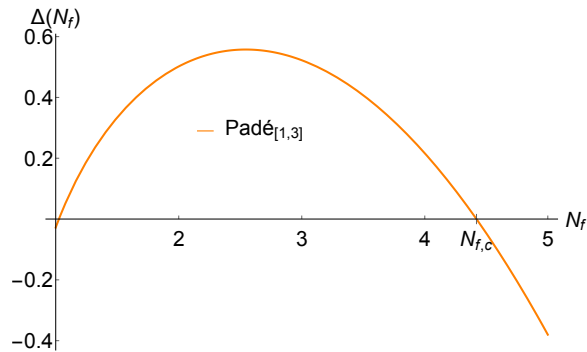


Figure 2.5: Plot of $\Delta(N_f) = F_{\text{conf}}(N_f) - F_{\text{SB}}(N_f)$, using $\text{Padé}_{[1,3]}$.

The plot in Fig. 2.5 implies that the RG flow from conformal to symmetry broken phase becomes impossible for N_f between 4 and 5. This value of N_f is found by solving the equation $F_{\text{conf}} = F_{\text{SB}}$; it provides an upper bound on the integer value of N_f where the conformal window may become unstable: $N_{\text{crit}} \leq 4$.

Now let us treat N_f as a continuous parameter and discuss the implications of conformal perturbation theory for the phase structure of the theory. As explained in the introduction, we expect that for N_f near N_{crit} , a $SU(2N_f)$ invariant quartic operator is nearly marginal, and we can work perturbatively in the small parameter $\delta = \Delta - 3$. The beta function for λ , the coefficient of the quartic operator, has the structure $\beta_\lambda = \delta\lambda + A\lambda^2 + O(\lambda^3)$. Thus, in addition to the QED_3 fixed point at $\lambda = 0$, we find a nearby fixed point at $\lambda_* = -\delta/A$. For $N_f \gtrsim N_{\text{crit}}$, this is a UV fixed point. It is another $SU(2N_f)$ invariant CFT which we could call QED_3^* . Its existence for N_f slightly above N_{crit} is guaranteed by the conformal perturbation theory. It also exists for large N_f , where it is a double-trace deformation of QED_3 . Therefore, QED_3^* may exist for all $N_f > N_{\text{crit}}$.

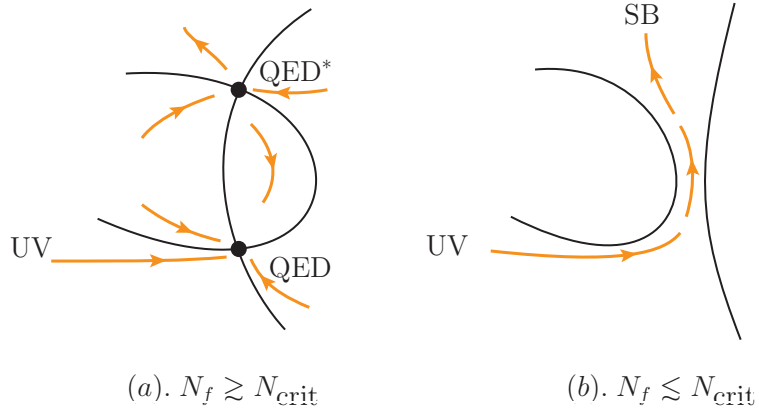


Figure 2.6: Schematic picture of RG flows for $N_f \gtrsim N_{\text{crit}}$ (a) and $N_f \lesssim N_{\text{crit}}$ (b). The QED_3 and QED_3^* fixed points merge at N_{crit} and acquire small imaginary parts for $N_f \lesssim N_{\text{crit}}$. In the latter case, the interacting conformal behavior is no longer possible, but the RG flow from the UV can “hover” near the complex fixed points before running away to large quartic coupling and presumably leading to the broken symmetry phase.

A commonly discussed scenario is that the QED_3 and QED_3^* fixed points merge at N_{crit} and acquire small imaginary parts for $N_f \lesssim N_{\text{crit}}$ [44, 48, 49, 46]. This means that the interacting conformal behavior is impossible for $N_f \lesssim N_{\text{crit}}$, but the RG flow from the UV can “hover” near the complex fixed points before running away to large

quartic coupling and presumably leading to the broken symmetry phase (see figure 2.6). During the hovering F can be made parametrically close to $F_{\text{conf}}(N_{\text{crit}})$. This is why the F -theorem requires $F_{\text{conf}}(N_{\text{crit}}) > F_{\text{SB}}$ (a similar argument involving the continuity of F was given in [38]). As we have seen, this gives a rather stringent bound $N_{\text{crit}} \lesssim 4.4$.

An alternate possibility is that both fixed points stay real and go through each other. Then the QED₃ fixed point continues to exist even after the appearance of a relevant operator; this relevant operator may create flow from QED₃ to the broken symmetry phase. Therefore, the F -theorem bound on N_{crit} is the same as with the “merger and annihilation” scenario.

2.7 Calculation of C_{J1} and C_{T1}

In what follows we calculate the two-point function of the $SU(N_f)$ current and stress-energy tensor, which are given by¹⁰

$$\begin{aligned} J_\nu^a &= -\bar{\psi}_i (t^a)_j^i \gamma_\nu \psi^j, \\ T_{\mu\nu} &= -\frac{1}{4} (\bar{\psi}_i \gamma_{(\mu} D_{\nu)} \psi^i - D_{(\mu}^* \bar{\psi}_i \gamma_{\nu)} \psi^i), \end{aligned} \quad (2.92)$$

where $\gamma_{(\mu} D_{\nu)} \equiv \gamma_\mu D_\nu + \gamma_\nu D_\mu$ and $D_\mu = \partial_\mu + iA_\mu$. Note that there is no Maxwell term contribution in $T_{\mu\nu}$, as this term was dropped in (2.47) in the critical limit.

We will work in flat Euclidean d -dimensional metric and introduce a null vector z^μ , which satisfies

$$z^2 = z^\mu z^\nu \delta_{\mu\nu} = 0. \quad (2.93)$$

¹⁰As it was pointed out in [96], for correlation functions with only gauge invariant operators we can omit the gauge fixing part and ghost part of the stress-energy tensor. This was explicitly checked in QCD in $d = 4$ up to three-loops in [97].

From (2.3), (2.5), we see that the two-point functions of the projected operators $T \equiv z^\mu z^\nu T_{\mu\nu}$ and $J \equiv z^\mu J_\mu$ have the form

$$\begin{aligned}\langle T(x)T(0) \rangle &= \frac{4C_T}{(x^2)^d} \frac{x_z^4}{x^4}, \\ \langle J^a(x)J^b(0) \rangle &= \delta^{ab} \frac{-2C_J}{(x^2)^{d-1}} \frac{x_z^2}{x^2},\end{aligned}\tag{2.94}$$

where we have introduced the notation $x_z \equiv z^\mu x_\mu$. It will be also useful to report the form of these two-point functions in momentum space, which may be obtained by Fourier transform and reads

$$\begin{aligned}\langle T(p)T(-p) \rangle &= C_T \frac{\pi^{\frac{d}{2}} \Gamma(2 - \frac{d}{2})}{2^{d-2} \Gamma(d+2)} \frac{p_z^4}{(p^2)^{2-\frac{d}{2}}}, \\ \langle J^a(p)J^b(-p) \rangle &= C_J \frac{\pi^{\frac{d}{2}} \Gamma(2 - \frac{d}{2})}{2^{d-3} \Gamma(d)} \frac{p_z^2}{(p^2)^{2-\frac{d}{2}}} \delta^{ab},\end{aligned}\tag{2.95}$$

where $p_z \equiv z^\mu p_\mu$.

For the stress-tensor of conformal QED, we may write $T = T_\psi + T_A$, where the two terms are given in momentum space by

$$\begin{aligned}T_\psi(p) &= -\frac{1}{2} \int \frac{d^d p_1}{(2\pi)^d} \bar{\psi}_i(-p_1) i\gamma_z (2p_{1z} + p_z) \psi^i(p + p_1), \\ T_A(p) &= - \int \frac{d^d p_1}{(2\pi)^d} \bar{\psi}_i(-p_1) i\gamma_z A_z \psi^i(p + p_1), \\ J^a(p) &= - \int \frac{d^d p_1}{(2\pi)^d} \bar{\psi}_i(-p_1) (t^a)_j^i \gamma_z \psi^j(p + p_1).\end{aligned}\tag{2.96}$$

The diagrammatic representation is shown in figure 2.7.

$$\begin{aligned}T_\psi(p) &= -\frac{1}{2} i (2p_{1z} + p_z) \gamma_z \delta_j^i \\ T_A(p) &= -i \gamma_z \delta_j^i \\ J^a(p) &= -\gamma_z (t^a)_j^i\end{aligned}$$

Figure 2.7: Diagrammatic representation for $T = T_\psi + T_A$ and J^a .

The diagrams contributing to $\langle JJ \rangle$ up to order $1/N$

$$\langle J^a(p)J^b(-p) \rangle = D_0 + D_1 + D_2 + \mathcal{O}(1/N^2) \quad (2.97)$$

are shown in figure 2.8. Their expressions in momentum space and explicit results are listed in Appendix 2.16.

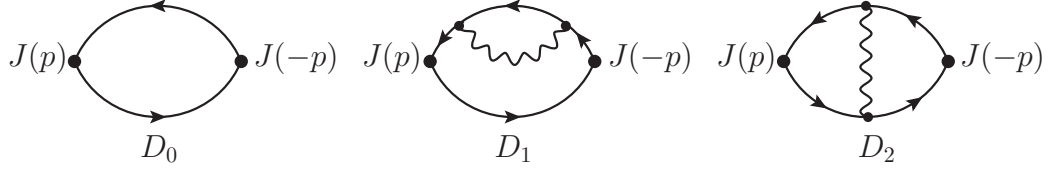


Figure 2.8: Diagrams contributing to C_J up to order $1/N$.

Putting together the results, we find

$$\langle J^a(p)J^b(-p) \rangle = -\text{Tr}(t^a t^b) C_{J0} \left(1 + \frac{C_{J1}(d)}{N} + \mathcal{O}(1/N^2) \right) \frac{\pi^{\frac{d}{2}} \Gamma(2 - \frac{d}{2})}{2^{d-3} \Gamma(d)} \frac{p_z^2}{(p^2)^{2-\frac{d}{2}}}, \quad (2.98)$$

where $C_{J1}(d)$ is given in (2.7), and

$$C_{J0} = \text{Tr} \mathbf{1} \frac{1}{S_d^2} \quad (2.99)$$

is the free fermion contribution. A plot of C_{J1} as a function of d is given in figure 2.9.

The value in $d = 3$ was given in (2.10) above. One may also extract the following

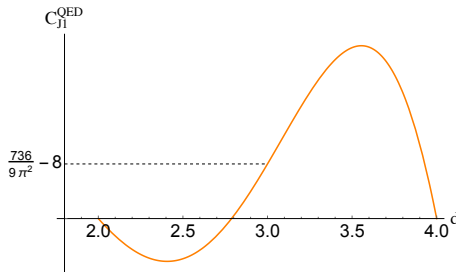


Figure 2.9: Plot of C_{J1} .

ϵ -expansions

$$C_{J1}|_{d=2+\epsilon} = -\epsilon + \mathcal{O}(\epsilon^2), \quad C_{J1}|_{d=4-\epsilon} = \frac{9\epsilon}{2} + \left(\frac{9}{2} - 9\zeta(3)\right)\epsilon^2 + \mathcal{O}(\epsilon^3). \quad (2.100)$$

In $d = 3$ the leading correction is quite small even for small N ; for $N = 4$, corresponding to $N_f = 1$, it makes C_J around 7% bigger than the free fermion result.

Let us now turn to the calculation of C_T . Up to order N^0 , the stress-tensor two-point function receives contribution from the diagrams shown in figure 2.10. Note that for some topologies we did not draw explicitly diagrams with the opposite fermion loop direction, but they have to be included. We list the integrands and results for these diagrams in Appendix B. We have

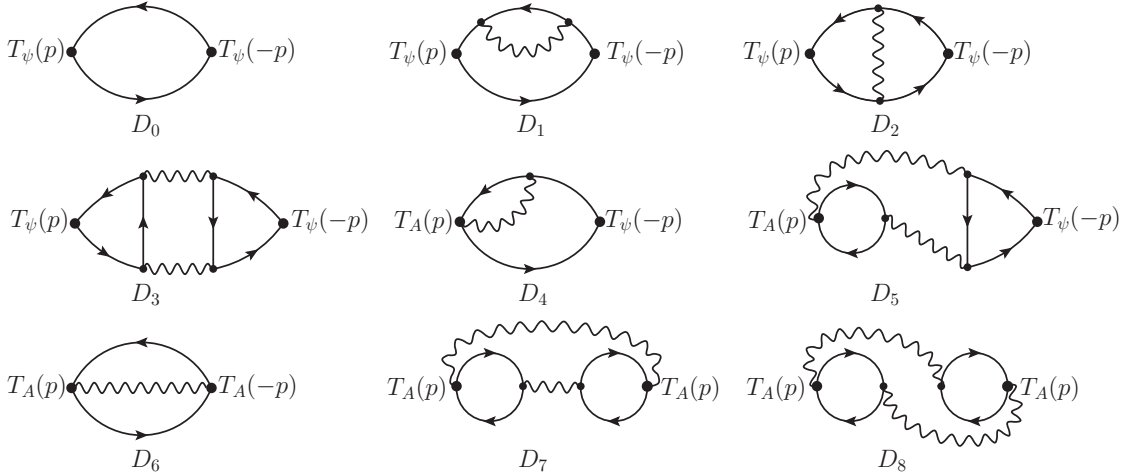


Figure 2.10: Diagrams contributing to C_T up to N^0 order.

$$\langle T^{\text{ren}}(p)T^{\text{ren}}(-p) \rangle = Z_T^2 \langle T(p)T(-p) \rangle = Z_T^2 \left(\sum_{n=0}^8 D_n + \mathcal{O}(1/N) \right), \quad (2.101)$$

where we have introduced a “ Z_T -factor” [68], which is computed in Appendix A from the Ward identity. It reads $Z_T = 1 + (Z_{T1}/\Delta + Z'_{T1})/N + \mathcal{O}(1/N^2)$, with

$$Z_{T1} = -\frac{d(d-2)\eta_{m1}}{2(d+2)(d-1)}, \quad Z'_{T1} = -\frac{(d-2)\eta_{m1}}{(d+2)(d-1)}, \quad (2.102)$$

where η_{m1} is given in (2.9). Putting together the results for the diagrams given in Appendix 2.16, we obtain

$$\langle T^{\text{ren}}(p)T^{\text{ren}}(-p) \rangle = C_{T0} \left(1 + \frac{C_{T1}(d)}{N} + \mathcal{O}(1/N^2) \right) \frac{\pi^{\frac{d}{2}} \Gamma(2 - \frac{d}{2})}{2^{d-2} \Gamma(d+2)} \frac{p_z^4}{(p^2)^{2-\frac{d}{2}}}, \quad (2.103)$$

where $C_{T1}(d)$ is given in (2.8), and the free fermion contribution is

$$C_{T0} = N \frac{d}{2S_d^2}. \quad (2.104)$$

As a check of our calculation, we note that the final result does not depend on the gauge parameter ξ .

A plot of $C_{T1}(d)$ in $2 < d < 4$ is given in figure 2.11. We see that C_{T1} is negative for $2 < d < 2.79$. This means that the inequality $C_T^{\text{UV}} > C_T^{\text{IR}}$ is violated for the flow from conformal QED_d (which may be thought of as the UV fixed point of the Thirring model) to the free fermion theory for $2 < d < 2.79$. However, it holds for $2.79 < d < 4$, including in particular $d = 3$.

Near some even dimensions we find

$$C_{T1}|_{d=2+\epsilon} = -2 - \frac{\epsilon}{4}, \quad C_{T1}|_{d=4-\epsilon} = 8 - \frac{\epsilon}{6}, \quad C_{T1}|_{d=6-\epsilon} = -30 + \frac{61\epsilon}{6}. \quad (2.105)$$

Note that in $d = 2$ we get

$$C_T|_{d=2} = \frac{N}{S_2^2} \left(1 - \frac{2}{N} \right). \quad (2.106)$$

This result is precisely as expected, since the conformal QED₂ corresponds to the multiflavor Schwinger model with $2N_f$ Dirac fermions, which is described by a CFT with central charge $c = 2N_f - 1$ [86, 87]. Normalizing (2.106) by the free scalar contribution $C_T^{\text{sc}} = d/((d-1)S_d^2)$, and recalling $N = 4N_f$, we obtain precisely this

central charge. In section 2.9 we will see that $C_{T1}|_{d=4-\epsilon}$ also agrees with the $4 - \epsilon$ expansion.

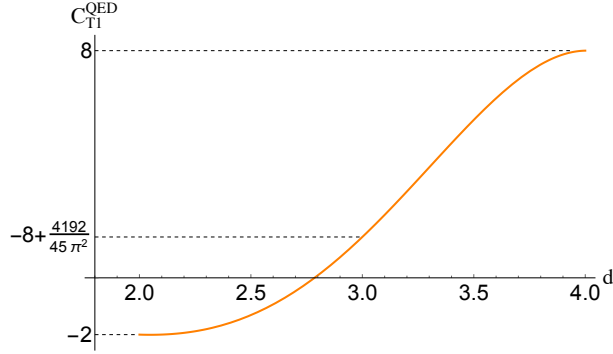


Figure 2.11: Plot of C_{T1} .

Near even dimensions the QED_d theory is expected to be described by the free fermions weakly coupled to a $U(1)$ gauge theory with the local kinetic term (2.11). For example, in $d = 6$ this higher-derivative theory was explored in [98, 99, 100, 101, 80, 33, 102]. We may use (2.8) to extract the C_T coefficient for the conformal Maxwell theory (2.11). From (2.8) it follows that

$$C_{T1}^{\text{QED}}|_{\text{even } d} = \frac{2(-1)^{\frac{d}{2}} d!}{(\frac{d}{2} - 1)! (\frac{d}{2} + 1)!} = 2(-1)^{\frac{d}{2}} \binom{d}{\frac{d}{2} - 1}. \quad (2.107)$$

Recalling that the contribution of the free massless fermions is given by (2.104), we find that the C_T of the conformal Maxwell theory is

$$C_T^{\text{conf. Maxwell}}|_{\text{even } d} = \frac{d}{2S_d^2} C_{T1}^{\text{QED}}|_{\text{even } d} = (-1)^{\frac{d}{2}} \frac{d}{S_d^2} \binom{d}{\frac{d}{2} - 1}. \quad (2.108)$$

In $d = 4, 6, 8, 10, \dots$ this formula gives $16, -90, 448, -2100, \dots$ times $1/S_d^2$. In $d = 4$ this agrees with the standard answer for the Maxwell theory. In $d = 6, 8, \dots$, eq. (2.108) gives new results for the values of C_T in the free conformal theory with the higher-derivative action (2.11).

2.8 C_J^{top} for the Topological Current in $d = 3$

In $d = 3$, it is interesting to compute C_J^{top} for the “topological” $U(1)$ current

$$j_{\text{top}}^\mu = \frac{i}{4\pi} \epsilon^{\mu\nu\lambda} F_{\nu\lambda}, \quad (2.109)$$

where the factor of i arises because we are working in Euclidean signature, and the normalization is such that the associated charges are integers. The diagrams contributing to the current two-point function up to order $1/N^2$ are shown in figure 2.12. The diagrams D_1 and D_2 have the same structure as the corresponding ones in fig.

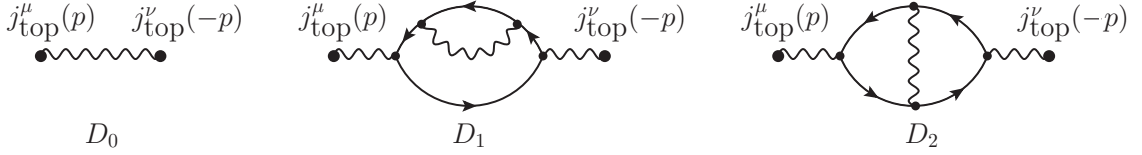


Figure 2.12: Diagrams contributing to C_J^{top} up to $1/N^2$ order.

2.9 for the $SU(N_f)$ current,¹¹ with the difference that at the external points we now have the gauge $U(1)$ current, to which we attach the two induced photon propagators. Thus, using the results from Appendix 2.16, we find

$$\begin{aligned} \langle j_{\text{top}}^\mu(p) j_{\text{top}}^\nu(-p) \rangle &= -\frac{1}{(4\pi)^2} \epsilon^{\mu\rho\sigma} e^{\nu\tau\lambda} \langle (p_\rho A_\sigma(p) - p_\sigma A_\rho(p)) (p_\tau A_\lambda(-p) - p_\lambda A_\tau(-p)) \rangle \\ &= -\frac{|p|}{4\pi^2} \frac{C_A}{N} \left(1 - \frac{C_{J_1}(3)}{N} + \mathcal{O}(1/N^2) \right) \left(\delta_{\mu\nu} - \frac{p_\mu p_\nu}{p^2} \right), \end{aligned} \quad (2.110)$$

where C_A and $C_{J_1}(d)$ are given in (2.49) and (2.7), which yield $C_A|_{d=3} = 32$ and the value of $C_{J_1}(3)$ given in (2.100). Therefore, we finally get

$$\langle j_{\text{top}}^\mu(p) j_{\text{top}}^\nu(-p) \rangle = -\frac{8|p|}{\pi^2 N} \left(1 + \frac{1}{N} \left(8 - \frac{736}{9\pi^2} \right) + \mathcal{O}(1/N^2) \right) \left(\delta_{\mu\nu} - \frac{p_\mu p_\nu}{p^2} \right). \quad (2.111)$$

¹¹In fact these diagrams can be extracted from the evaluation of the polarization operator, which was computed in case of QCD in [103].

Comparing with the momentum space normalization in (2.95), we find the result given in eq. (2.13). We note that this is related to C_J in (2.6)-(2.10) by an inversion, $C_A \sim 1/C_J$. This essentially follows from the fact that in the large N critical QED, A_μ and J_μ are related by a Legendre transformation [104, 105], see eq. (2.47).

The conformal bootstrap constraints on the values of C_J , C_T and C_J^{top} in QED₃ for $N_f = 1, 2, 3$ were recently discussed in [76]. In Table 2.3 we summarize our results for these coefficients in $d = 3$ and for different values of N_f (the number of 4-component fermions). These results appear to fall within the regions allowed by the bootstrap for $N_f = 1, 2, 3$.

N_f	1	2	3	4	5	10	20
C_T/C_{T0}	1.3597	1.1798	1.1199	1.0899	1.0719	1.0360	1.0180
C_J/C_{J0}	1.0715	1.0357	1.0238	1.0179	1.0143	1.0072	1.0036
$8\pi^2 C_J^{\text{top}}$	3.0106	1.5632	1.0550	0.7961	0.63919	0.3219	0.1615

Table 2.3: Results for C_T , C_J and C_J^{top} in $d = 3$ for different values of N_f , the number of 4-component fermions (half the number of 2-component Dirac spinors). C_T and C_J are normalized by the free field values in (2.104) and (2.99). To facilitate the comparison with [76], C_J^{top} is normalized by the free fermion contribution (2.99) for 2-component spinors ($\text{Tr}\mathbf{1} = 2$), which is $\text{Tr}\mathbf{1}/S_3^2 = 1/(8\pi^2)$.

2.9 $4 - \epsilon$ Expansion of C_J and C_T

To find C_J in the $4 - \epsilon$ expansion to the leading non-trivial order, we have to compute diagrams with the same topology as those in the large N approach, figure 2.8, but now the photon propagator is the standard one obtained from the Maxwell term. It reads

$$D_{\mu\nu}(p) = \frac{1}{p^2} \left(\delta_{\mu\nu} - (1 - \xi) \frac{p_\mu p_\nu}{p^2} \right), \quad (2.112)$$

where we have introduced an arbitrary gauge parameter ($\xi = 1$ is the usual Feynman gauge, and $\xi = 0$ Landau gauge).

The renormalization of the electric charge is well-known, and in minimal subtraction scheme it reads [15]:

$$e_0 = \mu^{\frac{\epsilon}{2}} \left(e + \frac{4N_f}{3\epsilon} \frac{e^3}{(4\pi)^2} + \left(\frac{8N_f^2}{3\epsilon^2} + \frac{2N_f}{\epsilon} \right) \frac{e^5}{(4\pi)^4} + \dots \right), \quad (2.113)$$

where e is the renormalized coupling, and the corresponding beta function is

$$\beta = -\frac{\epsilon}{2}e + \frac{4N_f}{3} \frac{e^3}{(4\pi)^2} + \frac{4N_f e^5}{(4\pi)^4} - \frac{2N_f(22N_f + 9)}{9} \frac{e^7}{(4\pi)^6} + \dots \quad (2.114)$$

Then, one finds an IR stable perturbative fixed point at

$$e_* = \pi \sqrt{\frac{6\epsilon}{N_f}} \left(1 - \frac{9}{16N_f} \epsilon + \frac{3(44N_f + 207)}{512N_f^2} \epsilon^2 + \mathcal{O}(\epsilon^3) \right). \quad (2.115)$$

Computing the diagrams in figure 2.8 with the photon propagator (2.112), taking a Fourier transform to coordinate space, and setting $e = e_*$ at the end, we obtain in $d = 4 - \epsilon$

$$C_J/C_J^{\text{free}} = 1 + \frac{9\epsilon}{8N_f} + \mathcal{O}(1/N_f^2). \quad (2.116)$$

which precisely agrees with (2.100) (recall that in this case we have $N = N_f \text{Tr} \mathbf{1} = 4N_f$).

To calculate the $4 - \epsilon$ expansion of C_T to order ϵ , we will use as a shortcut the fact that in $d = 4$ the C_T coefficient may be obtained as (see e.g. [106, 107])

$$C_T = \frac{640}{\pi^2} \beta_a, \quad (2.117)$$

where β_a is the beta function for the Weyl-squared term, which is known to be [61, 59]

$$\beta_a = \frac{N_f + 2}{20(4\pi)^2} + \frac{7N_f}{36} \frac{e^2}{(4\pi)^4} + \dots \quad (2.118)$$

The first term corresponds to the contributions of the free fermions and of the Maxwell field, while the second one encodes the leading interaction corrections. The second term, when evaluated at the IR fixed point (2.115) in $d = 4 - \epsilon$, gives $\frac{7\epsilon}{6(16\pi)^2}$. However, this is not the only contribution of order ϵ because the free field contributions need to be evaluated in $4 - \epsilon$ dimensions. The contribution of free massless fermions is given in (2.104). The contribution of the Maxwell field is more subtle, since this theory is scale invariant but not conformal away from four dimensions [11]. However, defining the projected stress-tensor $T_{\text{Maxwell}} = z^\mu z^\nu F_{\mu\alpha} F^\alpha_\nu$ (this selects the traceless part of $T_{\mu\nu}$), and using the field strength two-point function [11]

$$\langle F_{\mu\nu}(x) F_{\rho\sigma}(0) \rangle = \frac{(2d-4)\Gamma(\frac{d}{2}-1)}{4\pi^{\frac{d}{2}}(x^2)^{d/2}} \left[\left(\delta_{\mu\rho} - \frac{d}{2} \frac{x_\mu x_\rho}{x^2} \right) \left(\delta_{\nu\sigma} - \frac{d}{2} \frac{x_\nu x_\sigma}{x^2} \right) - \mu \leftrightarrow \nu \right] \quad (2.119)$$

we find that $\langle T_{\text{Maxwell}}(x) T_{\text{Maxwell}}(0) \rangle$ takes the form (2.94), just as in a conformal field theory, with the normalization given by

$$C_T^{\text{Maxwell}} = \frac{d^2(d-2)}{2S_d^2}. \quad (2.120)$$

This serves as the natural definition of C_T for the Maxwell theory (in $d = 4$, it agrees with the well-known result [66]). Putting these results together we find

$$C_T^{\text{QED}} = C_T^{\text{free ferm}} \left(1 + \frac{d(d-2) + 35\epsilon/6}{N} + \dots \right) = C_T^{\text{free ferm}} \left(1 + \frac{8 - \epsilon/6}{N} + \dots \right), \quad (2.121)$$

which exactly agrees with (2.105). This gives a highly non-trivial test of the dimension dependence of C_{T1} .

2.10 Another Estimate for Symmetry Breaking in QED₃

In $d = 3$, the QED Lagrangian has $SU(2N_f)$ global symmetry. For $N_f < N_{f,\text{crit}}$ it may be broken via the generation of vacuum expectation value of the operator $\sum_{j=1}^{N_f} \bar{\psi}_j \psi^j$ (this is written using the 4-component spinors ψ^i and gamma-matrices) [21, 14]. This operator preserves the 3-d time reversal symmetry, but it breaks the global symmetry to $SU(N_f) \times SU(N_f) \times U(1)$.

In an earlier paper [33], using the F -theorem inequality $F^{\text{UV}} > F^{\text{IR}}$ [34, 36, 37, 35, 51] we showed that theories with $N_f = 5$ and higher must be in the conformal phase. The F -theorem method is inconclusive, however, for theories with $N_f \leq 4$. There is lattice evidence that theories with $N_f = 1, 2$ are not conformal [64, 65],¹² but little is known about theories with $N_f = 3, 4$.

Let us now consider a different RG inequality:

$$C_T^{\text{UV}} > C_T^{\text{IR}} , \tag{2.122}$$

which is sometimes called “the C_T theorem”. While there is a known $d = 3$ counterexample to this inequality [77], which involves theories with $\mathcal{N} = 2$ supersymmetry, many known RG flows appear to obey (2.122). For example, it is obeyed for flows involving the scalar $O(N)$ [67, 68] and the Gross-Neveu model [68]. If we think of the conformal QED₃ theory as the UV fixed point of the Thirring model, then the inequality (2.122) is obeyed by the flow to the free fermion theory because $C_{T_1}(3) > 0$. We may also test this inequality for the flow from the QED theory in the extreme UV, which consists of the free decoupled Maxwell field and N_f 4-component fermions,

¹²See, however, the recent lattice work [108] suggesting that they are conformal.

to the conformal QED₃. For the former we find using (2.120) and (2.104)

$$C_T^{\text{UV}} = \frac{12N_f + 9}{32\pi^2}. \quad (2.123)$$

For the interacting conformal phase, using our result (2.10), we have

$$C_T^{\text{IR}} = \frac{6N_f}{16\pi^2} \left(1 + \frac{\frac{4192}{45\pi^2} - 8}{4N_f} + \mathcal{O}(1/N_f^2) \right). \quad (2.124)$$

We see that at large N_f (2.122) is obeyed to order N_f^0 because $9 > 3 \left(\frac{4192}{45\pi^2} - 8 \right) \approx 4.32$.

Let us now try applying (2.122) to the $d = 3$ flow from QED in the extreme UV to the broken symmetry phase. For the former we have (2.123). The latter is a free conformal field theory of $2N_f^2 + 1$ scalar fields; therefore, it has

$$C_T^{\text{IR}} = \frac{3(2N_f^2 + 1)}{32\pi^2}. \quad (2.125)$$

We find that the two expressions are equal for $N_f = N_{f,\text{crit}} = 1 + \sqrt{2} \approx 2.414$. This suggests that theories with $N_f = 3$ and higher are in the conformal phase. The inequality (2.122), however, does not require the $N_f = 1, 2$ theories to be conformal, and indeed there is lattice evidence that they are not [64, 65].¹³

2.11 C_T for Large N_f QCD _{d}

To the leading nontrivial order, the large N_f computations for QCD look similar to those in the QED case. The results for large N_f QCD at the critical point can be

¹³ A more stringent value $N_{f,\text{crit}} = 3/2$ follows from the RG inequality based on the coefficient of the thermal free energy [109]. This appears to be in contradiction with the lattice gauge theory work [65] claiming that the $N_f = 2$ theory is not conformal. However, both $N_{f,\text{crit}} = 3/2$ and $N_{f,\text{crit}} = 1 + \sqrt{2} \approx 2.414$ are consistent with the recent paper [108] claiming that the symmetry breaking does not take place even for $N_f = 1$.

deduced from the lagrangian [110, 111, 102, 112, 113, 114, 103, 73, 115]

$$\mathcal{L}_{\text{crit QCD}} = -\bar{\psi}_i \gamma^\mu (\partial_\mu + iA_\mu^a t^a) \psi^i + \frac{N_f}{2\xi} (\square^{(d-4)/2} \partial A)^2 + \partial_\mu \bar{c}^a \partial^\mu c^a + f^{abc} \partial^\mu \bar{c}^a A_\mu^b c^c, \quad (2.126)$$

where ψ^i with $i = 1, \dots, N_f$ are the quark fields belonging to the fundamental representation of the colour group G , A_μ^a is the gluon field and c^a and \bar{c}^a are the ghost fields in the adjoint representation of the colour group. We will use the following notation for the Casimirs of the Lie group generators t^a ($[t^a, t^b] = if^{abc}t^c$):

$$\text{Tr}(t^a t^b) = C(r) \delta^{ab}, \quad t^a t^a = C_2(r) \cdot I, \quad f^{acd} f^{bcd} = C_2(G) \cdot I \quad (2.127)$$

and also $\text{tr}(I) = d(r)$ and $\delta^{ab} \delta^{ab} = d(G)$. The stress-energy tensor is (2.92) with $D_\mu = \partial_\mu + iA_\mu^a t^a$, and as we mentioned above we can omit the gauge fixing and ghost parts of $T_{\mu\nu}$ when computing correlation functions of gauge invariant operators. The diagrams contributing to C_T to order $1/N_f$ are the same as in the QED case (see figure 2.10). It is not hard to show that the relations between QED and QCD diagrams are

$$D_0^{\text{QCD}} = d(r) D_0^{\text{QED}}, \quad D_n^{\text{QCD}} = d(G) D_n^{\text{QED}}, \quad n = 1, \dots, 8, \quad (2.128)$$

where for some diagrams we used the identity $d(r)C_2(r) = d(G)C(r)$. Therefore, we find

$$C_T^{\text{QCD}} = d(r) C_{T0} \left(1 + \frac{1}{N} \frac{d(G)}{d(r)} C_{T1} + \mathcal{O}(1/N^2) \right), \quad (2.129)$$

where C_{T_0} and C_{T_1} are the results for QED given in (2.104) and (2.8). For $SU(N_c)$ gauge group we have $d(r) = N_c$ and $d(G) = N_c^2 - 1$, thus

$$C_T^{\text{QCD}} = N_c C_{T_0} \left(1 + \frac{1}{N} \frac{N_c^2 - 1}{N_c} C_{T_1} + \mathcal{O}(1/N^2) \right). \quad (2.130)$$

Let us check that this agrees with the known exact result for central charge in $d = 2$ gauge theory with massless flavors. The conformal limit of $SU(N_c)$ gauge theory has central charge [85, 86, 87, 116]

$$c = c_{\text{free}} - \frac{(N_c^2 - 1)k}{k + N_c}. \quad (2.131)$$

The subtraction of the second term is due to the gauging of the $SU(N_c)$ Kac-Moody algebra with level k . Since there are $2N_f$ 2-d Dirac flavors in the fundamental representation of $SU(N_c)$, we have $k = 2N_f$. This theory may be described by a $SU(2N_f)_{N_c} \times U(1)$ WZW model [86, 87]. Its central charge is

$$c = 2N_f \frac{2N_f N_c + 1}{2N_f + N_c} = N_f N_c - \frac{2(N_c^2 - 1)N_f}{2N_f + N_c} = 2N_f N_c \left(1 - \frac{1}{2N_f} \frac{N_c^2 - 1}{N_c} + \dots \right), \quad (2.132)$$

which is in agreement with (2.130) evaluated in $d = 2$. For a general gauge group G we have

$$c = 2N_f d(r) - \frac{2d(G)N_f}{2N_f + d(r)} = 2N_f d(r) \left(1 - \frac{1}{2N_f} \frac{d(G)}{d(r)} + \dots \right), \quad (2.133)$$

which agrees with (2.129). Analogously, one can easily see that we have the same relation between C_J in QCD and QED:

$$C_J^{\text{QCD}} = d(r) C_{J_0} \left(1 + \frac{1}{N} \frac{d(G)}{d(r)} C_{J_1} + \mathcal{O}(1/N^2) \right), \quad (2.134)$$

where C_{J_0} and C_{J_1} are the results for QED given in (2.99) and (2.7). The value of C_T for the $d = 6$ conformal Maxwell theory was calculated directly in [117]. The result is in agreement with our (2.108), providing a check of our methods.

2.12 Appendix A. Eigenvalues of the kernel $K_{\mu\nu}$

On the S^d in stereographical coordinates the kernel $K_{\mu\nu} = -\langle J_\mu J_\nu \rangle$ has the form

$$K_{\mu\nu}(x, y) = -C_J \frac{4R^2}{(1+x^2)(1+y^2)} \frac{(\delta_{\mu\nu} - 2\frac{(x-y)_\mu(x-y)_\nu}{|x-y|^2})}{s(x, y)^{2\Delta}}. \quad (2.135)$$

We need to decompose the kernel on a sum of vector spherical harmonics:

$$K_{\mu\nu}(x, y) = \sum_{\ell, m} \sum_s \lambda_\ell^{(s)} Y_{\mu, \ell m}^{(s)*}(x) Y_{\nu, \ell m}^{(s)}(y), \quad (2.136)$$

where s denotes different types of vector spherical harmonics, ℓ is the principal angular quantum number and the range of m for given ℓ and s is $g_\ell^{(s)}$ (see (2.20)-(2.21)). The eigenvalue $\lambda_\ell^{(s)}$ has no m dependence because of rotational invariance. Because of vector spherical harmonics are orthonormal to each other we have¹⁴

$$\lambda_\ell^{(s)} = \int d^d x d^d y \sqrt{g_x} \sqrt{g_y} K^{\mu\nu}(x, y) Y_{\mu, \ell m}^{(s)}(x) Y_{\nu, \ell m}^{(s)*}(y). \quad (2.137)$$

We first consider longitudinal vector harmonics [78]

$$Y_{\mu, \ell m}^{(0)}(x) = \frac{\nabla_\mu Y_{\ell m}(x)}{\sqrt{\ell(\ell + d - 1)}}, \quad (2.138)$$

¹⁴We assume that $\int d^d x \sqrt{g_x} Y_{\mu, \ell m}^{(s)*}(x) Y_{\ell' m'}^{\mu(s')}(x) = \delta_{\ell\ell'} \delta_{mm'} \delta_{ss'}$.

where $Y_{\ell m}(x)$ are usual scalar spherical harmonics¹⁵. Integrating by parts in (2.137) we get

$$\lambda_\ell^{(0)} = \frac{1}{\ell(\ell+d-1)} \int d^d x d^d y \sqrt{g_x} \sqrt{g_y} \nabla_\mu \nabla_\nu K^{\mu\nu}(x, y) \frac{1}{g_\ell^{(0)}} \sum_m Y_{\ell m}(x) Y_{\ell m}^*(y), \quad (2.139)$$

where we sum over m and divide by the degeneracy $g_\ell^{(0)}$ ¹⁶. We use that¹⁷

$$\frac{1}{g_\ell^{(0)}} \sum_m Y_{\ell m}(x) Y_{\ell m}^*(y) = \frac{1}{\text{vol}(S^d)} \frac{C_\ell^{(d-1)/2}(1 - s^2(x, y)/2R^2)}{C_\ell^{(d-1)/2}(1)}, \quad (2.140)$$

where $C_\ell^{(d-1)/2}(x)$ is the Gegenbauer polynomial. Now due to rotational invariance we may choose $y = 0$ and find¹⁸

$$\nabla_\mu \nabla_\nu K^{\mu\nu}(x, 0) = -\frac{2C_J}{(4R^2)^{\Delta+1}} (\Delta - d + 1)(2 - d + 2\Delta + x^2 d) \frac{(1 + x^2)^\Delta}{(x^2)^{\Delta+1}}. \quad (2.141)$$

Therefore we obtain

$$\begin{aligned} \lambda_\ell^{(0)} &= -\frac{C_J(\Delta - d + 1)}{2^\Delta R^{2\Delta-d} \ell(d + \ell - 1)} \frac{\text{vol}(S^{d-1})}{C_\ell^{(d-1)/2}(1)} \\ &\quad \times \int_{-1}^1 dz (1+z)^{\frac{d-2}{2}} (1-z)^{\frac{d}{2}-\Delta-2} (2 + 2\Delta - d - (1-z)(1 + \Delta - d)) C_\ell^{(d-1)/2}(z), \end{aligned} \quad (2.142)$$

¹⁵We assume that $\nabla^2 Y_{\ell m} = -\ell(\ell+d-1)R^{-2}Y_{\ell m}$ and $\int d^d x \sqrt{g_x} Y_{\ell m}(x) Y_{\ell' m'}^*(x) = \delta_{\ell\ell'} \delta_{mm'}$.

¹⁶We are allowed to do this sum because on the l.h.s $\lambda_\ell^{(0)}$ doesn't depend on m .

¹⁷Notice that the $Y_{\ell m}(x)$ harmonics have a factor of $R^{-d/2}$, which is consistent with the formula (2.140) because $\text{vol}(S^d) = 2\pi^{\frac{d+1}{2}} R^d / \Gamma(\frac{d+1}{2})$ and $Y_{\mu, \ell m}^{(s)}$ have a factor of $R^{-d/2+1}$.

¹⁸Notice that we can not just take $y = 0$ in (2.139) without having the sum over m .

where we have changed the variable $x^2 = (1 - z)/(1 + z)$. Calculating the integral we get¹⁹

$$\lambda_\ell^{(0)} = -C_J \frac{2^{d-2\Delta} \pi^{d/2} (\Delta - 1) \Gamma\left(\frac{d}{2} - \Delta\right)}{\Gamma(\Delta + 1)} \frac{d - \Delta - 1}{\Delta - 1} \frac{\Gamma(l + \Delta)}{\Gamma(d + l - \Delta)} \frac{1}{R^{2\Delta - d}}. \quad (2.143)$$

The eigenvalues $\lambda_\ell^{(1)}$ for transverse spherical harmonics can be easily found for $\Delta = d - 1$, using the embedding formalism. In this case the kernel has the form [60]

$$K_{ab}(\eta_1, \eta_2) = -C_J \frac{R^{-2}}{(2d - 4)(d - 1)} P_{ac} \frac{\delta_{cb}}{|\eta_1 - \eta_2|^{2d-4}}, \quad (2.144)$$

where the operator $P_{ac} \equiv \frac{1}{2} L^2 \delta_{ac} + L_{ad} L_{dc} - (d - 1) L_{ac}$ acts on η_1 , and $L_{ab} \equiv \eta_a \frac{\partial}{\partial \eta_b} - \eta_b \frac{\partial}{\partial \eta_a}$ and $L^2 \equiv L_{ab} L_{ab}$. Now using the decomposition [60]

$$\frac{\delta_{cb}}{|\eta_1 - \eta_2|^{2d-4}} = \sum_{l,m} \sum_s (2R)^{4-d} \pi^{\frac{d}{2}} \frac{\Gamma(2 - \frac{d}{2}) \Gamma(\ell + d - 2)}{\Gamma(d - 2) \Gamma(\ell + 2)} Y_{c,\ell m}^{(s)}(\eta_1) Y_{b,\ell m}^{(s)}(\eta_2) \quad (2.145)$$

and the property of the operator P_{ab} : $P_{ab} Y_{b,\ell m}^{(s)} = 0$ for $s \neq 1$ and $P_{ab} Y_{b,\ell m}^{(1)} = -(\ell + 1)(\ell + d - 2) Y_{a,\ell m}^{(1)}$, we find

$$K_{ab}(\eta_1, \eta_2) = \sum_{\ell,m} C_J \frac{(2R)^{4-d} \pi^{\frac{d}{2}} (\ell + 1)(\ell + d - 2) \Gamma(2 - \frac{d}{2}) \Gamma(\ell + d - 2)}{R^2 (2d - 4)(d - 1) \Gamma(d - 2) \Gamma(\ell + 2)} Y_{a,\ell m}^{(1)}(\eta_1) Y_{b,\ell m}^{(1)}(\eta_2), \quad (2.146)$$

therefore for $\lambda_\ell^{(1)}$ we get

$$\lambda_\ell^{(1)} = C_J \frac{\pi^{\frac{d}{2}} \Gamma(2 - \frac{d}{2}) \Gamma(\ell + d - 1)}{2^{d-3} \Gamma(d) \Gamma(\ell + 1)} \frac{1}{R^{d-2}}, \quad (2.147)$$

¹⁹Here we used the integral $\int_{-1}^1 dz (1 + z)^{\nu - \frac{1}{2}} (1 - z)^\beta C_\ell^\nu(z) = (-1)^\ell \frac{2^{\beta + \nu + \frac{1}{2}} \Gamma(\beta + 1) \Gamma(\nu + \frac{1}{2}) \Gamma(2\nu + 1) \Gamma(\beta - \nu + \frac{3}{2})}{\ell! \Gamma(2\nu) \Gamma(\beta - \nu - \ell + \frac{3}{2}) \Gamma(\beta + \nu + \ell + \frac{3}{2})}$, which can be found with the help of [118] 7.311.3 and the relation $C_\ell^\nu(z) = (-1)^\ell C_\ell^\nu(-z)$. Also we used that $C_\ell^{\frac{d-1}{2}}(1) = \frac{(\ell + d - 2)!}{\ell! (d - 2)!}$.

which coincides with (2.54) for $\Delta = d - 1$.

2.13 Appendix B. Zonal spherical harmonics in continuous dimension

In this appendix we give more detailed derivation of the formula (2.54). As we already saw in the case of the conformal QED on the sphere in some physical computations one encounters a problem of decomposition of some kernel on the sphere S^d into a sum over tensor spherical harmonics [119, 83, 120]. In general it is quite difficult task to perform analytically. But in many cases the kernel in question has rotational invariance, which drastically simplifies the calculations.

We consider a decomposition of some general kernel

$$K_{\mu_1 \dots \mu_r, \nu_1 \dots \nu_r}(n, n') = \sum_{\ell, m, s} \lambda_\ell^{(s)} Y_{\mu_1 \dots \mu_r, \ell m}^{(s)}(n) Y_{\nu_1, \dots, \nu_r, \ell m}^{(s)*}(n'), \quad (2.148)$$

where n, n' are vectors on the sphere with unit radius, and $Y_{\mu_1 \dots \mu_r, \ell m}^{(s)}$ are tensor spherical harmonics of type s . The eigenvalues $\lambda_\ell^{(s)}$ depend only on ℓ due to rotational invariance of K ²⁰ and have degeneracy $g_\ell^{(s)}$.

Since all tensor spherical harmonics orthonormal to each other²¹

$$\int d^d n Y_{\mu_1 \dots \mu_r, \ell m}^{(s)}(n) Y_{\ell' m'}^{\mu_1 \dots \mu_r, (s')*}(n) = \delta_{\ell \ell'} \delta_{m m'} \delta_{s s'} \quad (2.149)$$

we find for the eigenvalues

$$\lambda_\ell^{(s)} = \int d^d n d^d n' K^{\mu_1 \dots \mu_r, \nu_1 \dots \nu_r}(n, n') Y_{\mu_1 \dots \mu_r, \ell m}^{(s)}(n) Y_{\nu_1, \dots, \nu_r, \ell m}^{(s)*}(n'). \quad (2.150)$$

²⁰This means that $K_{\mu_1 \dots \mu_r, \nu_1 \dots \nu_r}$ depends only on $z = n \cdot n'$ or equivalently $K_{\mu_1 \dots \mu_r, \nu_1 \dots \nu_r}(On, On') = O_{\mu_1}^{\alpha_1} \dots O_{\mu_r}^{\alpha_r} O_{\nu_1}^{\beta_1} \dots O_{\nu_r}^{\beta_r} K_{\alpha_1 \dots \alpha_r; \beta_1 \dots \beta_r}(n, n')$, where O is orthogonal matrix

²¹Here the summation over indices μ_1, \dots, μ_r is assumed. The indices are raised and lowered by metric tensor $g_{\mu\nu}$ on the sphere.

We can sum over m in the r.h.s of (2.150) and divide by the degeneracy of m : $g_\ell^{(s)}$, so we get

$$\lambda_\ell^{(s)} = \frac{1}{g_\ell^{(s)}} \int d^d n d^d n' K^{\mu_1 \dots \mu_r, \nu_1 \dots \nu_r}(n, n') Z_{\mu_1 \dots \mu_r, \nu_1 \dots \nu_r, \ell}^{(s)}(n, n'), \quad (2.151)$$

where we have introduced tensor zonal harmonics of spin s :

$$Z_{\mu_1 \dots \mu_r, \nu_1 \dots \nu_r, \ell}^{(s)}(n, n') \equiv \sum_m Y_{\mu_1 \dots \mu_r, \ell m}^{(s)}(n) Y_{\nu_1, \dots, \nu_r, \ell m}^{(s)*}(n'). \quad (2.152)$$

The important property of $Z(n, n')$ is that it is rotational invariant and thus depends only on $z = n \cdot n'$. Therefore in the integral (2.151) we may put n' to the north pole and integrate only over the angle between n and n' [83]:

$$\lambda_\ell^{(s)} = \frac{\text{vol}(S^d) \text{vol}(S^{d-1})}{g_\ell^{(s)}} \int_{-1}^1 dz (1 - z^2)^{\frac{d}{2}-1} K^{\mu_1 \dots \mu_r, \nu_1 \dots \nu_r}(z) Z_{\mu_1 \dots \mu_r, \nu_1 \dots \nu_r, \ell}^{(s)}(z). \quad (2.153)$$

Also we notice that zonal harmonics obey completeness condition

$$\sum_s \sum_\ell Z_{\mu_1 \dots \mu_r, \nu_1 \dots \nu_r, \ell}^{(s)}(n, n') = g_{\mu_1 \nu_1} \dots g_{\mu_r \nu_r} \delta(n - n'). \quad (2.154)$$

In the next subsections we find the explicit expressions for the tensor zonal spherical harmonics of rank zero and one.

2.13.1 Rank 0 zonal harmonics

In scalar case the zonal harmonics are known

$$Z_\ell(n, n') = \sum_m Y_{\ell m}(n) Y_{\ell m}^*(n') \equiv \frac{g_\ell}{\text{vol}(S^d)} \frac{C_\ell^{(d-1)/2}(n \cdot n')}{C_\ell^{(d-1)/2}(1)}, \quad (2.155)$$

where $C_\ell^{(d-1)/2}(z)$ is the Gegenbauer polynomial and g_ℓ is degeneracy of m in scalar case.

2.13.2 Rank 1 zonal harmonics

In vector case we have two types of the vector spherical harmonics. One type is longitudinal harmonics, for which we know the explicit form in terms of the scalar harmonics [121]

$$Y_{\mu,\ell m}^{(0)} = \frac{\nabla_\mu Y_{\ell m}}{\sqrt{\ell(\ell+d-1)}}. \quad (2.156)$$

The other type is the transverse vector harmonics $Y_{\mu,\ell m}^{(1)}$, $\nabla^\mu Y_{\mu,\ell m}^{(1)} = 0$. The explicit form for the transverse vector harmonics is not known. Using that $-\nabla^2 Y_{\ell m} = \ell(\ell+d-1)Y_{\ell m}$ we can find

$$Z_{\mu,\nu',\ell}^{(0)}(n, n') = \frac{1}{\ell(\ell+d-1)} \sum_m \nabla_\mu Y_{\ell m}(n) \nabla_{\nu'} Y_{\ell m}^*(n') = -\nabla_\mu \nabla_{\nu'} \frac{1}{\nabla^2} Z_\ell(n, n'). \quad (2.157)$$

Let us now try to find $Z_{\mu,\nu,\ell}^{(1)}(n, n')$. We know that it depends only on $z = n \cdot n'$, and it must obey the equation

$$-\nabla^2 Z_{\mu,\nu,\ell}^{(1)}(n, n') = (\ell(\ell+d-1) - 1) Z_{\mu,\nu,\ell}^{(1)}(n, n'). \quad (2.158)$$

and the same for $-\nabla'^2$ (but it is automatically fulfilled, because everything depends only on the relative angle between n and n'). Also we must have $\nabla^\mu Z_{\mu,\nu,\ell}^{(1)}(n, n') = \nabla_{\nu'} Z_{\mu,\nu,\ell}^{(1)}(n, n') = 0$.

2.13.3 Computations in stereographical coordinates

We consider the sphere of unit radius. In the stereographical coordinates the metric on the sphere is

$$g_{\mu\nu} = \frac{4\delta_{\mu\nu}}{(1+x^2)^2}, \quad g^{\mu\nu} = \frac{(1+x^2)^2}{4}\delta_{\mu\nu}. \quad (2.159)$$

One can find the Cristoffel symbols

$$\Gamma_{\mu\nu}^\lambda = -\frac{2}{(1+x^2)}(x_\mu\delta_{\lambda\nu} + x_\nu\delta_{\lambda\mu} - x_\lambda\delta_{\mu\nu}), \quad (2.160)$$

therefore

$$\Gamma_{\mu\nu}^\nu = -\frac{2dx_\mu}{(1+x^2)}, \quad \Gamma_{\mu\mu}^\lambda = \frac{2(d-2)}{1+x^2}x_\lambda. \quad (2.161)$$

The Riemann and Ricci tensors are given by the expressions

$$R_{\mu\nu\lambda\rho} = g_{\mu\lambda}g_{\nu\rho} - g_{\nu\lambda}g_{\mu\rho}, \quad R_{\mu\nu} = (d-1)g_{\mu\nu} \quad (2.162)$$

and one can find for the Laplacian of the scalar

$$\nabla^2\phi = \frac{(1+x^2)^2}{4}\left(\partial_\mu^2 - \frac{2(d-2)}{1+x^2}x_\mu\partial_\mu\right)\phi. \quad (2.163)$$

We denote the chordal distance by $s(x, y)$:

$$u = s(x, y)^2 = \frac{4(x-y)^2}{(1+x^2)(1+y^2)}, \quad (2.164)$$

where $(x-y)^2 = \delta_{\mu\nu}(x-y)_\mu(x-y)_\nu$. Then we have for $z = n \cdot n'$:

$$z = 1 - \frac{1}{2}s(x, y)^2. \quad (2.165)$$

We will use the following formulas²²

$$\begin{aligned}
\nabla^2 z &= -dz, \\
(\partial^\mu z)(\partial_\mu z) &= 1 - z^2, \\
\nabla_\mu \partial_\nu z &= -g_{\mu\nu} z, \\
(\partial^\mu z)(\nabla_\mu \partial_\nu \partial_{\nu'} z) &= -(\partial_\nu z)(\partial_{\nu'} z), \\
(\partial^\mu z)(\partial_\mu \partial_{\nu'} z) &= -z \partial_{\nu'} z, \\
(\partial^\mu \partial_{\mu'} z)(\partial_\mu \partial_{\nu'} z) &= g_{\mu'\nu'} - (\partial_{\mu'} z)(\partial_{\nu'} z), \\
\nabla_\mu \partial_\nu \partial_{\nu'} z &= -g_{\mu\nu} \partial_{\nu'} z.
\end{aligned} \tag{2.166}$$

And the additional identity

$$z_{\mu\mu'} z^{\mu\nu\nu'} = -z_{\nu\mu'} z_{\nu'}, \tag{2.167}$$

where $z_{\mu_1 \dots \mu_n \nu'_1 \dots \nu'_n} \equiv \nabla_{\mu_1} \dots \nabla_{\mu_n} \nabla_{\nu'_1} \dots \nabla_{\nu'_n} z$.

For the longitudinal zonal harmonics we find

$$Z_{\mu\nu',\ell}^{(0)}(u) = -\frac{1}{\ell(\ell+d-1)} \left(\partial_\mu z \partial_{\nu'} z Z_\ell''(z) + \partial_\mu \partial_{\nu'} z Z_\ell'(z) \right). \tag{2.168}$$

Using that

$$Z_\ell(u) = \frac{g_\ell^{(0)}}{\text{vol}(S^d)} \frac{C_\ell^{(d-1)/2}(z)}{C_\ell^{(d-1)/2}(1)}, \tag{2.169}$$

²²One has $\partial_\mu u = 2u \left(\frac{(x-y)_\mu}{(x-y)^2} - \frac{x_\mu}{1+x^2} \right)$, $\partial_{\nu'} u = 2u \left(\frac{(y-x)_{\nu'}}{(x-y)^2} - \frac{y_{\nu'}}{1+y^2} \right)$

and also that $\partial_z C_\ell^\alpha(z) = 2\alpha C_{\ell-1}^{\alpha+1}(z)$ we may write²³

$$Z_{\mu\nu',\ell}^{(0)}(z) = \frac{g_\ell^{(0)}}{dC_{\ell-1}^{(d+1)/2}(1)\text{vol}(S^d)} \left(\partial_\mu z \partial_{\nu'} z (d+1) C_{\ell-2}^{(d+3)/2}(z) + \partial_\mu \partial_{\nu'} z C_{\ell-1}^{(d+1)/2}(z) \right). \quad (2.170)$$

Now to find $Z_{\mu\nu',\ell}^{(1)}(z)$ we adopt the following ansatz

$$Z_{\mu\nu',\ell}^{(1)}(z) = \partial_\mu z \partial_{\nu'} z A_\ell(z) + \partial_\mu \partial_{\nu'} z B_\ell(z). \quad (2.171)$$

We can find functions A and B by solving the equations for $Z_{\mu\nu',\ell}^{(1)}(u)$:

$$\begin{aligned} \nabla^2 Z_{\mu\nu',\ell}^{(1)}(z) &= -(\ell(\ell+d-1) - 1) Z_{\mu\nu',\ell}^{(1)}(z), \\ \nabla^\mu Z_{\mu\nu',\ell}^{(1)}(z) &= 0. \end{aligned} \quad (2.172)$$

We find

$$\begin{aligned} \nabla^2(\partial_\mu \partial_{\nu'} z B_\ell) &= ((1-z^2)B_\ell'' - dzB_\ell' - B_\ell) \partial_\mu \partial_{\nu'} z - 2\partial_\mu z \partial_{\nu'} z B_\ell', \\ \nabla^\mu(\partial_\mu \partial_{\nu'} z B_\ell) &= -\partial_{\nu'} z (zB_\ell' + dB_\ell) \end{aligned} \quad (2.173)$$

and also

$$\begin{aligned} \nabla^2(\partial_\mu z \partial_{\nu'} z A_\ell) &= ((1-z^2)A_\ell'' - (d+4)zA_\ell' - (d+1)A_\ell) \partial_\mu z \partial_{\nu'} z - 2z\partial_\mu \partial_{\nu'} z A_\ell, \\ \nabla^\mu(\partial_\mu z \partial_{\nu'} z A_\ell) &= \partial_{\nu'} z ((1-z^2)A_\ell' - (d+1)zA_\ell). \end{aligned} \quad (2.174)$$

²³We use that $C_\ell^{(d-1)/2}(1) = \frac{(\ell+d-2)!}{\ell!(d-2)!}$

So we obtain

$$\begin{aligned}
(1 - z^2)A'_\ell - (d + 1)zA_\ell - zB'_\ell - dB_\ell &= 0, \\
(1 - z^2)A''_\ell - (d + 4)zA'_\ell - (d + 1)A_\ell - 2B'_\ell &= -(\ell(\ell + d - 1) - 1)A_\ell, \\
(1 - z^2)B''_\ell - dzB'_\ell - B_\ell - 2zA_\ell &= -(\ell(\ell + d - 1) - 1)B_\ell.
\end{aligned} \tag{2.175}$$

The explicit result in $d = 3$ helps to find the exact solution of these equations

$$\begin{aligned}
A_\ell &= c((d + 1)zC_{\ell-2}^{(d+3)/2}(z) + (d - 1)C_{\ell-1}^{(d+1)/2}(z)), \\
B_\ell &= c((d + 1)(1 - z^2)C_{\ell-2}^{(d+3)/2}(z) - (d - 1)zC_{\ell-1}^{(d+1)/2}(z))
\end{aligned} \tag{2.176}$$

and $Z_{\mu\nu',\ell}^{(1)}(z) = \partial_\mu z \partial_{\nu'} z A_\ell(z) + \partial_\mu \partial_{\nu'} z B_\ell(z)$. We can find normalization constant c by considering zonal harmonics for $n = n'$, so in general we have

$$\int d^d n Z_{\mu_1 \dots \mu_r, \ell}^{(s), \mu_1 \dots \mu_r}(1) = \sum_m \int d^d n Y_{\mu_1 \dots \mu_r, \ell m}^{(s)}(n) Y_{\ell m}^{\mu_1 \dots \mu_r, (s)*}(n) = g_\ell^{(s)}, \tag{2.177}$$

therefore

$$Z_{\mu_1 \dots \mu_r, \ell}^{(s), \mu_1 \dots \mu_r}(1) = \frac{g_\ell^{(s)}}{\text{vol}(S^d)}. \tag{2.178}$$

In case of rank 1 we have

$$Z_{\mu, \ell}^{(1), \mu}(1) = dB_\ell(1) = \frac{g_\ell^{(1)}}{\text{vol}(S^d)} \tag{2.179}$$

where we used that $g^{\mu\nu'} \partial_\mu z \partial_{\nu'} z|_{z=1} = 0$ and $g^{\mu\nu'} \partial_\mu \partial_{\nu'} z|_{z=1} = d$. Thus we find

$$c = -\frac{g_\ell^{(1)}}{d(d - 1)C_{\ell-1}^{(d+1)/2}(1)\text{vol}(S^d)}. \tag{2.180}$$

Therefore finally we have

$$Z_{\mu\nu',\ell}^{(1)}(z) = -\frac{g_\ell^{(1)}}{d(d-1)C_{\ell-1}^{(d+1)/2}(1)\text{vol}(S^d)} \left(\partial_\mu z \partial_{\nu'} z ((d+1)z C_{\ell-2}^{(d+3)/2}(z) + (d-1)C_{\ell-1}^{(d+1)/2}(z)) \right. \\ \left. + \partial_\mu \partial_{\nu'} z ((d+1)(1-z^2)C_{\ell-2}^{(d+3)/2}(z) - (d-1)z C_{\ell-1}^{(d+1)/2}(z)) \right). \quad (2.181)$$

2.13.4 Rank 1 kernel decomposition

We have the following kernel in stereographical coordinates

$$K_{\mu\nu'}(x, y) = -C_J \frac{4}{(1+x^2)(1+y^2)} \frac{(\delta_{\mu\nu'} - 2\frac{(x-y)_\mu(x-y)_{\nu'}}{|x-y|^2})}{s(x, y)^{2\Delta}}, \quad (2.182)$$

We put $y = 0$ and get

$$K^{\mu\nu'}(x, 0) = -\frac{C_J(1+x^2)^{\Delta+1}}{4^{\Delta+1}(x^2)^\Delta} (\delta_{\mu\nu'} - 2\frac{x_\mu x_{\nu'}}{x^2}). \quad (2.183)$$

Then one can find at $y = 0$:

$$\partial_\mu z = -\frac{4x_\mu}{(1+x^2)^2}, \quad \partial_{\nu'} z = \frac{4x_{\nu'}}{1+x^2}, \\ \partial_\mu z \partial_{\nu'} z = -\frac{4^2 x_\mu x_{\nu'}}{(1+x^2)^3}, \quad \partial_\mu \partial_{\nu'} z = \frac{4}{1+x^2} (\delta_{\mu\nu'} - \frac{2x_\mu x_{\nu'}}{1+x^2}). \quad (2.184)$$

Therefore we obtain

$$K^{\mu\nu'}(x, 0) \partial_\mu z \partial_{\nu'} z = -C_J 2^{-\Delta} (1-z)^{-\Delta+1} (1+z), \\ K^{\mu\nu'}(x, 0) \partial_\mu \partial_{\nu'} z = C_J 2^{-\Delta} (1-z)^{-\Delta} (1+z-d), \quad (2.185)$$

where we used that $x^2 = (1-z)/(1+z)$. Then we have

$$\lambda_\ell^{(s)} = \frac{\text{vol}(S^d)\text{vol}(S^{d-1})}{g_\ell^{(s)}} \int_{-1}^1 dz (1-z^2)^{\frac{d}{2}-1} K^{\mu,\nu'}(z) Z_{\mu,\nu',\ell}^{(s)}(z), \quad (2.186)$$

where [122, 78, 123]

$$g_\ell^{(0)} = \frac{(2\ell + d - 1)(\ell + d - 2)!}{\ell!(d - 1)!}, \quad g_\ell^{(1)} = \frac{\ell(\ell + d - 1)(2\ell + d - 1)(\ell + d - 3)!}{(d - 2)!(\ell + 1)!}. \quad (2.187)$$

Using expressions (2.170) and (2.181) we find

$$\begin{aligned} \lambda_\ell^{(0)} &= \frac{C_J 2^{-\Delta} \text{vol}(S^{d-1})}{d C_{\ell-1}^{(d+1)/2}(1)} (1 + \Delta - d) \int_{-1}^1 dz (1+z)^{\frac{d}{2}} (1-z)^{\frac{d}{2}-\Delta-1} C_{\ell-1}^{(d+1)/2}(z), \\ \lambda_\ell^{(1)} &= -\frac{C_J 2^{-\Delta} \text{vol}(S^{d-1})}{d(d-1) C_{\ell-1}^{(d+1)/2}(1)} (d-1)(\Delta-1) \int_{-1}^1 dz (1+z)^{\frac{d}{2}} (1-z)^{\frac{d}{2}-\Delta-1} C_{\ell-1}^{(d+1)/2}(z). \end{aligned} \quad (2.188)$$

Calculating the integrals we finally get²⁴

$$\begin{aligned} \lambda_\ell^{(0)} &= -C_J \frac{2^{d-2\Delta} \pi^{d/2} (\Delta-1) \Gamma(\frac{d}{2}-\Delta)}{\Gamma(\Delta+1)} \frac{\Gamma(\ell+\Delta)}{\Gamma(\ell+d-\Delta)} \frac{d-1-\Delta}{\Delta-1}, \\ \lambda_\ell^{(1)} &= -C_J \frac{2^{d-2\Delta} \pi^{d/2} (\Delta-1) \Gamma(\frac{d}{2}-\Delta)}{\Gamma(\Delta+1)} \frac{\Gamma(\ell+\Delta)}{\Gamma(\ell+d-\Delta)}. \end{aligned} \quad (2.189)$$

which is in agreement with (2.54).

2.14 Appendix C. Calculation of G_2 and G_4

Using the propagators and vertex in (2.80), (2.79), (2.78) we find for the two-point function

$$G_2 = -N_f \int d^d \eta_1 d^d \eta_2 \text{Tr}(Q_{ab}(\eta_1) \alpha_b S(\eta_1, \eta_2) Q_{cd}(\eta_2) \alpha_d S(\eta_2, \eta_1)) D_{ac}(\eta_1, \eta_2). \quad (2.190)$$

²⁴Here we used the integral $\int_{-1}^1 dz (1+z)^{\nu-\frac{1}{2}} (1-z)^\beta C_\ell^\nu(z) = (-1)^\ell \frac{2^{\beta+\nu+\frac{1}{2}} \Gamma(\beta+1) \Gamma(\nu+\frac{1}{2}) \Gamma(2\nu+1) \Gamma(\beta-\nu+\frac{3}{2})}{\ell! \Gamma(2\nu) \Gamma(\beta-\nu-\ell+\frac{3}{2}) \Gamma(\beta+\nu+\ell+\frac{3}{2})}$, which can be found with the help of [118] 7.311.3 and the relation $C_\ell^\nu(z) = (-1)^\ell C_\ell^\nu(-z)$.

After calculation we obtain

$$G_2 = -\frac{(N_f \text{Tr} \mathbf{1}) \Gamma(\frac{d}{2}) \Gamma(d-2)}{2^{d+2} \pi^{\frac{3d}{2}} R^{d-2}} \int d^d \eta_1 d^d \eta_2 \frac{(d-2 + \frac{1}{2R^2}(\eta_1 - \eta_2)^2)}{|\eta_1 - \eta_2|^{2d-2}} {}_2F_1(1, d-2, \frac{d}{2}, 1 - \frac{(\eta_1 - \eta_2)^2}{4R^2}). \quad (2.191)$$

Due to rotational invariance we can put η_2 to the north pole of the sphere and get in stereographic coordinates

$$G_2 = -\frac{(N_f \text{Tr} \mathbf{1}) R^{4-d} \Gamma(d-2)}{(16\pi)^{\frac{d-1}{2}} \Gamma(\frac{d+1}{2})} \int_0^\infty \frac{dx}{(1+x^2)x^{d-1}} \left(d - \frac{2}{1+x^2} \right) {}_2F_1(1, d-2, \frac{d}{2}, \frac{1}{1+x^2}). \quad (2.192)$$

Now introducing the variable $z = 1/(1+x^2)$ we find

$$G_2 = -\frac{(N_f \text{Tr} \mathbf{1}) R^{4-d} \Gamma(d-2)}{2(16\pi)^{\frac{d-1}{2}} \Gamma(\frac{d+1}{2})} \int_0^1 dz z^{\frac{d}{2}-1} (1-z)^{-\frac{d}{2}} (d-2z) {}_2F_1(1, d-2, \frac{d}{2}, z). \quad (2.193)$$

The integral can be calculated exactly and we obtain²⁵

$$G_2 = -\frac{(N_f \text{Tr} \mathbf{1}) R^{4-d} \Gamma(d-1)}{(d-3) 4^{\frac{d+2}{2}} (4\pi)^{\frac{d-3}{2}} \sin(\frac{\pi d}{2}) \Gamma(\frac{d+1}{2})}. \quad (2.194)$$

²⁵ G_2 was also computed in [62, 63] by different methods.

After doing combinatorics for G_4 we find that it consists of the sum of 34 integrals of the form

$$\begin{aligned}
I_4(a_1, \dots, a_6) &= \\
&= \left(\frac{\Gamma(\frac{d}{2})}{2\pi^{\frac{d}{2}}} \right)^4 \left(\frac{R^{2-d}\Gamma(d-2)}{(4\pi)^{\frac{d}{2}}\Gamma(\frac{d}{2})} \right)^2 \\
&\quad \times \int \prod_{i=1}^4 d^d \eta_i \frac{{}_2F_1(1, d-2, \frac{d}{2}; 1 - \frac{s(\eta_1, \eta_2)^2}{4R^2}) {}_2F_1(1, d-2, \frac{d}{2}; 1 - \frac{s(\eta_3, \eta_4)^2}{4R^2})}{s(\eta_1, \eta_2)^{2a_1} s(\eta_2, \eta_3)^{2a_2} s(\eta_3, \eta_4)^{2a_3} s(\eta_1, \eta_4)^{2a_4} s(\eta_1, \eta_3)^{2a_5} s(\eta_2, \eta_4)^{2a_6}},
\end{aligned} \tag{2.195}$$

where we used the exact form of the photon propagator (2.79). The integral I_4 is represented diagrammatically in figure 2.13.

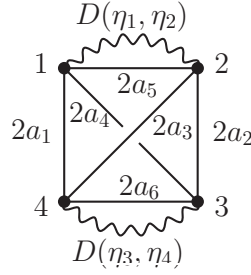


Figure 2.13: The diagrammatic representation for the integral $I_4(a_1, \dots, a_6)$.

The next step is to write the integral I_4 in the Mellin-Barnes (MB) representation and then use the Mathematica program [124, 125] to find I_4 as a series in ϵ [126]. For the photon propagator we use the Mellin-Barnes representation²⁶

$$\begin{aligned}
D(\eta_1, \eta_2) &= - \frac{\sin(\frac{\pi d}{2})}{2^d \pi^{\frac{d}{2}+1} R^{d-2}} \frac{1}{2\pi i} \int_{-i\infty}^{+i\infty} dz \Gamma(-z) \Gamma(1+z) \Gamma(d-2+z) \\
&\quad \times \Gamma(1 - \frac{d}{2} - z) \left(\frac{s(\eta_1, \eta_2)^2}{4R^2} \right)^z.
\end{aligned} \tag{2.196}$$

²⁶We use the formula ${}_2F_1(a, b, c; x) = \frac{\Gamma(c)}{\Gamma(a)\Gamma(b)\Gamma(c-a)\Gamma(c-b)} \frac{1}{2\pi i} \int_{-i\infty}^{+i\infty} dz \Gamma(-z) \Gamma(a+z) \Gamma(b+z) \Gamma(c-a-b-z) (1-x)^z$.

Then using methods similar as discussed in [54] one can write the general MB form for the integral

$$\begin{aligned}
I_4(a_1, \dots, a_6) &= \frac{\sin^2(\frac{\pi d}{2})\Gamma(\frac{d}{2})^4}{2^{d+7}\pi^{\frac{1}{2}(5d+3)}\Gamma(\frac{d+1}{2})} (2R)^{2d+4-2\sum_{i=1}^6 a_i} \frac{1}{(2\pi i)^5} \int \prod_{i=1}^5 dz_i \Gamma(-z_1)\Gamma(-z_2)\Gamma(z_1+1) \\
&\quad \times \Gamma(z_2+1)\Gamma(d-2+z_1)\Gamma(1-\frac{d}{2}-z_1)\Gamma(d-2+z_2)\Gamma(1-\frac{d}{2}-z_2) \\
&\quad \times \Gamma_2(d-a_{145}+z_1, a_1, a_5-z_1|z_3, z_4, z_5) \\
&\quad \times \Gamma_0(d-a_{235}+z_1-z_4, d-a_{136}+z_2-z_3, a_3-z_5), \tag{2.197}
\end{aligned}$$

where $a_{mnk\dots} \equiv a_m + a_n + a_k + \dots$ and Γ -blocks are

$$\begin{aligned}
\Gamma_0(a_1, a_2, b) &= \frac{\pi^d}{\Gamma(\frac{d}{2})} \frac{\Gamma(\frac{d}{2}-b)\Gamma(a_1+b-\frac{d}{2})\Gamma(a_2+b-\frac{d}{2})\Gamma(a_1+a_2+b-d)}{\Gamma(a_1)\Gamma(a_2)\Gamma(a_1+a_2+2b-d)}, \\
\Gamma_2(a, b_1, b_2|z_1, z_2, z_3) &= \frac{\pi^{d/2} \prod_{i=1}^3 \Gamma(-z_i)\Gamma(a+b_1+b_2-\frac{d}{2}+\sum_{i=1}^3 z_i)}{\Gamma(a)\Gamma(b_1)\Gamma(b_2)\Gamma(d-a-b_1-b_2)} \Gamma(b_1+z_1+z_3) \\
&\quad \times \Gamma(b_2+z_2+z_3)\Gamma(d-a-2b_1-2b_2-z_1-z_2-2z_3). \tag{2.198}
\end{aligned}$$

For some values of a_1, \dots, a_6 the MB representation (2.197) is divergent or exactly zero for any d (due to the term $\Gamma(0)$). To handle this problem we used an additional regulator δ , so we were consistently calculating the integrals

$$I_4^{\text{reg}}(a_1, \dots, a_6) = I_4(a_1 + \delta, \dots, a_6 + \delta). \tag{2.199}$$

Each integral out of 34 in G_4 depends on δ and ϵ . But the G_4 itself is free of δ and depends only on ϵ as it should.

In general MB approach gives a result in terms of a series in ϵ and δ and each coefficient of this series is a sum of convergent Mellin-Barnes integrals, which are independent of ϵ and δ and can be calculated numerically. The numerical result is usually equal to some exact combinations of constants like $\pi^4, \zeta(3)$, e.t.c. To get an

exact answer we used integer relation search algorithm PSLQ [127]. The final result reads

$$\begin{aligned}
G_4 = & \frac{N_f^2}{6\pi^4\epsilon^2} + \frac{N_f(8N_f(5 + 3(\log(4\pi R^2) + \gamma)) - 18)}{12^2\pi^4\epsilon} \\
& + \frac{1}{12^3\pi^4} \left(16N_f^2(5 + 3(\log(4\pi R^2) + \gamma))^2 \right. \\
& \left. - 72N_f(5 + 3(\log(4\pi R^2) + \gamma)) + 4(77 + 9\pi^2)N_f^2 + 9N_f(72\zeta(3) - 47) \right).
\end{aligned} \tag{2.200}$$

Note that in this calculation of G_4 we have used $d = 4 - \epsilon$ and $N = N_f \text{tr} \mathbf{1} = 4N_f$.

2.15 Appendix D. Calculation of Z_T

In this appendix we present the computation of the Z_T factor for the stress-energy tensor in the theory of Critical QED. As we show below, a non-trivial Z_T is required for the Ward identity to hold. We define the ‘‘renormalized’’ stress-energy tensor $T_{\mu\nu}^{\text{ren}}$ by

$$T_{\mu\nu}^{\text{ren}}(x) = Z_T T_{\mu\nu}(x), \tag{2.201}$$

where $Z_T = 1 + (Z_{T1}/\Delta + Z'_{T1})/N + \mathcal{O}(1/N^2)$, and $T_{\mu\nu}$ is the ‘‘bare’’ stress-tensor. To find Z_T we will use the three-point function $\langle T_{\mu\nu}^{\text{ren}}(x_1) O_m^{\text{ren}}(x_2) O_m^{\text{ren}}(x_3) \rangle$, where $O_m^{\text{ren}} = Z_{O_m} O_m$ is the electron mass operator, Z_{O_m} is its renormalization constant and the bare operator is

$$O_m = \bar{\psi}\psi. \tag{2.202}$$

This three point function is gauge invariant. So using conformal invariance and conservation of the stress-tensor, one has the general expression for the three-point

function

$$\begin{aligned} \langle T_{\mu\nu}^{\text{ren}}(x_1)O_m^{\text{ren}}(x_2)O_m^{\text{ren}}(x_3) \rangle &= \\ &= \frac{-C_{TO_mO_m}}{(x_{12}^2x_{13}^2)^{\frac{d}{2}-1}(x_{23}^2)^{\Delta_{O_m}-\frac{d}{2}+1}} \left((X_{23})_\mu(X_{23})_\nu - \frac{1}{d}\delta_{\mu\nu}(X_{23})^2 \right), \end{aligned} \quad (2.203)$$

where

$$(X_{23})_\nu = \frac{(x_{12})_\nu}{x_{12}^2} - \frac{(x_{13})_\nu}{x_{13}^2}. \quad (2.204)$$

The conformal Ward identity gives

$$C_{TO_mO_m} = \frac{1}{S_d} \frac{d\Delta_{O_m}}{d-1} C_{O_m}, \quad (2.205)$$

where C_{O_m} and Δ_{O_m} are two-point constant and anomalous dimension of the operator O_m in coordinate space:

$$\langle O_m^{\text{ren}}(x)O_m^{\text{ren}}(0) \rangle = \frac{C_{O_m}}{(x^2)^{\Delta_{O_m}}}. \quad (2.206)$$

Taking the Fourier transform of (2.203) and setting the momentum of the stress-energy tensor to zero for simplicity, one finds in terms of the projected stress tensor $T = z^\mu z^\nu T_{\mu\nu}$

$$\langle T^{\text{ren}}(0)O_m^{\text{ren}}(p)O_m^{\text{ren}}(-p) \rangle = (d - 2\Delta_{O_m})\tilde{C}_{O_m} \frac{p_z^2}{(p^2)^{\frac{d}{2}-\Delta_{O_m}+1}}, \quad (2.207)$$

where \tilde{C}_{O_m} is the two-point constant of $\langle O_m^{\text{ren}}O_m^{\text{ren}} \rangle$ correlator in the momentum space:

$$\langle O_m^{\text{ren}}(p)O_m^{\text{ren}}(-p) \rangle = \frac{\tilde{C}_{O_m}}{(p^2)^{1-\frac{d}{2}-\eta_m}}, \quad (2.208)$$

and $\Delta_{O_m} = d - 1 + \eta_m$, where $\eta_m = \eta_{m1}/N + \mathcal{O}(1/N^2)$. In order to find \tilde{C}_{O_m} , Z_{O_m} and η_{m1} up to $1/N$ order, we have to calculate the diagrams depicted in figure 2.14. The expressions for the diagrams are

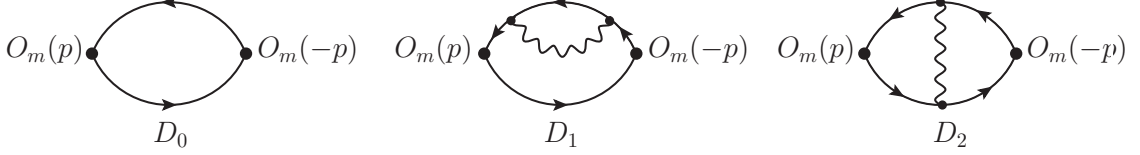


Figure 2.14: Diagrams contributing to $\langle O_m(p)O_m(-p) \rangle$ up to order $1/N$.

$$\begin{aligned}
D_0 &= \int \frac{d^d p_1}{(2\pi)^d} (-1) \text{Tr}(G(p+p_1)G(p_1)), \\
D_1 &= 2(i)^2 \mu^{2\Delta} \int \frac{d^d p_1 d^d p_2}{(2\pi)^{2d}} (-1) \text{Tr}(G(p+p_1)G(p_1)\gamma^{\nu_1}G(p_2)\gamma^{\nu_2}G(p_1)) D_{\nu_1\nu_2}(p_1-p_2), \\
D_2 &= (i)^2 \mu^{2\Delta} \int \frac{d^d p_1 d^d p_2}{(2\pi)^{2d}} (-1) \text{Tr}(G(p+p_1)\gamma^{\nu_1}G(p+p_2)G(p_2)\gamma^{\nu_2}G(p_1)) D_{\nu_1\nu_2}(p_1-p_2)
\end{aligned} \tag{2.209}$$

and

$$\begin{aligned}
\langle O_m^{\text{ren}}(p)O_m^{\text{ren}}(-p) \rangle &= Z_{O_m}^2 \langle O_m(p)O_m(-p) \rangle \\
&= Z_{O_m}^2 (D_0 + D_1 + D_2 + \mathcal{O}(1/N^2)).
\end{aligned} \tag{2.210}$$

Computing these diagrams one finds

$$2Z_{O_m1} = \eta_{m1} = -\frac{2(d-1)\Gamma(d)}{\Gamma(\frac{d}{2})^2\Gamma(\frac{d}{2}+1)\Gamma(2-\frac{d}{2})} \tag{2.211}$$

and

$$\tilde{C}_{O_m} = \frac{4^{1-d}\pi^{\frac{3-d}{2}}\text{Tr}\mathbf{1}}{\Gamma(\frac{d-1}{2})\sin(\pi\frac{d}{2})} \left(1 + \frac{1}{N}\eta_{m1} \left(\frac{3d(d-2)}{8(d-1)}\Theta(d) - \Psi(d) + \frac{d-2}{d} \right) \right), \tag{2.212}$$

where $\Theta(d) \equiv \psi'(d/2) - \psi'(1)$ and $\Psi(d) \equiv \psi(d-1) + \psi(2-d/2) - \psi(1) - \psi(d/2-1)$.

Now we can calculate the three-point function $\langle T^{\text{ren}}(0)O_m^{\text{ren}}(p)O_m^{\text{ren}}(-p) \rangle$ using Feynman diagrams, namely we have

$$\langle T^{\text{ren}}(0)O_m^{\text{ren}}(p)O_m^{\text{ren}}(-p) \rangle = Z_T Z_{O_m}^2 \langle T(0)O_m(p)O_m(-p) \rangle \quad (2.213)$$

and the diagrams contributing to $\langle T(0)O_m(p)O_m(-p) \rangle$ up to order $1/N$ are shown in figure 2.15, and the explicit results are listed in eq. (2.215) below. Putting these diagrams together and equating the expression (2.207) required by conformal symmetry with the diagrammatic result for (2.213), we find that the required Z_T factor is the one given in (2.102). As a check of our calculation, we note that dependence on the gauge parameter ξ drops out from the final result.

Let us end this section by listing the results for the diagrams in figure 2.15. They are given by

$$\begin{aligned} D_0 &= -\text{Tr} \mathbf{1} \frac{\pi \csc(\pi \frac{d}{2}) \Gamma(\frac{d}{2})}{(4\pi)^{\frac{d}{2}} \Gamma(d-2)} \frac{p_z^2}{(p^2)^{2-\frac{d}{2}}}, \\ D_1 &= \frac{1}{N} D_0 \eta_{m1} \left(\left(\frac{1}{\Delta} - \log\left(\frac{p^2}{\mu^2}\right) \right) \left(\frac{d-4}{4} + \frac{d\xi}{4(d-1)} \right) \right. \\ &\quad \left. + \left(\left(\frac{d-4}{4} + \frac{d\xi}{4(d-1)} \right) \Psi(d) - \frac{d^3 - 8d^2 + 16d - 16}{4(d-2)d} - \frac{d^2 \xi}{4(d-2)(d-1)} \right) \right), \\ D_2 &= \frac{1}{N} D_0 \eta_{m1} \left(- \left(\frac{1}{\Delta} - \log\left(\frac{p^2}{\mu^2}\right) \right) \left(\frac{d^3 - 7d^2 + 10d - 8}{8(d-1)(d+2)} + \frac{d\xi}{8(d-1)} \right) \right. \\ &\quad - \left(\left(\frac{d^3 - 7d^2 + 10d - 8}{8(d-1)(d+2)} + \frac{d\xi}{8(d-1)} \right) \Psi \right. \\ &\quad - \left. \frac{2d^7 - 21d^6 + 63d^5 - 68d^4 - 60d^3 + 192d^2 - 160d + 64}{8(d-2)(d-1)^2 d(d+2)^2} \right. \\ &\quad \left. - \frac{(2d^3 - 7d^2 + 12d - 8)\xi}{8(d-2)(d-1)^2} \right) \right), \\ D_3 &= \frac{1}{N} D_0 \eta_{m1} \left(- \left(\frac{1}{\Delta} - \log\left(\frac{p^2}{\mu^2}\right) \right) \left(\frac{d}{4} + \frac{d\xi}{4(d-1)} \right) + \left(\frac{3d(d-2)^2}{8(d-1)^2} \Theta(d) \right. \right. \\ &\quad \left. \left. - \left(\frac{d}{4} + \frac{d\xi}{4(d-1)} \right) \Psi(d) + \frac{d^3 - d^2 + 2d - 4}{4(d-2)(d-1)^2} + \frac{(3d^2 - 6d + 4)\xi}{4(d-2)(d-1)^2} \right) \right), \end{aligned} \quad (2.214)$$

$$\begin{aligned}
D_4 &= \frac{1}{N} D_0 \eta_{m1} \left(\left(\frac{1}{\Delta} - \log\left(\frac{p^2}{\mu^2}\right) \right) \left(\frac{d-4}{8} + \frac{d\xi}{8(d-1)} \right) + \left(\left(\frac{d-4}{8} + \frac{d\xi}{8(d-1)} \right) \Psi(d) \right. \right. \\
&\quad \left. \left. + \frac{3d^3 - 16d^2 + 32d - 16}{8(d-2)(d-1)d} - \frac{d^2\xi}{8(d-2)(d-1)^2} \right) \right), \\
D_5 &= \frac{1}{N} D_0 \eta_{m1} \left(- \left(\frac{1}{\Delta} - 2\log\left(\frac{p^2}{\mu^2}\right) \right) \left(\frac{(d-2)^2}{4(d-1)(d+2)} \right) - \left(\frac{(d-2)^2}{2(d-1)(d+2)} \Psi(d) \right. \right. \\
&\quad \left. \left. - \frac{(d-2)(5d^4 - 9d^3 + 4d^2 + 28d - 16)}{4(d-1)^2 d(d+2)^2} - \frac{(d-2)\xi}{2(d-1)^2} \right) \right), \\
D_6 &= \frac{1}{N} D_0 \eta_{m1} \left(\frac{3d(d-2)}{8(d-1)^2} \Theta(d) + \frac{d-2}{4(d-1)} - \frac{(d-2)\xi}{2(d-1)^2} \right), \\
D_7 &= \frac{1}{N} D_0 \eta_{m1} \left(\frac{3d(d-2)}{8(d-1)^2} \Theta(d) + \frac{1}{2(d-1)} - \frac{\xi}{2(d-1)} \right), \\
D_8 &= \frac{1}{N} D_0 \eta_{m1} \left(\left(\frac{1}{\Delta} - \log\left(\frac{p^2}{\mu^2}\right) \right) \left(\frac{d-2}{2(d-1)} \right) + \left(\frac{(d-2)}{2(d-1)} \Psi(d) \right. \right. \\
&\quad \left. \left. - \frac{d^2 - 3d + 4}{2(d-1)d} + \frac{\xi}{2(d-1)} \right) \right), \\
D_9 &= \frac{1}{N} D_0 \eta_{m1} \left(- \left(\frac{1}{\Delta} - 2\log\left(\frac{p^2}{\mu^2}\right) \right) \left(\frac{d-2}{4(d-1)} \right) - \left(\frac{(d-2)}{2(d-1)} \Psi(d) \right. \right. \\
&\quad \left. \left. - \frac{d^3 - 3d^2 + 5d - 4}{2(d-1)^2 d} + \frac{(d-2)\xi}{2(d-1)^2} \right) \right), \\
D_{10} &= \frac{1}{N} D_0 \eta_{m1} \left(- \frac{3d(d-2)}{8(d-1)^2} \Theta(d) - \frac{2d-3}{2(d-1)^2} + \frac{(d-2)\xi}{2(d-1)^2} \right), \tag{2.215}
\end{aligned}$$

where $\Theta(d) \equiv \psi'(d/2) - \psi'(1)$ and $\Psi(d) \equiv \psi(d-1) + \psi(2-d/2) - \psi(1) - \psi(d/2-1)$ and η_{m1} is given in (2.211). We notice that

$$D_7 + D_8 + D_9 + D_{10} = \frac{D_0 \eta_{m1}}{N \Delta} \frac{(d-2)}{4(d-1)}. \tag{2.216}$$

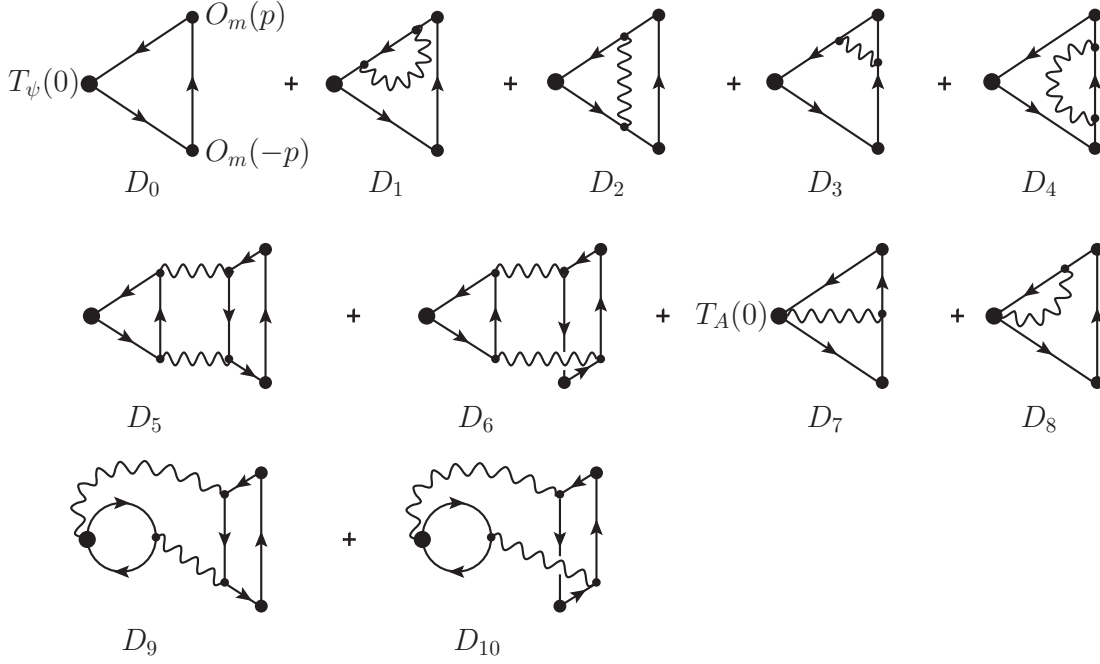


Figure 2.15: Diagrams contributing to $\langle T(0)O_m(p)O_m(-p) \rangle$ up to order $1/N$.

2.16 Appendix E. Results for $\langle JJ \rangle$ and $\langle TT \rangle$ diagrams

The diagrams for $\langle JJ \rangle$ shown in figure 2.8 are given explicitly by

$$\begin{aligned}
D_0 &= \text{Tr}(t^a t^b) \int \frac{d^d p_1}{(2\pi)^d} (-1) \text{Tr}(\gamma_z G(p_1) \gamma_z G(p + p_1)), \\
D_1 &= 2 \text{Tr}(t^a t^b) (i)^2 \mu^{2\Delta} \int \frac{d^d p_1 d^d p_2}{(2\pi)^{2d}} (-1) \text{Tr}(\gamma_z G(p + p_1) \gamma_z G(p_1) \gamma^{\nu_1} G(p_2) \gamma^{\nu_2} G(p_1)) \\
&\quad \times D_{\nu_1 \nu_2}(p_1 - p_2), \\
D_2 &= \text{Tr}(t^a t^b) (i)^2 \mu^{2\Delta} \int \frac{d^d p_1 d^d p_2}{(2\pi)^{2d}} (-1) \text{Tr}(\gamma_z G(p + p_1) \gamma^{\nu_1} G(p + p_2) \gamma_z G(p_2) \gamma^{\nu_2} G(p_1)) \\
&\quad \times D_{\nu_1 \nu_2}(p_1 - p_2)
\end{aligned} \tag{2.217}$$

and the results are

$$\begin{aligned}
D_0 &= \text{Tr}(t^a t^b) \text{Tr} \mathbf{1} \frac{\pi \csc\left(\frac{\pi d}{2}\right) \Gamma\left(\frac{d}{2}\right)}{(4\pi)^{\frac{d}{2}} (d-1) \Gamma(d-2)} \frac{p_z^2}{(p^2)^{2-\frac{d}{2}}}, \\
D_1 &= \frac{1}{N} D_0 \eta_{m1} \left(\left(\frac{1}{\Delta} - \log\left(\frac{p^2}{\mu^2}\right) \right) \left(\frac{d-4}{4} + \frac{d\xi}{4(d-1)} \right) + \left(\left(\frac{d-4}{4} + \frac{d\xi}{4(d-1)} \right) \Psi(d) \right. \right. \\
&\quad \left. \left. + \frac{3d^3 - 16d^2 + 32d - 16}{4(d-2)(d-1)d} - \frac{d^2 \xi}{4(d-2)(d-1)^2} \right) \right), \\
D_2 &= \frac{1}{N} D_0 \eta_{m1} \left(- \left(\frac{1}{\Delta} - \log\left(\frac{p^2}{\mu^2}\right) \right) \left(\frac{d-4}{4} + \frac{d\xi}{4(d-1)} \right) - \left(\left(\frac{d-4}{4} + \frac{d\xi}{4(d-1)} \right) \Psi(d) \right. \right. \\
&\quad \left. \left. - \frac{3d(d-2)}{8(d-1)} \Theta(d) - \frac{(d-4)d}{4(d-2)(d-1)} - \frac{d^2 \xi}{4(d-2)(d-1)^2} \right) \right). \tag{2.218}
\end{aligned}$$

The diagrams for $\langle TT \rangle$ depicted in figure 2.10 are given explicitly by

$$\begin{aligned}
D_0 &= N_f \left(\frac{-i}{2}\right)^2 \int \frac{d^d p_1}{(2\pi)^d} (2p_{1z} + p_z)^2 (-1) \text{Tr}(\gamma_z G(p + p_1) \gamma_z G(p_1)), \\
D_1 &= 2N_f \mu^{2\Delta} \left(\frac{-i}{2}\right)^2 (i)^2 \int \frac{d^d p_1 d^d p_2}{(2\pi)^{2d}} (2p_{1z} + p_z)^2 (-1) \text{Tr}(\gamma_z G(p + p_1) \gamma_z G(p_1) \gamma^{\nu_1} \\
&\quad \times G(p_2) \gamma^{\nu_2} G_{p_1}) D_{\nu_1 \nu_2}(p_1 - p_2), \\
D_2 &= N_f \mu^{2\Delta} \left(\frac{-i}{2}\right)^2 (i)^2 \int \frac{d^d p_1 d^d p_2}{(2\pi)^{2d}} (2p_{1z} + p_z)(2p_{2z} + p_z) (-1) \text{Tr}(\gamma_z G(p + p_1) \gamma^{\nu_1} \\
&\quad \times G(p + p_2) \gamma_z G(p_2) \gamma^{\nu_2} G_{p_1}) D_{\nu_1 \nu_2}(p_1 - p_2), \\
D_3 &= N_f^2 \mu^{4\Delta} \left(\frac{-i}{2}\right)^2 (i)^4 \int \frac{d^d p_1 d^d p_2 d^d p_3}{(2\pi)^{3d}} (2p_{1z} + p_z) (-1) \text{Tr}(\gamma_z G(p + p_1) \gamma^{\nu_1} G(p_1 - p_3) \\
&\quad \times \gamma^{\nu_2} G(p_1)) D_{\nu_1 \nu_3}(p + p_3) D_{\nu_2 \nu_4}(p_3) (2p_{2z} + p_z) \\
&\quad \times (-1) \text{Tr}(\gamma_z G(p_2) \gamma^{\nu_4} G(p_2 - p_3) \gamma^{\nu_3} G(p + p_2)) + \dots, \tag{2.219}
\end{aligned}$$

$$\begin{aligned}
D_4 &= 2N_f \mu^{2\Delta} \left(\frac{-i}{2}\right) (-i)(i) \int \frac{d^d p_1 d^d p_2}{(2\pi)^{2d}} (2p_{1z} + p_z) (-1) \text{Tr}(\gamma_z G(p + p_1) \gamma_z G(p_2)) \\
&\quad \times \gamma^{\nu_1} G(p_1) D_{\nu_1 z}(p_1 - p_2), \\
D_5 &= 2N_f^2 \mu^{4\Delta} \left(\frac{-i}{2}\right) (-i)(i)^3 \int \frac{d^d p_1 d^d p_2 d^d p_3}{(2\pi)^{3d}} (-1) \text{Tr}(\gamma_z G(p_1 - p_3) \gamma^{\nu_1} G(p_1)) D_{\nu_1 \nu_2}(p_3) \\
&\quad \times D_{z\nu_3}(p + p_3) (2p_{2z} + p_z) (-1) \text{Tr}(\gamma_z G(p_2) \gamma^{\nu_2} G(p_2 - p_3) \gamma^{\nu_3} G(p + p_2)) + \dots, \\
D_6 &= N_f \mu^{2\Delta} (-i)^2 \int \frac{d^d p_1 d^d p_2}{(2\pi)^{2d}} (-1) \text{Tr}(\gamma_z G(p + p_2) \gamma_z G(p_1)) D_{zz}(p_1 - p_2), \\
D_7 &= N_f^2 \mu^{4\Delta} (-i)^2 (i)^2 \int \frac{d^d p_1 d^d p_2 d^d p_3}{(2\pi)^{3d}} (-1) \text{Tr}(\gamma_z G(p_1 - p_3) \gamma^{\nu_1} G(p_1)) D_{zz}(p + p_3) \\
&\quad \times D_{\nu_1 \nu_2}(p_3) (-1) \text{Tr}(\gamma_z G(p_2) \gamma^{\nu_2} G(p_2 - p_3)), \\
D_8 &= N_f^2 \mu^{4\Delta} (-i)^2 (i)^2 \int \frac{d^d p_1 d^d p_2 d^d p_3}{(2\pi)^{3d}} (-1) \text{Tr}(\gamma_z G(p_1 - p_3) \gamma^{\nu_1} G(p_1)) D_{\nu_1 z}(p_3) \\
&\quad \times D_{z\nu_2}(p + p_3) (-1) \text{Tr}(\gamma_z G(p_2 - p_3) \gamma^{\nu_2} G(p + p_2)), \tag{2.220}
\end{aligned}$$

where dots mean that there is also an expression which corresponds to the opposite direction of the fermion loop. After carrying out the momentum integrals using techniques similar to the ones described in the appendices of [68], we find

$$\begin{aligned}
D_0 &= -N \frac{\pi^{1-\frac{d}{2}} \csc(\frac{\pi d}{2}) \Gamma(\frac{d}{2})}{4^{\frac{d}{2}+1} (d-1)(d+1) \Gamma(d-2)} \frac{p_z^4}{(p^2)^{2-\frac{d}{2}}}, \\
D_1 &= \frac{1}{N} D_0 \eta_{m1} \left(\left(\frac{1}{\Delta} - \log\left(\frac{p^2}{\mu^2}\right) \right) \left(\frac{d-4}{4} + \frac{d\xi}{4(d-1)} \right) + \left(\left(\frac{d-4}{4} + \frac{d\xi}{4(d-1)} \right) \Psi(d) \right. \right. \\
&\quad \left. \left. + \frac{2d^4 - 10d^3 + 15d^2 + 4d - 8}{2(d-2)(d-1)d(d+1)} - \frac{d(2d-1)\xi}{2(d-2)(d-1)^2(d+1)} \right) \right), \\
D_2 &= \frac{1}{N} D_0 \eta_{m1} \left(- \left(\frac{1}{\Delta} - \log\left(\frac{p^2}{\mu^2}\right) \right) \left(\frac{d^3 - 7d^2 + 10d - 8}{4(d-1)(d+2)} + \frac{d\xi}{4(d-1)} \right) \right. \\
&\quad \left. + \left(\frac{3d(d-2)}{8(d-1)} \Theta(d) - \left(\frac{d^3 - 7d^2 + 10d - 8}{4(d-1)(d+2)} + \frac{d\xi}{4(d-1)} \right) \Psi(d) \right. \right. \\
&\quad \left. \left. + \frac{5d^5 - 27d^4 + 44d^3 - 30d^2 - 12d + 16}{2(d-2)(d-1)^2 d(d+1)(d+2)} - \frac{(d^3 - 4d^2 + 2)\xi}{2(d-2)(d-1)^2(d+1)} \right) \right), \\
D_3 &= \frac{1}{N} D_0 \eta_{m1} \left(- \left(\frac{1}{\Delta} - 2 \log\left(\frac{p^2}{\mu^2}\right) \right) \left(\frac{(d-2)^2}{2(d-1)(d+2)} \right) + \left(\frac{2(d-2)}{(d-1)(d+2)} \Psi(d) \right. \right. \\
&\quad \left. \left. - \frac{d(d^3 - 8d + 11)}{(d-1)^2(d+1)(d+2)} + \frac{\xi}{2(d-1)} \right) \right) + dD_0/(2N), \tag{2.221}
\end{aligned}$$

and

$$\begin{aligned}
D_4 &= \frac{1}{N} D_0 \eta_{m_1} \left(\left(\frac{1}{\Delta} - \log\left(\frac{p^2}{\mu^2}\right) \right) \left(\frac{d-2}{d-1} \right) \right. \\
&\quad \left. + \left(\frac{(d-2)\Psi(d)}{d-1} - \frac{d^4 - 4d^3 + 5d^2 + 2d - 2}{(d-1)^2 d(d+1)} + \frac{\xi}{d-1} \right) \right), \\
D_5 &= \frac{1}{N} D_0 \eta_{m_1} \left(- \left(\frac{1}{\Delta} - 2 \log\left(\frac{p^2}{\mu^2}\right) \right) \left(\frac{d-2}{2(d-1)} \right) - \left(\frac{(d-2)\Psi(d)}{d-1} \right. \right. \\
&\quad \left. \left. - \frac{d^4 - 4d^3 + 5d^2 + 2d - 2}{(d-1)^2 d(d+1)} + \frac{\xi}{d-1} \right) \right) - dD_0/N, \\
D_6 &= \frac{1}{N} D_0 \eta_{m_1} \left(- \frac{\xi - 1}{2(d-1)} \right), \\
D_7 &= \frac{1}{N} D_0 \eta_{m_1} \left(\frac{\xi - 1}{2(d-1)} \right), \\
D_8 &= dD_0/(2N), \tag{2.222}
\end{aligned}$$

where $\Theta(d) \equiv \psi'(d/2) - \psi'(1)$ and $\Psi(d) \equiv \psi(d-1) + \psi(2-d/2) - \psi(1) - \psi(d/2-1)$ and η_{m_1} is given in (2.211). We notice that

$$D_4 + D_5 + D_6 + D_7 + D_8 = \frac{D_0 \eta_{m_1}}{N \Delta} \frac{(d-2)}{2(d-1)} - dD_0/(2N). \tag{2.223}$$

Chapter 3

Particle Production in 1 + 1 CFT

This chapter is an edited version of ref. [128] written in collaboration with Guilherme Pimentel and Alexander Polyakov.

3.1 Introduction

In this chapter we discuss vacuum decay in 1 + 1 dimensional Conformal Field Theories with external fixed background fields. As an example, we consider a theory of massless fermions in 1+1 dimensions coupled to Abelian, non-Abelian or gravitational background fields. The computation of the vacuum decay rate involves evaluating the effective action, which is given by the logarithm of the determinant of the quantum fields in the fixed background. The pioneering example, due to Schwinger [129], is of fermions in a constant background electric field. The example we study in our paper is interesting, as we can find formulas for vacuum decay in generic field profiles (which satisfy a few technical assumptions that we state below). Some exact results for generic field profiles were also obtained in [130, 131], in 1 + 1 dimensional QED.

Let us briefly review a case with no particle production. Consider free massless fermions interacting with a fixed non-Abelian gauge field background. The effective action is obtained by the Gaussian integration over the fermion fields, and is given

by a one loop determinant. If the field profile satisfies a “good” behavior, that we specify later, the effective action is real and is expressed [132] in terms of the Wess-Zumino-Novikov-Witten (WZNW) action [133, 134, 135]. In this case particles are not created, since the vacuum decay rate is nonzero only when the effective action has an imaginary part.

Our goal is to determine the effective action for background fields that do lead to particle production. In this case, we have to discuss the in/out effective action which has an imaginary part, reflecting vacuum decay. The imaginary piece in the effective action is determined by a careful treatment of the Feynman $i\epsilon$ prescription in a massless theory.

Our main result is that the effective action is modified by the inclusion of extra boundary terms, which are complex, and whose imaginary part gives the vacuum decay rate. The boundary term is a two-form which appears to be novel. To compute the boundary terms we need a certain Riemann-Hilbert decomposition. While the Abelian and non-Abelian decompositions are standard Riemann-Hilbert problems, the gravitational case has not been considered before. The vacuum decay rate for Abelian background fields is given by the same formula of dissipative quantum mechanics obtained by Caldeira and Leggett [136, 137]. Our results generalize their formulas for non-Abelian and gravitational backgrounds.

The rest of the chapter is organized as follows. In section 3.2 we compute the effective action and the new boundary term for an Abelian gauge field and discuss the general logic of the computation, which helps in the more complicated cases. In section 3.3 we find the effective action and the new boundary term for the non-Abelian gauge field. Finally, in section 3.4 we find the effective action and the new boundary term in the case of the gravitational field. In appendix 3.5, we discuss an alternative method of computation of the boundary terms. In appendix 3.6, we review the gauge-gravity duality between the non-Abelian and gravitational cases [138, 139, 140].

Finally, in appendix 3.7, we show the first perturbative correction to the Caldeira-Leggett formula coming from non-Abelian and gravitational backgrounds.

3.2 Vacuum decay in an Abelian background

To set the stage, let us look at the Abelian case first. The Lagrangian is

$$\mathcal{L} = \bar{\psi}\gamma^\mu(i\partial_\mu + A_\mu)\psi = \bar{\psi}_-(i\partial_+ + A_+)\psi_- + \bar{\psi}_+(i\partial_- + A_-)\psi_+, \quad (3.1)$$

where the metric is $\eta^{\mu\nu} = (1, -1)$, and we introduced light cone coordinates $x^\pm = (x^0 \pm x^1)/\sqrt{2}$. From the Lagrangian it is clear that the left movers ψ_+ and right movers ψ_- are sourced by A_- and A_+ fields, respectively. Therefore, the determinant will split into a right-moving piece, a left-moving piece, and a contact term that ensures gauge invariance [132]¹

$$S(A_+, A_-) = \log \det(\gamma^\mu(i\partial_\mu + A_\mu)) = W_+(A_+) + W_-(A_-) - 2 \int d^2x A_+ A_- . \quad (3.2)$$

The contact term comes from short distance cutoff regulators; it is not related to particle production. In the case of strong fields which lead to particle production, W_+ and W_- have imaginary parts. The vacuum decay rate factorizes and is given by

$$|{}_{\text{out}}\langle 0|0\rangle_{\text{in}}|^2 = e^{-2\text{Im}S(A)} = e^{-2\text{Im}W_+} e^{-2\text{Im}W_-} . \quad (3.3)$$

Let us compute the contribution to the effective action coming from A_+ . We will treat x^+ as a time coordinate, while in the x^- direction we assume that $A_+(x^+, x^-) \rightarrow 0$ as $x^- \rightarrow \pm\infty$. An easy calculation of the diagram

¹In this section we write the effective action up to an unimportant overall factor $-\frac{e^2}{4\pi}$. In other words, we set $e^2 = -4\pi$. The charge e can be restored by the substitution $A_\mu \rightarrow eA_\mu$.

$$W_+(A_+) = \begin{array}{c} A_+(p) \\ \text{---} \end{array} \text{---} \text{---} \begin{array}{c} A_+(-p) \\ \text{---} \end{array}$$

leads to ($d^2p = dp_+ dp_-$)

$$W_+(A_+) = \int \frac{d^2p}{(2\pi)^2} \frac{p_-}{p_+ + i\varepsilon \operatorname{sgn} p_-} A_+(p) A_+(-p). \quad (3.4)$$

As is well known, this result is exact and higher order corrections in A_+ are zero. The “ $i\varepsilon$ ” prescription follows from the Feynman rule $\frac{1}{p^2} \Rightarrow \frac{1}{p^2 + i\varepsilon} = \frac{1}{p_-} \left(\frac{1}{p_+ + i\varepsilon \operatorname{sgn} p_-} \right)$. The term in parenthesis is the Feynman Green’s function. We see that²

$$\operatorname{Im} W_+(A_+) = - \int \frac{d^2p}{4\pi} |p_-| \delta(p_+) A_+(p) A_+(-p) = - \frac{1}{4\pi} \int dp_- |p_-| A_+(0, p_-) A_+(0, -p_-). \quad (3.5)$$

The condition of vacuum stability ($\operatorname{Im} W_+ = 0$) is thus $\int_{-\infty}^{+\infty} A_+(y^+, x^-) dy^+ = 0$. It is useful to rewrite the formula (3.5) in position space. If we denote

$$\omega(x^-) \equiv \int_{-\infty}^{+\infty} A_+(y^+, x^-) dy^+, \quad (3.6)$$

from (3.5) we obtain³

$$\operatorname{Im} W_+(A_+) = \frac{1}{4\pi} \int_{-\infty}^{+\infty} dx^- dy^- \frac{(\omega(x^-) - \omega(y^-))^2}{(x^- - y^-)^2}. \quad (3.7)$$

We recognize this formula as the friction term in Caldeira-Leggett’s dissipative quantum mechanics [136, 137]. Below we will find the non-Abelian and gravitational generalizations of this action.

²We use $1/(p_+ + i\varepsilon \operatorname{sgn} p_-) = \mathcal{P}(1/p_+) - i\pi \operatorname{sgn}(p_-) \delta(p_+)$.

³The fact that the effective action depends on $\omega(x^-)$ demonstrates that the gauge symmetry in our system is restricted by the condition that gauge transformations for A_+ and A_- must be trivial at the boundary of spacetime.

It is instructive to rewrite (3.7) in a slightly different form. Let us introduce two complex functions $\omega_{\text{up}}(x^-)$ and $\omega_{\text{down}}(x^-)$, which are analytic in the upper and lower half-planes, respectively. They are related to $\omega(x^-)$ as

$$\omega_{\text{up}}(x^-) - \omega_{\text{down}}(x^-) = \omega(x^-) \quad (3.8)$$

for real x^- . This decomposition of the function $\omega(x^-)$ is called the *scalar Riemann-Hilbert problem* and the explicit solution in this case is given by

$$\omega_{\text{up/down}}(x^-) = \frac{1}{2\pi i} \int_{-\infty}^{+\infty} \frac{\omega(y^-) dy^-}{y^- - x^- \mp i\varepsilon}. \quad (3.9)$$

In terms of $\omega_{\text{up/down}}$, the imaginary part of the effective action can be written as

$$\text{Im } W_+(A_+) = \text{Im} \int_{-\infty}^{+\infty} dx^- (\omega_{\text{down}} \partial_- \omega_{\text{up}}). \quad (3.10)$$

The generalization of the formula (3.10) for the strong non-Abelian and gravitational cases is the main goal of this paper.

There is yet another way of obtaining (3.10), which will be useful below. We can parametrize A_+ as

$$A_+(x^+, x^-) = \partial_+ \phi(x^+, x^-) \quad (3.11)$$

and we notice that the “Wilson line” $\phi(x^+, x^-)$ has residual gauge invariance $\phi \rightarrow \phi + u(x^-)$. We say that $\phi = \phi_R(x^+, x^-)$ is in *retarded* gauge if it obeys the boundary condition $\phi_R(-\infty, x^-) \rightarrow 0$ and therefore

$$\phi_R(x^+, x^-) = \int_{-\infty}^{x^+} A_+(y^+, x^-) dy^+. \quad (3.12)$$

We see that ϕ_R is manifestly real and causal, as $\phi_R(x^+, x^-)$ only depends on $A_+(y^+, x^-)$ for $y^+ < x^+$; moreover, $\phi_R(+\infty, x^-) = \omega(x^-)$, so the imaginary part of the effective action (3.10) is written in terms of the boundary value of ϕ_R and the whole $W_+(A_+)$ reads

$$W_+(A_+) = \int d^2x \partial_+ \phi_R \partial_- \phi_R + \int_{-\infty}^{+\infty} dx^- (\omega_{\text{down}} \partial_- \omega_{\text{up}}). \quad (3.13)$$

We can use the solution of the Riemann-Hilbert problem (3.8) and the residual gauge invariance of ϕ to define a *spectral* (or Feynman) gauge, namely

$$\phi_S(x^+, x^-) \equiv \phi_R(x^+, x^-) - \omega_{\text{down}}(x^-) \rightarrow \begin{cases} \omega_{\text{up}}(x^-), & x^+ \rightarrow +\infty \\ -\omega_{\text{down}}(x^-), & x^+ \rightarrow -\infty \end{cases}. \quad (3.14)$$

In the spectral gauge the effective action (3.13) reads

$$W_+(A_+) = \int d^2x \partial_+ \phi_S \partial_- \phi_S, \quad (3.15)$$

and has the form of the usual result [12]. In our case, the difference is that the function ϕ_S is complex valued and (3.15) contains both real and imaginary parts of the effective action! The conclusion is that in the *spectral* gauge, we do not require boundary terms in the effective action, whereas in the *retarded* gauge, we have boundary terms, which are complex and account for the vacuum decay.

The logic is summarized as follows. If we use the *spectral* gauge, then the expressions for the effective actions are well known [12, 132, 141], as the boundary terms evaluate to zero. Then passing from the *spectral* gauge to *retarded* gauge we determine the functional form of the boundary terms. In the retarded gauge, the boundary term contains the imaginary part of the effective action. In Appendix 3.5 we discuss an

alternative method to compute the full effective action, by exploiting (chiral or trace) anomaly equations.

3.3 Vacuum decay in a non-Abelian background

In the non-Abelian case the general form of the effective action reads

$$S(A_+, A_-) = \log \det(\gamma^\mu(i\partial_\mu + A_\mu)) = W_+(A_+) + W_-(A_-) + 2 \int d^2x \operatorname{Tr}(A_+ A_-) \quad (3.16)$$

and imaginary terms responsible for the particle production are present only in W_+ and W_- . We concentrate again on $W_+(A_+)$, which is formally given by the following sum of Feynman diagrams

$$W_+(A_+) = \text{---} \bigcirc \text{---} + \text{---} \bigcirc \text{---} + \text{---} \bigcirc \text{---} + \dots$$

The diagram shows a series of Feynman diagrams representing the expansion of the effective action $W_+(A_+)$. The first diagram is a circle with two external dashed lines. The second diagram is a circle with four external dashed lines, two on the left and two on the right. The third diagram is a circle with six external dashed lines, three on the left and three on the right. The diagrams are separated by plus signs and followed by an ellipsis.

If we parametrize $A_+ = g^{-1}\partial_+g$ we get $W_+(g)$. If $g(x^+ \rightarrow \pm\infty, x^-) = \mathbb{1}$ then $W_+(g)$ is the WZNW action [142]

$$W_{\text{WZNW}}(g) \equiv \frac{1}{2} \int d^2x \operatorname{Tr}(\partial^\mu g^{-1} \partial_\mu g) - \frac{1}{3} \int d^2x dt \varepsilon^{\mu\nu\lambda} \operatorname{Tr}(g^{-1} \partial_\mu g g^{-1} \partial_\nu g g^{-1} \partial_\lambda g), \quad (3.17)$$

where in the last Wess-Zumino (WZ) term we introduced the extra t -dependence: $g(x^+, x^-, t)$ such that $g(x^+, x^-, 0) = \mathbb{1}$ and $g(x^+, x^-, 1) = g(x^+, x^-)$; and $\mu, \nu, \lambda = (\pm, 0)$, and $\varepsilon^{0-+} = 1$, where zero corresponds to the t coordinate.

From the Abelian case, we expect that vacuum decay occurs for A_+ with $g^{-1}(-\infty, x^-) \cdot g(+\infty, x^-) \neq \mathbb{1}$, or, in different notation:

$$\Omega(x^-) \equiv P \exp \int_{-\infty}^{\infty} A_+(y^+, x^-) dy^+ \neq \mathbb{1}, \quad (3.18)$$

where “ $P \exp$ ” is the path-ordered exponential. In this case the effective action is not given by (3.17); it must include new boundary terms. Indeed, looking at the variation of the WZ term

$$S_{\text{WZ}} \equiv \int d^2x dt \varepsilon^{\mu\nu\lambda} \text{Tr}(a_\mu a_\nu a_\lambda), \quad (3.19)$$

where $a_\mu \equiv g^{-1} \partial_\mu g$, with $\delta a_\mu = \nabla_\mu \varepsilon$, we obtain

$$\begin{aligned} \delta S_{\text{WZ}} &= \int d^2x dt \varepsilon^{\mu\nu\lambda} \text{Tr}(a_\mu a_\nu \nabla_\lambda \varepsilon) \sim \int d^2x dt \varepsilon^{\mu\nu\lambda} \nabla_\lambda \text{Tr}((\partial_\mu a_\nu - \partial_\nu a_\mu) \varepsilon) \\ &= \int d^2x dt \varepsilon^{ij} \partial_0 \text{Tr}(\partial_i a_j \varepsilon) - \int d^2x dt \partial_+ \text{Tr}((\partial_- a_0 - \partial_0 a_-) \varepsilon) \\ &= \int d^2x \varepsilon^{ij} \text{Tr}(\partial_i a_j \varepsilon) - \int dx^- dt \text{Tr}((\partial_- a_0 - \partial_0 a_-) \varepsilon) \Big|_{x^+ = -\infty}^{x^+ = +\infty}. \end{aligned} \quad (3.20)$$

The first term here is standard while the time-boundary term explicitly violates t -symmetry. In other words, S_{WZ} is dependent on the t -parametrization. This unphysical dependence on the extrapolation disappears when the right boundary terms are added to WZNW action.

Notice that the matrix g has a gauge symmetry

$$g(x^+, x^-) \rightarrow u(x^-) g(x^+, x^-), \quad (3.21)$$

where $u(x^-)$ is an arbitrary complex matrix. The retarded gauge is defined by

$$g_R(x^+ \rightarrow -\infty, x^-) = \mathbb{1} \Rightarrow g_R(x^+, x^-) = P \exp \int_{-\infty}^{x^+} dy^+ A_+(y^+, x^-). \quad (3.22)$$

Like in the Abelian case, we see that $\Omega(x^-) = g_R(+\infty, x^-)$.

Proceeding by analogy, we should look for complex valued matrices $\Omega_{\text{down}}(x^-)$ and $\Omega_{\text{up}}(x^-)$ that are a solution to the *matrix Riemann-Hilbert problem*

$$\Omega_{\text{down}}(x^-)\Omega_{\text{up}}(x^-) = \Omega(x^-), \quad (3.23)$$

for real values of x^- . We assume that $\Omega_{\text{up}}^{-1}(x^-)$ and $\Omega_{\text{down}}^{-1}(x^-)$ are also analytic in the upper and lower half-planes, respectively. Unfortunately, the matrix Riemann-Hilbert problem does not have an explicit general solution.⁴

As we see from (3.20) the retarded gauge choice requires extra terms in the WZ term in order to cancel the unacceptable boundary contributions. However, we can use our gauge freedom in choosing g to eliminate the boundary terms. Let us introduce the spectral (or Feynman) gauge:

$$g_S(x^+, x^-) \equiv \Omega_{\text{down}}^{-1}(x^-) g_R(x^+, x^-) \rightarrow \begin{cases} \Omega_{\text{up}}(x^-), & x^+ \rightarrow +\infty \\ \Omega_{\text{down}}^{-1}(x^-), & x^+ \rightarrow -\infty \end{cases}. \quad (3.24)$$

It follows from here that $g_S(x^+, x^-)$ at $x^+ \rightarrow \pm\infty$ is analytic in the lower/upper half-planes and thus all boundary terms vanish after x^- integration. By analogy with the Abelian case, we come to the conclusion that in the spectral gauge there are no boundary terms! The effective action is just the standard WZNW action (3.17), which is complex valued, as g_S is complex

$$W_+(A_+) = W_{\text{WZNW}}(g_S). \quad (3.25)$$

⁴For a review on the subject and the cases where an explicit solution is available, see [143]. Notice that the right and left decompositions are inequivalent, namely, we could look for $\Omega(x^-) = \tilde{\Omega}_{\text{up}}(x^-)\tilde{\Omega}_{\text{down}}(x^-)$, but in terms of these matrices we do not obtain spectral boundary conditions in a simple way. In general $\tilde{\Omega}_{\text{up/down}}(x^-) \neq \Omega_{\text{up/down}}(x^-)$.

A more physical justification of the absence of boundary terms in the spectral gauge is discussed in the Appendix 3.5.

From (3.25), we now determine the boundary term that must be present in the effective action written in an arbitrary gauge. For example, in going from spectral to retarded gauge, we do not change $A_+ = g^{-1}\partial_+g$, therefore the effective actions must be the same,

$$W_+(A_+) = W_{\text{WZNW}}(\Omega_{\text{down}}^{-1}g_R) = W_{\text{WZNW}}(g_R) + W_B(\Omega_{\text{up}}, \Omega_{\text{down}}). \quad (3.26)$$

In order to proceed we use exterior calculus to derive a composition formula for the WZ term. Let us introduce two 1-forms a and b , with $a = g^{-1}dg, b = dh h^{-1}$. a and b satisfy the equations $da = -a \wedge a, db = b \wedge b$. Consider the 1-form $c = (gh)^{-1}d(gh) = h^{-1}(a + b)h$. Then we have

$$\text{Tr}(c \wedge c \wedge c) = \text{Tr}(a \wedge a \wedge a) + \text{Tr}(b \wedge b \wedge b) - 3d(\text{Tr} a \wedge b). \quad (3.27)$$

Now we apply (3.27) with $g_S = \Omega_{\text{down}}^{-1}g_R$. From the quadratic term in the WZNW action we obtain⁵

$$\frac{1}{2} \int d^2x \text{Tr}(\partial^\mu g_S^{-1} \partial_\mu g_S) = \frac{1}{2} \int d^2x \text{Tr}(\partial^\mu g_R^{-1} \partial_\mu g_R) + \int d^2x \text{Tr}(\partial_- \Omega_{\text{down}} \Omega_{\text{down}}^{-1} \partial_+ g_R g_R^{-1}), \quad (3.28)$$

and using (3.26) and (3.27) for the WZ term in (3.17) we find

$$W_{\text{WZ}}(g_S) = W_{\text{WZ}}(g_R) - 3 \int_{(x^+, x^-, t)} d(\text{Tr}(\Omega_{\text{down}} d\Omega_{\text{down}}^{-1} \wedge dg_R g_R^{-1})). \quad (3.29)$$

Notice that the Penrose diagram for our space-time with the embedding dimension is a pyramid; we call it the Penrose-Nefertiti diagram (see figure 3.1).

⁵In light-cone coordinates $\text{Tr}(\partial^\mu g^{-1} \partial_\mu g) = \text{Tr}(\partial_- g^{-1} \partial_+ g) + \text{Tr}(\partial_+ g^{-1} \partial_- g) = 2\text{Tr}(\partial_+ g^{-1} \partial_- g)$.

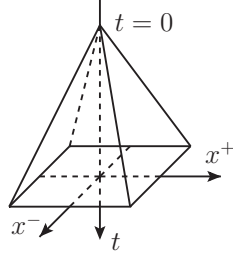


Figure 3.1: Penrose-Nefertiti diagram. The usual Penrose diagram of 1+1 dimensional Minkowski spacetime is the base of a pyramid. The embedding coordinate t runs from the apex ($t = 0$) to the base ($t = 1$). The new boundary terms in the effective action are supported at the $t - x$ faces of the pyramid.

The first term in (3.29) is real (we assume A_+ is real), while the boundary term, which has support at the faces of the pyramid, is complex valued. Using Stokes' theorem in (3.29), we obtain

$$\begin{aligned}
W_{\text{WZ}}(g_S) = & W_{\text{WZ}}(g_R) - 3 \int d^2x \text{Tr}(\Omega_{\text{down}} \partial_- \Omega_{\text{down}}^{-1} \partial_+ g_R g_R^{-1}) \\
& + 3 \int_{(x^-, t)} \text{Tr}(\Omega_{\text{down}}^{-1} d\Omega_{\text{down}} \wedge \Omega_{\text{up}} d\Omega_{\text{up}}^{-1}). \quad (3.30)
\end{aligned}$$

Using (3.26), (3.28) and (3.30) we finally obtain

$$W_B(\Omega_{\text{up}}, \Omega_{\text{down}}) = \int_{(x^-, t)} \text{Tr}(\Omega_{\text{down}}^{-1} d\Omega_{\text{down}} \wedge \Omega_{\text{up}} d\Omega_{\text{up}}^{-1}). \quad (3.31)$$

The formula (3.31) is one of the main results of our paper.⁶ The boundary term is complex valued, and although not manifestly imaginary, contains the imaginary part of the effective action⁷.

⁶The effective action for arbitrary g is $W_+(A_+) = W_{\text{WZNW}}(g^{-1}(-\infty, x^-)g) + W_B(\Omega_{\text{up}}, \Omega_{\text{down}})$.

⁷Notice that, although the boundary term does depend on the t -interpolation, its imaginary part does not! One can see this by looking at the variation of (3.31), $\delta W_B = \frac{1}{2} \int dx^- \text{Tr}(\Omega_{\text{down}}^{-1} \delta \Omega_{\text{down}} \Omega_{\text{up}} \partial_- \Omega_{\text{up}}^{-1} + \Omega_{\text{down}}^{-1} \partial_- \Omega_{\text{down}} \delta \Omega_{\text{up}} \Omega_{\text{up}}^{-1}) + \frac{1}{2} \int dt dx^- \text{Tr}([\Omega^{-1} \partial_0 \Omega, \Omega^{-1} \partial_- \Omega] \Omega^{-1} \delta \Omega)$. We see that the last term is t -dependent but explicitly real (Ω is a real matrix), whereas the first term is t -independent and complex. We also notice that the t -dependent term cancels with the t -dependent term in the variation of the WZ term (3.20) in the effective action. Thus the variation of the effective action is also t -independent.

We emphasize that this boundary term is the non-Abelian generalization of the Caldeira-Leggett dissipative term, and is given by a two-form⁸. We also notice that our two-form is a Minkowski space counterpart of the Atiyah-Patodi-Singer η -invariant [146, 147, 148], which appears in Euclidean manifolds with boundary. We present the leading order, non-Abelian correction to the Caldeira-Leggett formula in Appendix 3.7.

3.4 Vacuum decay in the gravitational field

Now we consider a theory of fermions coupled to a fixed gravitational field. It is convenient to parametrize the metric in the light cone coordinates,

$$ds^2 = h_{+-}(x^+, x^-)dx^+dx^- + h_{++}(x^+, x^-)dx^+dx^+ + h_{--}(x^+, x^-)dx^-dx^-. \quad (3.32)$$

We assume that the background fields are asymptotically flat, i.e. $h_{++}(x^+, x^-) \rightarrow 0$, $h_{--}(x^+, x^-) \rightarrow 0$ and $h_{+-}(x^+, x^-) \rightarrow 1$ as $x^\pm \rightarrow \pm\infty$. The Lagrangian is⁹

$$\mathcal{L} = \psi_-(\partial_+ - h_{++}\partial_-)\psi_- + \psi_+(\partial_- - h_{--}\partial_+)\psi_+. \quad (3.33)$$

Like in the non-Abelian case, the effective action is

$$S(h_{++}, h_{--}, h_{+-}) = W_+(h_{++}) + W_-(h_{--}) + L(h_{++}, h_{--}, h_{+-}), \quad (3.34)$$

where the last term L is a local and real term and appears due to the UV regulator.

We concentrate on the calculation of the contribution from left-moving fermions, $W_+(h_{++})$. For gravity we use the same logic as in the non-Abelian case. We

⁸A similar two-form was found in Euclidean manifolds with a boundary, in [144, 145].

⁹For simplicity, we consider Majorana fermions. As in [149], we perform a field redefinition to write the Lagrangian in the form (3.33). In the previous sections, we considered Dirac fermions, as these can carry electric and color charge.

parametrize the metric tensor $h_{++}(x^+, x^-)$ using the function $f(x^+, x^-)$ defined by the equation

$$(\partial_+ - h_{++}\partial_-)f = 0, \quad (3.35)$$

which is a gravitational analog of the Wilson line. Lines of constant f correspond to the characteristics of light-like, right-moving geodesics in the background spacetime. Notice that there is an ambiguity in f , namely

$$f(x^+, x^-) \Rightarrow u(f(x^+, x^-)), \quad (3.36)$$

where $u(x^-)$ is an arbitrary invertible complex function of one variable. The *retarded* gauge is defined by

$$f_R(x^+ \rightarrow -\infty, x^-) = x^- \Rightarrow f_R(x^+, x^-) \equiv P \exp \left(\int_{-\infty}^{x^+} dy^+ h_{++}(y^+, x^-) \partial_- \right) x^-. \quad (3.37)$$

As in the case of gauge fields, we need to add a suitable boundary term to the effective action [141]

$$W_{\text{gWZ}}(f) \equiv \int d^2x \left(\frac{\partial_-^2 f \partial_+ \partial_- f}{(\partial_- f)^2} - \frac{(\partial_-^2 f)^2 \partial_+ f}{(\partial_- f)^3} \right), \quad (3.38)$$

where gWZ stands for ‘‘gravitational Wess-Zumino’’ and we omit an overall normalization factor, which is $-1/48\pi$ in our case. Alternatively, we can use the gauge symmetry (3.36) to eliminate the boundary term. Let us introduce the *spectral* gauge by

$$f_S(x^+, x^-) \equiv \Gamma_{\text{down}}^{-1}(f_R(x^+, x^-)) = \begin{cases} \Gamma_{\text{up}}(x^-), & x^+ \rightarrow +\infty, \\ \Gamma_{\text{down}}^{-1}(x^-), & x^+ \rightarrow -\infty, \end{cases} \quad (3.39)$$

where $\Gamma_{\text{up}}(x^-)$ and $\Gamma_{\text{down}}(x^-)$ are analytic functions in the upper and lower x^- half-plane. We also assume that the inverse functions $\Gamma_{\text{up}}^{-1}(x^-)$ and $\Gamma_{\text{down}}^{-1}(x^-)$ are analytic in the upper and lower x^- half-plane respectively. In this case, to determine $\Gamma_{\text{up,down}}$, we need to solve a “functional” Riemann-Hilbert problem ¹⁰,

$$\Gamma_{\text{down}}(\Gamma_{\text{up}}(x^-)) = \Gamma(x^-), \quad (3.40)$$

where

$$\Gamma(x^-) \equiv P \exp \left(\int_{-\infty}^{+\infty} dy^+ h_{++}(y^+, x^-) \partial_- \right) x^- = f_R(+\infty, x^-). \quad (3.41)$$

To our knowledge, the Riemann-Hilbert problem (3.40) has not been considered in the mathematics literature before. We also notice that (3.40) doesn't have an explicit solution. ¹¹

By similar arguments as in the previous sections, the effective action is

$$W_+(h_{++}) = W_{\text{gWZ}}(f_S), \quad (3.42)$$

where W_{gWZ} is given by (3.38). See also Appendix 3.5 for a different derivation of (3.42). This effective action is complex valued. In retarded and spectral gauges the metric $h_{++}(x^+, x^-)$ is the same, therefore we have the equality

$$W_+(h_{++}) = W_{\text{gWZ}}(\Gamma_{\text{down}}^{-1}(f_R)) = W_{\text{gWZ}}(f_R) + W_B(\Gamma_{\text{up}}, \Gamma_{\text{down}}). \quad (3.43)$$

¹⁰In an analogous fashion to the matrix Riemann-Hilbert problem, we can have right and left decompositions of the function f . Namely, we can consider functions $\tilde{\Gamma}_{\text{up/down}}$ such that $\tilde{\Gamma}_{\text{up}}(\tilde{\Gamma}_{\text{down}}(x^-)) = \Gamma(x^-)$ in the real line. In general, $\tilde{\Gamma}_{\text{up/down}} \neq \Gamma_{\text{up/down}}$.

¹¹Finding a physically relevant explicit solution to (3.40) seems to be hard. On the other hand one can find solutions in terms of meromorphic functions. For example, $\Gamma_{\text{down}}(x) = \frac{\epsilon}{1-x_3^2} \frac{(x-a)^2}{(x-ix_1)(x-ix_2)}$, $\Gamma_{\text{up}}(x) = \frac{ax-b}{x+ix_3}$ and $\Gamma(x) = \frac{\epsilon}{1+x^2}$ is a solution to (3.40), where $a = \frac{i}{2}(x_1 + x_2 + (x_1 - x_2)x_3)$, $b = \frac{1}{2}(x_1 - x_2 + (x_1 + x_2)x_3)$, $x_1, x_2, x_3 > 0$ and ϵ is an arbitrary real parameter.

Using (3.38), (3.43) we get

$$W_B(\Gamma_{\text{up}}, \Gamma_{\text{down}}) = \int d^2x \partial_- f_R \frac{(\Gamma_{\text{down}}^{-1})''}{(\Gamma_{\text{down}}^{-1})'} \partial_- \left(\frac{\partial_+ f_R}{\partial_- f_R} \right). \quad (3.44)$$

Now, introducing new variables $y^- = f_R(x^+, x^-)$, $y^+ = x^+$ one can get¹²

$$W_B(\Gamma_{\text{up}}, \Gamma_{\text{down}}) = \int dy^- \frac{\partial}{\partial y^-} \log((\Gamma_{\text{down}}^{-1})'(y^-)) \log(\Gamma'(\Gamma^{-1}(y^-))). \quad (3.45)$$

Finally introducing a coordinate $s = \Gamma^{-1}(y^-)$ and using that $(\Gamma_{\text{down}}^{-1})'(\Gamma(s)) = 1/\Gamma'_{\text{down}}(\Gamma_{\text{up}}(s))$ and $\Gamma'(s) = \Gamma'_{\text{down}}(\Gamma_{\text{up}}(s))\Gamma'_{\text{up}}(s)$ we obtain¹³

$$W_B(\Gamma_{\text{up}}, \Gamma_{\text{down}}) = \int ds \log(\Gamma'_{\text{down}}(\Gamma_{\text{up}}(s))) \frac{\partial}{\partial s} \log(\Gamma'_{\text{up}}(s)). \quad (3.46)$$

Therefore the effective action in the retarded gauge is

$$W_+(h_{++}) = \int d^2x \left(\frac{\partial_-^2 f_R \partial_+ f_R}{(\partial_- f_R)^2} - \frac{(\partial_-^2 f_R)^2 \partial_+ f_R}{(\partial_- f_R)^3} \right) + \int ds \log(\Gamma'_{\text{down}}(\Gamma_{\text{up}}(s))) \frac{\partial}{\partial s} \log(\Gamma'_{\text{up}}(s)). \quad (3.47)$$

The bulk term is manifestly real, while the boundary term is complex, and, in particular, contains the imaginary piece of the effective action.

In appendix 3.6, we review a connection between gauge theory and gravity in two dimensions [138, 139, 140], and phrase (3.40) in terms of a matrix Riemann-Hilbert problem, in the hope that this simple connection might be useful in finding explicit solutions of the functional Riemann-Hilbert problem.

¹²To arrive at this formula we need two steps. At step 1 we define the inverse function $f_R^{-1}(\cdot, \cdot)$ by $f_R^{-1}(x^+, f_R(x^+, x^-)) = x^-$ and notice that $\int d^2x \partial_- f_R = \int d^2y$ and $\partial_- = (\partial_- f_R) \partial / \partial y^- = (\partial f_R^{-1} / \partial y^-)^{-1} \partial / \partial y^-$ and $\partial_+ f_R / \partial_- f_R = -\partial f_R^{-1} / \partial y^+$. At step 2 we integrate over y^+ and use that $\partial f_R^{-1} / \partial y^- (+\infty, y^-) = 1/\Gamma'(\Gamma^{-1}(y^-))$ and $\partial f_R^{-1} / \partial y^- (-\infty, y^-) = 1$. It was crucial here to assume that $f_R(x^+, x^-)$ is invertible for all x^+ .

¹³The expression (3.45) is very similar to formula (5.23) in [150]. The reason for the similarity of the results is puzzling to us and is an interesting open question.

3.5 Appendix A. Boundary conditions on induced currents and alternative derivation of the boundary actions

In this appendix we derive the effective action for non-Abelian and gravitational cases using the anomaly equations. We start with the non-Abelian case. We define $J_\mu \equiv \delta W / \delta A_\mu$; then the anomaly equations read [142]¹⁴

$$\begin{cases} \partial_\mu J^\mu + [A_\mu, J^\mu] = 0, \\ \varepsilon^{\mu\nu} (\partial_\mu J_\nu + [A_\mu, J_\nu]) = \varepsilon^{\mu\nu} F_{\mu\nu}. \end{cases} \quad (3.48)$$

Working in the light-cone cone coordinates x^\pm and choosing the axial gauge $A_- = 0$, we get $\partial_-(A_+ - J_+) = 0$ and $(\varepsilon^{-+} = 1)$

$$\partial_- A_+ + \partial_+ J_- - [J_-, A_+] = 0. \quad (3.49)$$

Parametrizing $A_+ = g^{-1} \partial_+ g$ one can find that the general solution of (3.49) is

$$J_- = -g^{-1} \partial_- g - g^{-1} j_- g, \quad (3.50)$$

where $j_- = j_-(x^-)$ is, at this stage, an arbitrary complex matrix function, which depends only on x^- , and has to be fixed by additional physical arguments. On the other hand the variation of the effective action is

$$\delta W(A_+) = \int d^2x \operatorname{Tr}(J_- \delta A_+). \quad (3.51)$$

¹⁴To restore the unimportant overall factor in front of the effective action one needs to replace $\varepsilon^{\mu\nu} F_{\mu\nu} \rightarrow \frac{\varepsilon^{\mu\nu}}{2\pi} F_{\mu\nu}$.

As we will see below, it is exactly the term $g^{-1}j_-g$ in the current J_- which is responsible for the imaginary part of the effective action.

In order to fix $j_-(x^-)$ we use the ‘‘analyticity’’ argument. Namely we say that the induced current ${}_{\text{out}}\langle J_-(x^+, x^-)\rangle_{\text{in}}$ must satisfy the analytical (spectral) boundary conditions¹⁵:

$${}_{\text{out}}\langle J_-(x^+, x^-)\rangle_{\text{in}} \rightarrow \begin{cases} J_{\text{up}}(x^-), & x^+ \rightarrow +\infty, \\ J_{\text{down}}(x^-), & x^+ \rightarrow -\infty, \end{cases} \quad (3.52)$$

where $J_{\text{up}}(x^-)$ and $J_{\text{down}}(x^-)$ are complex matrix functions analytic in the upper and lower x^- half-planes correspondingly¹⁶.

Now we return to determining j_- in the expression for the induced current. Working in the retarded gauge $g_R(x^+, x^-) \equiv P \exp \int_{-\infty}^{x^+} dy^+ A_+(y^+, x^-)$ and using (3.52) one finds

$$j_{-R}(x^-) = -\partial_- \Omega_{\text{down}} \Omega_{\text{down}}^{-1}, \quad (3.53)$$

where Ω_{down} and Ω_{up} are matrices analytic in the lower and upper half-planes, and solve the matrix Riemann-Hilbert problem

$$\Omega_{\text{down}}(x^-) \Omega_{\text{up}}(x^-) = P \exp \int_{-\infty}^{+\infty} dy^+ A_+(y^+, x^-). \quad (3.54)$$

Correspondingly we find $J_{\text{up}}(x^-) = -\Omega_{\text{up}}^{-1} \partial_- \Omega_{\text{up}}$ and $J_{\text{down}}(x^-) = \partial_- \Omega_{\text{down}} \Omega_{\text{down}}^{-1}$.

¹⁵Although $J_-(x^+, x^-)$ is a hermitian operator, the matrix element ${}_{\text{out}}\langle J_-(x^+, x^-)\rangle_{\text{in}}$ can be complex valued, as we are not computing an expectation value of the current for a given state, but rather evaluating a transition amplitude between states without particles in the past and without particles in the future.

¹⁶We can justify (3.52) as follows. First, we checked (3.52) diagrammatically in perturbation theory, to third order in the background field. The other general argument invokes consideration of the correlation function ${}_{\text{out}}\langle 0 | \bar{\psi}_+(y^+, y^-) \psi_+(x^+, x^-) | 0 \rangle_{\text{in}}$, where $x^+ \rightarrow -\infty$. In this limit $\psi_+(x^+, x^-)$ is a free field and we have $\psi_+(-\infty, x^-) = \sum_{p>0} (a_p e^{ipx^-} + a_p^\dagger e^{-ipx^-})$. As $a_p | 0 \rangle_{\text{in}} = 0$ we see that only e^{-ipx^-} modes survive. These modes define an analytic function in x^- in the lower half plane because e^{-ipx^-} decays when $p > 0$ and $\text{Im } x^- < 0$. This argument can be applied for any operator $O(\psi_+)$, to show that a correlation function $\langle \dots O(-\infty, x^-) \rangle$ is analytic in x^- in the lower half-plane.

Notice that in the spectral gauge (3.24) we have $j_{-S}(x^-) = 0$. From this it follows that, in the spectral gauge, the effective action is the WZNW action (3.25), evaluated at g_S , and there are no boundary terms. Now, as we determined the current

$$J_- = -g_R^{-1} \partial_- g_R - g_R^{-1} j_{-R} g_R, \quad (3.55)$$

one can check that the variation of $W_+(A_+)$ (see (3.17) and (3.31)) indeed equals to (3.51).

In the gravitational case everything is similar to the non-Abelian case. In the light-cone coordinates and the axial gauge $h_{--} = 0$, the anomaly equation reads [141]¹⁷

$$(\partial_+ - h_{++} \partial_- - 2(\partial_- h_{++})) T_{--} = -2\partial_-^3 h_{++}. \quad (3.56)$$

Parametrizing h_{++} by $f(x^+, x^-)$, with $(\partial_+ - h_{++} \partial_-)f = 0$, the general solution of the equation (3.56) is

$$T_{--}(x^+, x^-) = -2\mathcal{D}_- f + (\partial_- f)^2 t_-(f), \quad (3.57)$$

where we define the Schwarzian

$$\mathcal{D}_- f \equiv \frac{\partial_-^3 f}{\partial_- f} - \frac{3}{2} \frac{(\partial_-^2 f)^2}{(\partial_- f)^2} \quad (3.58)$$

and $t_-(f)$ is at this stage is an arbitrary complex function, which has to be fixed by additional physical arguments¹⁸. So analogously to the non-Abelian case we say that the induced current ${}_{\text{out}}\langle T_{--}(x^+, x^-) \rangle_{\text{in}}$ must satisfy the analytical (spectral) boundary

¹⁷To restore the overall factor in front of the effective action one needs to replace $-2\partial_-^3 h_{++} \rightarrow \frac{1}{24\pi} \partial_-^3 h_{++}$.

¹⁸The logic is very similar to that of the paper [151], where the term $t_-(f)$ in the stress-energy tensor is fixed by choosing a particular state.

conditions:

$$\text{out} \langle T_{--}(x^+, x^-) \rangle_{\text{in}} \rightarrow \begin{cases} T_{\text{up}}(x^-), & x^+ \rightarrow +\infty, \\ T_{\text{down}}(x^-), & x^+ \rightarrow -\infty, \end{cases} \quad (3.59)$$

where $T_{\text{up}}(x^-)$ and $T_{\text{down}}(x^-)$ are some complex functions analytic in the upper and lower x^- half-planes correspondingly. Again, working in the retarded gauge, defined by the condition $f_R(x^+ \rightarrow -\infty, x^-) = x^-$ we find that¹⁹

$$t_{-R}(f) = -2\mathcal{D}_f \Gamma_{\text{down}}^{-1}(f), \quad (3.60)$$

where $\Gamma_{\text{up}}(x^-)$ and $\Gamma_{\text{down}}(x^-)$ are invertible, analytic functions in the upper and lower x^- half-plane, and they are solutions of the functional Riemann-Hilbert problem ($\Gamma(x^-) \equiv f_R(+\infty, x^-)$)

$$\Gamma_{\text{down}}(\Gamma_{\text{up}}(x^-)) = \Gamma(x^-). \quad (3.61)$$

We have $T_{\text{up}}(x^-) = -2\mathcal{D}_-\Gamma_{\text{up}}$ and $T_{\text{down}}(x^-) = -2\mathcal{D}_-\Gamma_{\text{down}}^{-1}$ and we again notice that $t_{-S}(f) = 0$ in the spectral gauge f_S , defined in (3.39), which leads to the formula (3.42).

Having the expression for the current $T_{--} = -2\mathcal{D}_-\Gamma_{\text{down}}^{-1}(f_R)$, we can check that the variation of (3.47) is indeed equal to

$$\delta W(h_{++}) = \int d^2x T_{--} \delta h_{++}. \quad (3.62)$$

¹⁹It is convenient here to use the composition formula for the Schwarzian: $\mathcal{D}_x g(f) = \mathcal{D}_x f + (\partial_x f)^2 \mathcal{D}_f g$.

3.6 Appendix B. Gauge-gravity duality in two dimensions

In this appendix, we review the duality between 2-dimensional gravity and $\text{SL}(2, \mathbb{C})$ gauge theory [138, 139, 140]. We find it useful, as the functional Riemann-Hilbert problem can be related to $\text{SL}(2, \mathbb{C})$ matrix Riemann-Hilbert problem.²⁰

The main idea is to consider the gauge theory on a nontrivial background, and study one particular component of the gauge field. The gauge field has three flavor indices and two spacetime indices, A_μ^a , $a = +, 0, -$ (a new occurrence of \pm , unrelated to the others in the paper) and $\mu = +, -$. Now, instead of fixing the axial gauge $A_-^a = 0$, we partially fix the gauge by setting

$$A_-^+ \equiv T_{--}, \quad A_-^- = 1, \quad A_-^0 = 0. \quad (3.63)$$

It turns out that the remaining gauge freedom on the component A_-^+ acts as the Virasoro generators on a stress tensor T_{--} . Thus, there is a beautiful duality between a component of a gauge field and the stress tensor of a certain gravitational theory. To complete the duality, one notices that the anomaly equations for the gauge field A are equivalent to the anomaly equations for a metric g_{++} , if we identify the induced current in the gauge theory with the metric in the gravitational theory, $J_+^- = g_{++}$.

In terms of the action functionals, for the $\text{SL}(2, \mathbb{C})$ non-Abelian gauge theory one can establish a relation

$$W_{\text{WZ}}(h) = W_{\text{gWZ}}(g_{++}), \quad (3.64)$$

²⁰We need to extend the gauge group to be complex valued, as we are interested in both real and imaginary parts of the action. Originally the duality was found using $\text{SL}(2, \mathbb{R})$ gauge group. The only new subtleties arise in treating integrations by parts, but, as long as we use the spectral gauge condition, the formulas are similar to the ones in the literature.

where the Wess-Zumino action and gravitational Wess-Zumino actions are given by the formulas

$$\begin{aligned} W_{\text{gWZ}}(g_{++}) &= \frac{1}{4} \int d^2x \left(\frac{\partial_-^2 f \partial_+ \partial_- f}{(\partial_- f)^2} - \frac{(\partial_-^2 f)^2 \partial_+ f}{(\partial_- f)^3} \right), \\ W_{\text{WZ}}(h) &= \frac{1}{2} \int_0^1 dt d^2x \text{Tr}(h^{-1} \dot{h} [h^{-1} \partial_- h, h^{-1} \partial_+ h]), \end{aligned} \quad (3.65)$$

and the $\text{SL}(2, \mathbb{C})$ matrix $h(x^+, x^-, t)$ and the metric $g_{++}(x^+, x^-)$ are related as follows:

$$\begin{aligned} A_- = h^{-1} \partial_- h &= \begin{pmatrix} 0 & T_{--} \\ 1 & 0 \end{pmatrix}, \quad J_+^- = (-h^{-1} \partial_+ h)_{21} = g_{++}, \quad (\partial_+ - g_{++} \partial_-) f = 0, \\ \partial_+ T_{--} - g_{++} \partial_- T_{--} - 2(\partial_- g_{++}) T_{--} &= -\frac{1}{2} \partial_-^3 g_{++}. \end{aligned} \quad (3.66)$$

One can prove these relations using a nice parametrization for the matrix h :

$$h = \begin{pmatrix} a & \partial_- a \\ b & \partial_- b \end{pmatrix}, \quad \text{with} \quad a \partial_- b - b \partial_- a = 1. \quad (3.67)$$

In this parametrization one has $g_{++} = a \partial_+ b - b \partial_+ a$ and $T_{--} = \partial_-^2 a / a = \partial_-^2 b / b$ and $f = \mathcal{F}(a/b)$, where \mathcal{F} is an arbitrary invertible function. Thus, in terms of h , we can find the characteristic function f . It is interesting to understand whether this makes a connection between functional and matrix Riemann-Hilbert problems.

3.7 Appendix C. Non-Abelian and gravitational corrections to Caldeira-Leggett formula

In the case of a weak non-Abelian field profile, we may try to solve the matrix Riemann-Hilbert problem perturbatively

$$\Omega_{\text{down}}(x^-)\Omega_{\text{up}}(x^-) = \Omega(x^-), \quad (3.68)$$

where $\Omega(x^-) \equiv P \exp \int_{-\infty}^{\infty} A_+(y^+, x^-) dy^+$ and we assume the following perturbative decomposition for Ω_{down} and Ω_{up} :

$$\Omega_{\text{up}} = \mathbb{1} + \Omega_{\text{up}}^{(1)} + \Omega_{\text{up}}^{(2)} + \dots, \quad \Omega_{\text{down}} = \mathbb{1} - \Omega_{\text{down}}^{(1)} - \Omega_{\text{down}}^{(2)} + \dots \quad (3.69)$$

Expanding $\Omega(x^-)$ to first order we get

$$\Omega_{\text{up}}^{(1)}(x^-) - \Omega_{\text{down}}^{(1)}(x^-) = \omega(x^-), \quad (3.70)$$

where $\omega(x^-) \equiv \int_{-\infty}^{\infty} A_+(y^+, x^-) dy^+$, thus

$$\Omega_{\text{up}}^{(1)} = \omega_{\text{up}}(x^-), \quad \Omega_{\text{down}}^{(1)} = \omega_{\text{down}}(x^-), \quad (3.71)$$

where $\omega_{\text{up/down}}(x^-)$ are given in (3.9). At second order we have

$$\Omega_{\text{up}}^{(2)} - \Omega_{\text{down}}^{(2)} = \int_{-\infty}^{+\infty} dy_1^+ \int_{-\infty}^{y_1^+} dy_2^+ \text{Tr}(A_+(y_1^+, x^-)A_+(y_2^+, x^-)) + \omega_{\text{down}}\omega_{\text{up}}, \quad (3.72)$$

where we used (3.71), and so we have just a scalar Riemann-Hilbert problem, which we can solve explicitly. Now plugging this perturbative decomposition in the

2-form (3.31) we obtain

$$\begin{aligned} \text{Im } W_B(\Omega_{\text{up}}, \Omega_{\text{down}}) = & \text{Im} \int dx^- \text{Tr} \left(\omega_{\text{down}} \partial_- \omega_{\text{up}} + \right. \\ & \left. + \Omega_{\text{down}}^{(2)} \partial_- \omega_{\text{up}} + \omega_{\text{down}} \partial_- \Omega_{\text{up}}^{(2)} - \frac{1}{2} (\omega_{\text{up}} \partial_- \omega_{\text{down}}^2 + \omega_{\text{down}} \partial_- \omega_{\text{up}}^2) + \dots \right), \end{aligned} \quad (3.73)$$

where the term in the first line is the standard Caldeira-Leggett formula, and the terms in the second line are the first perturbative corrections to it, cubic in A_+ . Notice that, perturbatively, it is clear that the imaginary part of W_B does not depend on the t -interpolation.

Now, in analogy with the non-Abelian case, we can solve the functional Riemann-Hilbert problem perturbatively. This assumes that the gravitational field is weak. It is convenient to write $\Gamma_{\text{up/down}}(x^-) = x^- \pm \gamma_{\text{up/down}}(x^-)$ and $\Gamma(x^-) = x^- + \gamma(x^-)$, then for (3.40) we have

$$\gamma_{\text{up}}(x^-) - \gamma_{\text{down}}(x^- + \gamma_{\text{up}}(x^-)) = \gamma(x^-). \quad (3.74)$$

Then writing a perturbative decomposition for $\gamma_{\text{up/down}}$

$$\gamma_{\text{up}} = \gamma_{\text{up}}^{(1)} + \gamma_{\text{up}}^{(2)} + \dots, \quad \gamma_{\text{down}} = \gamma_{\text{down}}^{(1)} + \gamma_{\text{down}}^{(2)} + \dots \quad (3.75)$$

we find at the first and the second order

$$\begin{aligned} \gamma_{\text{up}}^{(1)}(x^-) - \gamma_{\text{down}}^{(1)}(x^-) &= \gamma(x^-), \\ \gamma_{\text{up}}^{(2)}(x^-) - \gamma_{\text{down}}^{(2)}(x^-) &= \gamma_{\text{up}}^{(1)}(x^-) \partial_- \gamma_{\text{down}}^{(1)}(x^-). \end{aligned} \quad (3.76)$$

So we see that step by step we just need to solve the scalar Riemann-Hilbert problem, which has the explicit solution (3.9). Thus, the boundary action (3.46) reads

$$W_B = \int dx^- \left(\gamma_{\text{down}}^{(1)} \partial_-^3 \gamma_{\text{up}}^{(1)} - ((\partial_- \gamma_{\text{up}}^{(1)})^2 \partial_-^2 \gamma_{\text{down}}^{(1)} + (\partial_- \gamma_{\text{down}}^{(1)})^2 \partial_-^2 \gamma_{\text{up}}^{(1)} - (\partial_-^2 \gamma_{\text{down}}^{(1)})^2 \gamma_{\text{up}}^{(1)} + \dots) \right). \quad (3.77)$$

We also checked this result using Feynman diagrams.

Chapter 4

Tensor Models

This chapter is an edited version of ref. [31] and [152] written in collaboration with Simone Giombi and Igor Klebanov.

4.1 Introduction

An important tool in theoretical physics is the study of certain models in the limit where they have a large number of degrees of freedom. Several different broad classes of such “large N limits” have been explored. Perhaps the most tractable large N limit applies to theories where the degrees of freedom transform as N -component vectors under a symmetry group. A well-known example is the $O(N)$ symmetric theory of N scalar fields ϕ^a in d dimensions with interaction $g(\phi^a\phi^a)^2$ (for reviews see [6, 15]). It is exactly solvable in the large N limit where gN is held fixed, since summation over the necessary class of bubble diagrams is not hard to evaluate. Another famous class of examples are models of interacting $N \times N$ matrix fields, so that the number of degrees of freedom scales as N^2 ; here one can introduce single-trace interactions like $g\text{tr}\phi^4$. A significant simplification occurs in the 't Hooft large N limit where gN is held fixed: the perturbative expansion is dominated by the planar diagrams [24]. While

such planar matrix theories are exactly solvable in some special low-dimensional cases [25], the problem does not appear to be solvable in general.

In view of these classic results, it is natural to study theories with rank- m tensor degrees of freedom $\phi^{a_1 \dots a_m}$, where each index takes N values so that the net number of degrees of freedom scales as N^m [26, 27, 28]. Since the complexity of taking the large N limit increases from $m = 1$ to $m = 2$, one might expect that the tensor models with $m > 2$ are much more difficult than the matrix models. However, Gurau and collaborators [153, 154, 155, 156, 157, 29] have discovered that, by adjusting the interactions appropriately, it is possible to find models with $m > 2$ where a large N limit is solvable. The perturbative expansion is then dominated by a special class of “melon diagrams” (for some examples with $m = 3$ see figures 4.1).

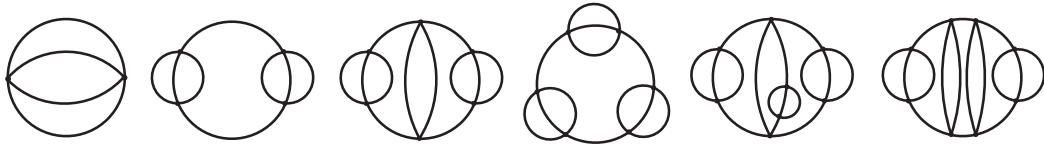


Figure 4.1: Some melonic contributions to the free energy.

Gurau’s original example [153] was a so-called colored tensor model where complex fermionic tensors $\psi_A^{a_1 \dots a_m}$ carry an additional label A which takes $m+1$ possible values $0, 1, \dots, m$. In the smallest non-trivial case $m = 3$ this model has the interaction

$$g \psi_0^{abc} \psi_1^{ade} \psi_2^{fbe} \psi_3^{fdc} + \text{c.c.} \quad (4.1)$$

The label A may be thought of as corresponding to the 4 different vertices of a tetrahedron. Each pair of fields has one pair of indices in common, just as every pair of vertices of a tetrahedron is connected by one edge. The interaction (4.1) has $U(N)^6$ symmetry, where each $U(N)$ corresponds to one of the edges of the tetrahedron. Including the quadratic piece $\psi_A^{abc} \bar{\psi}_A^{abc}$ and integrating over the fermionic tensors with interaction (4.1) generates a summation over a particular class of 3-dimensional in-

trinsic geometries made out of tetrahedra. Apart from this interpretation, this model is of much interest because it exhibits a novel type of large N limit, where the coupling constant is scaled so that $g^2 N^3$ is held constant, and the theory has N^3 degrees of freedom.¹ Thus, it is interesting to try generalizing Gurau’s construction² from the $d = 0$ tensor integral case to d -dimensional quantum theories. An important step in this direction was recently made by Witten [163], who studied a quantum mechanical model of colored anti-commuting tensors and observed that its large N limit is similar to that in the Sachdev-Ye-Kitaev (SYK) model [164, 165, 166, 167].

The quantum mechanical model introduced by Witten uses, in the $m = 3$ case, real fermionic tensors ψ_A^{abc} and possesses $O(N)^6$ symmetry. The action of this model is

$$S_{\text{Gurau-Witten}} = \int dt \left(\frac{i}{2} \psi_A^{abc} \partial_t \psi_A^{abc} + g \psi_0^{abc} \psi_1^{ade} \psi_2^{fbe} \psi_3^{fdc} \right), \quad (4.2)$$

It was shown [163, 168] that, in the large N limit of this model only the “melonic” Feynman graphs survive, just as in the SYK model. Very importantly, gauging the $O(N)^6$ symmetry gets rid of the non-singlet states. This removes a crucial conceptual obstacle in the search for the gravity dual of this model, in the spirit of the AdS/CFT correspondence for gauge theories [169, 170, 171].

In work subsequent to [153] it was shown that the “coloring” is not necessary for obtaining a large N limit where the melon graphs dominate, and theories of just one complex bosonic tensor were shown to have this property [29, 172, 173, 174]. More recently, a model of a single real rank-3 tensor with $O(N)^3$ symmetry was studied by Carrozza and Tanasa and shown to possess a melonic large N limit [30]. We will

¹The N^3 scaling of the degrees of freedom is also found for 6-dimensional CFTs on N coincident M5-branes [158, 159]. An interpretation of this scaling in terms of M2-branes with three holes attached to three different M5-branes, thus giving rise to tri-fundamental matter, was proposed in section 5.2 of [160]. One may wonder if there is a precise connection between theories on M5-branes and tensor models.

²The random tensor models also have connections with the “holographic space-time” approach to quantum gravity [161, 162].

study such a theory of one real rank- m fermionic tensor with interaction ψ^{m+1} . For $m = 3$ the interaction assumes explicit form

$$V_{O(N)^3} = \frac{1}{4}g\psi^{a_1b_1c_1}\psi^{a_1b_2c_2}\psi^{a_2b_1c_2}\psi^{a_2b_2c_1} \quad (4.3)$$

The three indices are distinguishable, and the theory has $O(N)^3$ symmetry under

$$\psi^{abc} \rightarrow M_1^{aa'}M_2^{bb'}M_3^{cc'}\psi^{a'b'c'}, \quad M_1, M_2, M_3 \in O(N). \quad (4.4)$$

Thus, the real field ψ^{abc} transforms in the tri-fundamental representation of $O(N)^3$. Such an $O(N)^3$ fermionic model does not work in $d = 0$ because the invariant quadratic term vanishes, $\psi^{abc}\psi^{abc} = 0$, but in $d = 1$ there is a non-trivial model with the kinetic term $\frac{i}{2}\psi^{abc}\partial_t\psi^{abc}$. We will also consider analogous bosonic models where the anti-commuting field in (4.3) is replaced by a commuting one, ϕ^{abc} . Then in $d = 0$ we may add the quadratic term $\phi^{abc}\phi^{abc}$, while in $d > 0$ the standard kinetic term $\frac{1}{2}\partial_\mu\phi^{abc}\partial^\mu\phi^{abc}$. While the bosonic potential is generally not positive definite, the model may still be studied in perturbation theory. One may hope that, as in the matrix models, the restriction to leading large N limit can formally stabilize the theory.

In section 4.2 we study the index structure of the expansion of the path integral in g and demonstrate that the large N limit is dominated by the melon diagrams.

³ The argument, which applies to both the $O(N)^3$ fermionic and bosonic models, contains a new ingredient compared to other models. In $O(N)^3$ models with complex tensors, which were studied in [29], each index loop necessarily passed through an even number of vertices, but in models with real tensors a loop can also pass through

³We constructed the argument before the existence of [30] was pointed out to us, so it may provide an independent perspective on the $O(N)^3$ theories.

an odd number of vertices. However, the diagrams dominant in the large N limit do not contain any index loops that pass through 3 vertices.

In section 4.3 we show that the $O(N)^3$ fermionic theory with interaction (4.3) is equivalent to the SYK model in the large N limit. We comment on the spectrum of operators in the gauged tensor models, pointing out that it appears to be vastly bigger than the “single Regge trajectory” which has been studied in the SYK model so far [175, 176, 177, 178]. In section 4.3.1 we write down a $U(N)^2 \times O(N)$ symmetric quantum mechanical model with a complex fermionic 3-tensor. We study the large N limit of this model and derive the scaling dimensions of two-particle operators. We argue that this model is related in the large N limit to the generalization of SYK model which contains complex fermions [179, 180].

It is of obvious interest to extend the SYK and tensor models to dimensions higher than $d = 1$. Such extensions were considered in [31, 181, 182, 183, 184]. Some of our work in this chapter will be following the observation that, in a theory of a rank-3 bosonic tensor field one may introduce quartic interactions with $O(N)^3$ symmetry [31]. Although the action is typically unbounded from below, such a QFT is perturbatively renormalizable in $d = 4$, so it may be studied using the $4 - \epsilon$ expansion [3].

In this chapter we explore the $4 - \epsilon$ expansion and compare it with the large N Schwinger-Dyson equations, finding perfect agreement. We present results on the large N scaling dimensions of two-particle operators of arbitrary spin as a function of d , found using the Schwinger-Dyson equations. A salient feature of the large N spectrum of this theory in $d < 4$ is that the lowest scalar operator has a complex dimension of the form $\frac{d}{2} + i\alpha(d)$.⁴ We confirm this using the $4 - \epsilon$ expansion in section 4.4.3. In that calculation it is necessary to include the mixing of the basic

⁴However, the scaling dimension of the lowest scalar operator is real for $4 < d < 4.155$.

“tetrahedron” interaction term,

$$O_t(x) = \phi^{a_1 b_1 c_1} \phi^{a_1 b_2 c_2} \phi^{a_2 b_1 c_2} \phi^{a_2 b_2 c_1}, \quad (4.5)$$

with two additional $O(N)^3$ invariant terms: the so-called pillow and double-sum invariants (4.76). The coefficients of these additional terms turn out to be complex at the “melonic” large N IR fixed point; as a result, the scaling dimension of the leading operator $\phi^{abc}\phi^{abc}$ is complex. A similar phenomenon for the $O(N)^2$ symmetric theory of a matrix ϕ^{ab} is discussed in the Appendix A. In that case it is necessary to include the $O(N)^2$ invariant double-trace operator $(\phi^{ab}\phi^{ab})^2$ whose coefficient is complex at the IR fixed point; as a result, the scaling dimension of operator $\phi^{ab}\phi^{ab}$ is complex.

We also extend our results to rank $q - 1$ tensors with ϕ^q interactions. In each dimension d it is found that the two-particle mode with complex scaling dimension disappears for q greater than some critical value q_{crit} (for example, in $d = 2$, $q_{\text{crit}} \approx 64.3$ [184]). We study the spectrum of bilinear operators in the large N bosonic theory with $q = 6$ in $3 - \epsilon$ dimensions and point out that it is free of the problem with the complex dimension of ϕ^2 for $\epsilon < 0.03$. Thus, this theory is a candidate for a stable large N CFT, albeit in a non-integer dimension. However, an obvious danger, which we have not investigated, is that the coupling constants for some of the $O(N)^5$ invariant sextic operators may be complex in $d = 3 - \epsilon$.

A more promising direction towards finding melonic CFTs in $d \geq 2$ is to explore the supersymmetric versions of tensor or SYK-like models [31, 184] and a successful construction of such theory in $d = 2$ was achieved recently [184].

4.2 Melonic Dominance in the $O(N)^3$ Symmetric Theories

The arguments in this section, which are analogous to those in [30], apply to the $O(N)^3$ models, both in the fermionic and bosonic cases and for any d . We will ignore the coordinate dependence and just focus on the index structure.



Figure 4.2: The resolved propagator $\langle \phi^{abc} \phi^{a'b'c'} \rangle = \delta^{aa'} \delta^{bb'} \delta^{cc'}$.

The propagator of the ϕ^{abc} field has the index structure depicted in figure 4.2. The three colored wires (also called “strands” in the earlier literature) represent propagation of the three indices of the ϕ^{abc} field. The vertex has the index structure depicted in the figure 4.3. There are three equivalent ways to draw the vertex; for concreteness we will use the first way. “Forgetting” the middle lines we obtain the standard matrix model vertex as in figure 4.4.

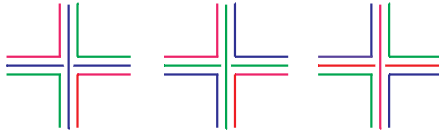


Figure 4.3: Three equivalent ways to represent the resolved vertex.



Figure 4.4: The standard matrix model vertex obtained after “forgetting” the middle lines.

Let us consider the vacuum Feynman diagrams. Examples of melonic and non-melonic diagrams with their resolved representations and fat (double-line) subgraphs are depicted in figures 4.5 and 4.6.



Figure 4.5: A melonic second-order diagram and all its fat subgraphs.

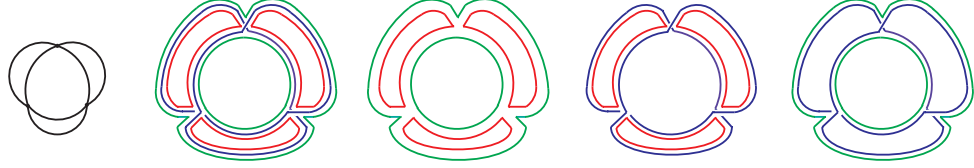


Figure 4.6: A non-melonic third-order diagram and all its fat subgraphs.

Each resolved Feynman diagram consists of loops of three different colors and is proportional to $N^{f_{\text{total}}}$, where f_{total} is the total number of index loops. Suppose we “forget” all wires of some particular color in our diagram, as in the pictures 4.5 and 4.6. Then we get a double-line fat graph (ribbon graph) of the kind one finds in matrix models. One can count the number of all index loops f in this fat graph using the Euler characteristic χ

$$f = \chi + e - v, \quad (4.6)$$

where e is the number of edges and v is the number of vertices. In our theory we obviously have $e = 2v$, therefore $f = \chi + v$. We can forget red, blue or green wires, and in each case we get a fat graph made of the remaining two colors. If we forget, say, all red wires, then using the formula (4.6) we find $f_{bg} = \chi_{bg} + v$, where $f_{bg} = f_b + f_g$ is the number of blue and green loops and χ_{bg} is the Euler characteristic of this blue-green fat graph. Analogously we get $f_{rg} = \chi_{rg} + v$ and $f_{br} = \chi_{br} + v$. Adding up all these formulas we find

$$f_{bg} + f_{rg} + f_{br} = 2(f_b + f_g + f_r) = \chi_{bg} + \chi_{br} + \chi_{rg} + 3v. \quad (4.7)$$

Thus, the total number of loops is

$$f_{\text{total}} = f_b + f_g + f_r = \frac{3v}{2} + 3 - g_{bg} - g_{br} - g_{rg}, \quad (4.8)$$

where $g = 1 - \chi/2$ is the genus of a graph. Because $g \geq 0$ we obtain

$$f_{\text{total}} \leq 3 + \frac{3v}{2}. \quad (4.9)$$

Now the goal is to show that the equality $f_{\text{total}} = 3 + 3v/2$ is satisfied only for the melonic diagrams. We will call the graphs which satisfy $f_{\text{total}} = 3 + 3v/2$ the maximal graphs. Thus we should argue that maximal graphs are necessarily melonic. We note that, due to (4.8), each double-line fat subgraph of a maximal graph has genus zero.

Now let us classify all loops in our graph according to how many vertices they pass through (a loop can pass the same vertex twice). Let us denote by $\mathcal{F}_s \geq 0$ the number of loops, which pass through s vertices. For a maximal graph

$$f_{\text{total}} = \mathcal{F}_2 + \mathcal{F}_3 + \mathcal{F}_4 + \mathcal{F}_5 + \dots = 3 + \frac{3v}{2}, \quad (4.10)$$

where we set $\mathcal{F}_1 = 0$ because we assume that there are no tadpole diagrams. Since each vertex must be passed 6 times, we also get

$$2\mathcal{F}_2 + 3\mathcal{F}_3 + 4\mathcal{F}_4 + 5\mathcal{F}_5 + \dots = 6v. \quad (4.11)$$

Combining these two equations we find

$$2\mathcal{F}_2 + \mathcal{F}_3 = 12 + \mathcal{F}_5 + 2\mathcal{F}_6 + \dots \quad (4.12)$$

Now our goal is to show that $\mathcal{F}_2 > 0$ using this formula (in fact, $\mathcal{F}_2 \geq 6$, but all we will need is that it is non-vanishing).

Let us first argue that a maximal graph must have $\mathcal{F}_3 = 0$. To have $\mathcal{F}_3 > 0$ we need a closed index loop passing through 3 vertices. Without a loss of generality we can assume that this loop is formed by the middle lines in each vertex (blue lines). The only possibility with a closed loop of an internal (blue) index, which passes through three vertices, is shown in fig. 4.7 a). After "forgetting" the color of this loop we get a fat graph in fig. 4.7 b), which is non-planar due a twisted propagator. So, a graph with $\mathcal{F}_3 > 0$ cannot be maximal. Thus, setting $\mathcal{F}_3 = 0$ in (4.12), we deduce that a maximal graph should have $\mathcal{F}_2 > 0$.

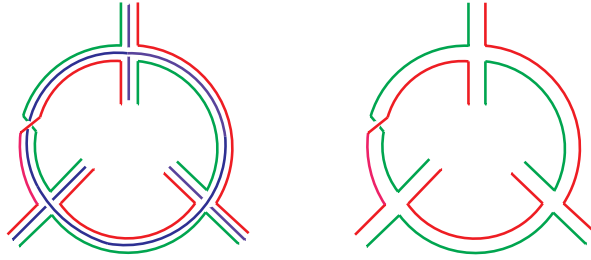


Figure 4.7: a) Local part of a graph with a middle index loop passing through 3 vertices. b) The same figure where the middle index has been “forgotten.”

Finally, we need to show that the graphs with $\mathcal{F}_2 > 0$ are melonic. To do this we will follow Proposition 3 in [157]. Without a loss of generality we assume that the loop passing through 2 vertices is formed by the middle lines in each vertex (blue lines). The only such possibility is shown in fig. 4.8 a). After "forgetting" the color of this loop we get a fat graph in fig. 4.8 b).

Now we uncolor the lines in our fat graph and cut and sew two edges as in figure 4.9. We cut two edges but did not change the number of loops; therefore, the Euler



Figure 4.8: a) Local part of a graph with a middle index loop passing through two vertices v_1 and v_2 . b) The same figure where the middle index has been “forgotten.”

characteristic of the new graph is $\chi = 4$. This is possible only if we separated our original graph into two genus zero parts. Therefore, our graph is two-particle reducible for the internal and external couples of lines. Thus, the whole unresolved graph looks like figure 4.10. Then, if graphs G' and G'' are empty we get a second-order melon graph as in figure 4.5. If they are not empty one can argue (see [157]) that they are also maximal graphs. So, we can recursively apply the same above argument to them, implying that the complete diagram is melonic.

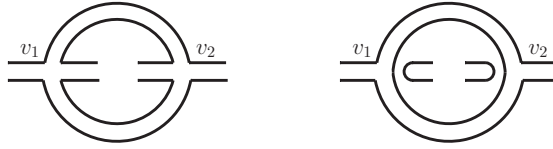


Figure 4.9: Cutting and sewing lines.

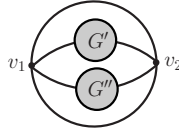


Figure 4.10: General structure of the maximal graph.

4.3 $O(N)^3$ Quantum Mechanics and the SYK Model

Using the interaction (4.3) we will now consider an $O(N)^3$ quantum mechanical model with real anti-commuting variables $\psi^{abc}(t)$ and the action

$$S = \int dt \left(\frac{i}{2} \psi^{abc} \partial_t \psi^{abc} + \frac{1}{4} g \psi^{a_1 b_1 c_1} \psi^{a_1 b_2 c_2} \psi^{a_2 b_1 c_2} \psi^{a_2 b_2 c_1} \right). \quad (4.13)$$

It has 1/4 of the degrees of freedom of the colored Gurau-Witten model (4.2). We will argue that the $O(N)^3$ model (4.13) is equivalent to the SYK model in the large N limit.

We recall that ψ^{abc} are the N^3 anticommuting fields and the indices, each of which runs from 1 to N , are treated as distinguishable. The Fermi statistics implies

$$\psi^{a_1 b_1 c_1} \psi^{a_1 b_2 c_2} \psi^{a_2 b_1 c_2} \psi^{a_2 b_2 c_1} = -\psi^{a_1 b_2 c_2} \psi^{a_1 b_1 c_1} \psi^{a_2 b_1 c_2} \psi^{a_2 b_2 c_1} . \quad (4.14)$$

After relabeling $b_1 \leftrightarrow c_2$ and $b_2 \leftrightarrow c_1$ we get the relation

$$\psi^{a_1 b_1 c_1} \psi^{a_1 b_2 c_2} \psi^{a_2 b_1 c_2} \psi^{a_2 b_2 c_1} = -\psi^{a_1 c_1 b_1} \psi^{a_1 c_2 b_2} \psi^{a_2 c_2 b_1} \psi^{a_2 c_1 b_2} . \quad (4.15)$$

This demonstrates the vanishing of the interaction term in the $O(N)$ symmetric theory with a fully symmetric or fully anti-symmetric fermionic tensor. Fortunately, in the theory with general 3-index fermionic tensors the interaction is non-trivial.

Let us return, therefore, to the theory (4.13) with $O(N)^3$ symmetry, where the three indices are distinguishable. The symmetry may be gauged by the replacement

$$\partial_t \psi^{abc} \rightarrow (D_t \psi)^{abc} = \partial_t \psi^{abc} + A_1^{aa'} \psi^{a'bc} + A_2^{bb'} \psi^{ab'c} + A_3^{cc'} \psi^{abc'} , \quad (4.16)$$

where A_i is the gauge field corresponding to the i -th $O(N)$ group. In $d = 1$ the gauge fields are non-dynamical, and their only effect is to restrict the operators to be gauge singlets. There is a sequence of such operators of the form

$$O_2^n = \psi^{abc} (D_t^n \psi)^{abc} , \quad (4.17)$$

where n is odd. This set of operators is analogous to the ‘‘single Regge trajectory’’ [175, 176, 178] found in the Sachdev-Ye-Kitaev (SYK) model [164, 165, 166, 167].

We should note, however, that theory (4.13) contains an abundance of additional ‘‘single-trace’’ $O(N)^3$ symmetric operators. A large class of them contains an even number of ψ fields without derivatives and with all indices contracted. One of such

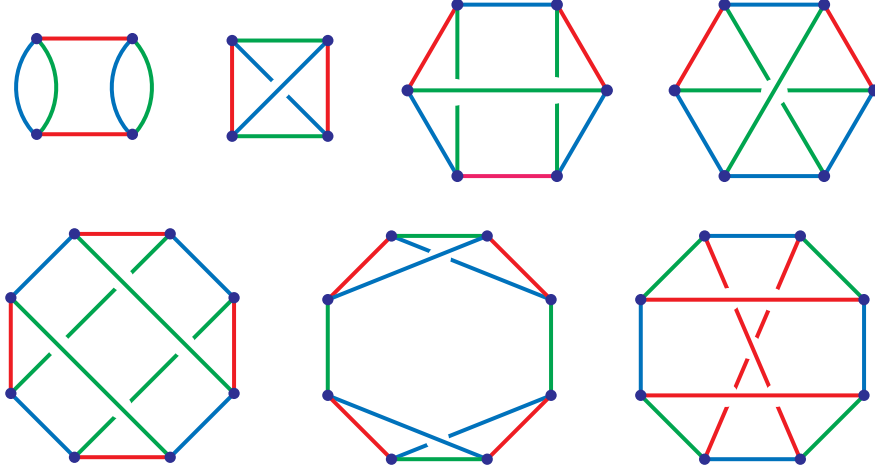


Figure 4.11: Graphical representation of different operators

ψ^4 operators is the interaction term in the action, which is related by the equation of motion to $\psi^{abc}(D_t\psi)^{abc}$. Another type of ψ^4 operator is

$$O_4 = \psi^{a_1 b_1 c_1} \psi^{a_1 b_1 c_2} \psi^{a_2 b_2 c_1} \psi^{a_2 b_2 c_2} , \quad (4.18)$$

and there are similar operators where the second and third or the first and third indices have pairwise contractions (however, in the theory where the $O(N)^3$ symmetry is gauged such operators vanish because they are squares of the gauge symmetry generators). Moving on to the higher operators we can try writing down the following ψ^6 operator:

$$O_6 = \psi^{a_1 b_1 c_1} \psi^{a_1 b_2 c_2} \psi^{a_2 b_1 c_3} \psi^{a_2 b_3 c_1} \psi^{a_3 b_2 c_3} \psi^{a_3 b_3 c_2} . \quad (4.19)$$

Due to the fermi statistics this operator actually vanishes, but an operator with ψ fields replaced by scalars ϕ is present in the bosonic model that we study in section 4.4. The following ψ^8 operator does not vanish in the fermionic model:

$$O_8 = \psi^{a_1 b_1 c_1} \psi^{a_1 b_2 c_2} \psi^{a_2 b_3 c_3} \psi^{a_2 b_4 c_4} \psi^{a_3 b_1 c_3} \psi^{a_3 b_3 c_1} \psi^{a_4 b_2 c_4} \psi^{a_4 b_4 c_2} . \quad (4.20)$$

All such operators can be represented graphically with ψ -fields corresponding to vertices and index contractions to edges (see figure 4.11). These representations are similar to the Feynman diagrams in ϕ^3 theory. A feature of the latter two operators is that each pair of ψ -fields has either one or no indices in common. We expect to find an infinite class of operators of this type – they should correspond to some number of tetrahedra glued together. Since there is no parametrically large dimension gap in the set of operator dimensions, the holographic dual of this theory should be highly curved.

Let us study some of the diagrammatics of the $O(N)^3$ quantum mechanics model (4.13). We will study the ungauged model; the effect of the gauging may be imposed later by restricting to the gauge invariant operators. The bare propagator is

$$\langle T(\psi^{abc}(t)\psi^{a'b'c'}(0)) \rangle_0 = \delta^{aa'} \delta^{bb'} \delta^{cc'} G_0(t) = \delta^{aa'} \delta^{bb'} \delta^{cc'} \frac{1}{2} \text{sgn}(t). \quad (4.21)$$

The full propagator in the large N limit receives corrections from the melonic diagrams represented in figure 4.12. Resummation of all melonic diagrams leads to the

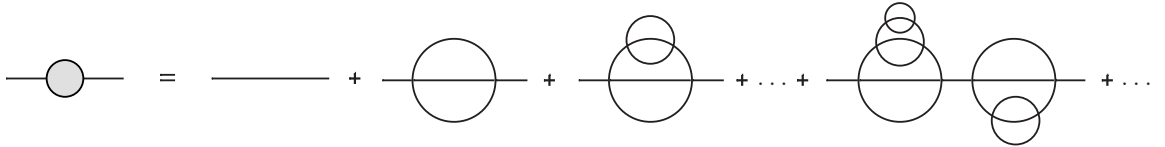


Figure 4.12: Diagrams contributing to the two-point function in the leading large N order. The line with the gray circle represents the full two-point function. Each simple line is the bare propagator.

Schwinger-Dyson equation for the two-point function

$$G(t_1 - t_2) = G_0(t_1 - t_2) + g^2 N^3 \int dt dt' G_0(t_1 - t) G(t - t')^3 G(t' - t_2), \quad (4.22)$$

represented graphically in figure 4.13. This is the same equation as derived in [175, 176, 178] for the large N SYK model. The solution to (4.22) in the IR limit is

$$G(t_1 - t_2) = -\left(\frac{1}{4\pi g^2 N^3}\right)^{1/4} \frac{\text{sgn}(t_1 - t_2)}{|t_1 - t_2|^{1/2}}. \quad (4.23)$$

To uncover the spectrum of the bilinear operators in the model, we need to study

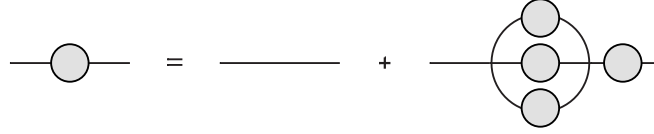


Figure 4.13: The graphical representation of the Schwinger-Dyson equation for the two-point function.

the 4-point function $\langle \psi^{a_1 b_1 c_1}(t_1) \psi^{a_1 b_1 c_1}(t_2) \psi^{a_2 b_2 c_2}(t_3) \psi^{a_2 b_2 c_2}(t_4) \rangle$. Its structure is again the same as in the large N SYK model [176, 175]:

$$\langle \psi^{a_1 b_1 c_1}(t_1) \psi^{a_1 b_1 c_1}(t_2) \psi^{a_2 b_2 c_2}(t_3) \psi^{a_2 b_2 c_2}(t_4) \rangle = N^6 G(t_{12}) G(t_{34}) + \Gamma(t_1, \dots, t_4), \quad (4.24)$$

where $\Gamma(t_1, \dots, t_4)$ is given by a series of ladder diagrams depicted in fig 4.14.

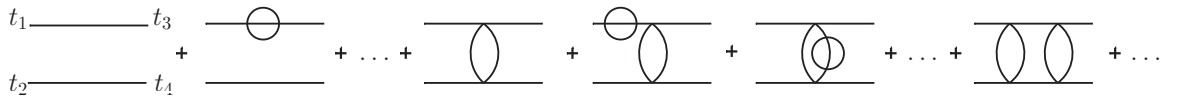


Figure 4.14: Ladder diagrams contributing to $\Gamma(t_1, \dots, t_4)$

Resumming the diagrams in fig. 4.14 one finds a contribution to $\Gamma(t_1, \dots, t_4)$ as a series of diagrams in terms of the full propagators, see fig. 4.15

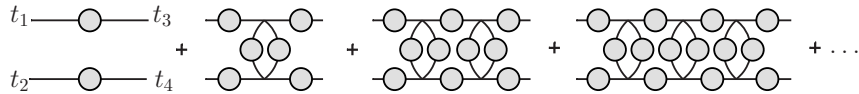


Figure 4.15: Ladder diagrams contributing to $\Gamma(t_1, \dots, t_4)$

If we denote by Γ_n the ladder with n rungs, so $\Gamma = \sum_n \Gamma_n$, we have

$$\Gamma_0(t_1, \dots, t_4) = N^3(-G(t_{13})G(t_{24}) + G(t_{14})G(t_{23})). \quad (4.25)$$

For the next coefficient one gets

$$\Gamma_1(t_1, \dots, t_4) = 3g^2 N^6 \int dt dt' (G(t_1 - t)G(t_2 - t')G(t - t')^2 G(t - t_3)G(t - t_4) - (t_3 \leftrightarrow t_4)), \quad (4.26)$$

and one can check further that

$$\Gamma_2(t_1, \dots, t_4) = -3g^2 N^3 \int dt dt' (G(t_1 - t)G(t_2 - t')G(t - t')^2 \Gamma_1(t, t', t_3, t_4) - (t_3 \leftrightarrow t_4)). \quad (4.27)$$

So, in general, one gets exactly the same recursion relation as in the SYK model

$$\Gamma_{n+1}(t_1, \dots, t_4) = \int dt dt' K(t_1, t_2; t, t') \Gamma_n(t, t', t_3, t_4), \quad (4.28)$$

where the kernel is

$$K(t_1, t_2; t_3, t_4) = -3g^2 N^3 G(t_{13})G(t_{24})G(t_{34})^2. \quad (4.29)$$

In order to find the spectrum of the two-particle operators O_2^n , following [176, 178] one has to solve the integral eigenvalue equation

$$v(t_0, t_1, t_2) = g(h) \int dt_3 dt_4 K(t_1, t_2; t_3, t_4) v(t_0, t_3, t_4), \quad (4.30)$$

where

$$v(t_0, t_1, t_2) = \langle O_2^n(t_0) \psi^{abc}(t_1) \psi^{abc}(t_2) \rangle = \frac{\text{sgn}(t_1 - t_2)}{|t_0 - t_1|^h |t_0 - t_2|^h |t_1 - t_2|^{1/2-h}}, \quad (4.31)$$

is the conformal three-point function. Then the scaling dimensions are determined by the equation $g(h) = 1$. To find $g(h)$ one can use $SL(2)$ invariance to take t_0 to infinity and just consider eigenfunctions of the form

$$v(t_1, t_2) = \frac{\text{sgn}(t_1 - t_2)}{|t_1 - t_2|^{1/2-h}}. \quad (4.32)$$

It is not hard to find $g(h)$ using two basic integrals

$$\begin{aligned} \int_{-\infty}^{+\infty} du \frac{\text{sgn}(u - t_1) \text{sgn}(u - t_2)}{|u - t_1|^a |u - t_2|^b} &= l_{a,b}^+ \frac{1}{|t_1 - t_2|^{a+b-1}}, \\ \int_{-\infty}^{+\infty} du \frac{\text{sgn}(u - t_2)}{|u - t_1|^a |u - t_2|^b} &= l_{a,b}^- \frac{\text{sgn}(t_1 - t_2)}{|t_1 - t_2|^{a+b-1}}, \\ l_{a,b}^\pm &= \beta(1 - a, a + b - 1) \pm (\beta(1 - b, a + b - 1) - \beta(1 - a, 1 - b)), \end{aligned} \quad (4.33)$$

where $\beta(x, y) = \Gamma(x)\Gamma(y)/\Gamma(x + y)$ is the Euler beta function. Plugging (4.32) into (4.30) and using (4.33), we find [176, 178]

$$g(h) = -\frac{3}{4\pi} l_{\frac{3}{2}-h, \frac{1}{2}}^+ l_{1-h, \frac{1}{2}}^- = -\frac{3 \tan(\frac{\pi}{2}(h - \frac{1}{2}))}{2(h - 1/2)}. \quad (4.34)$$

The scaling dimensions are given by the solutions of $g(h) = 1$. The first solution is exact, $h = 2$; this is the important mode dual to gravity and responsible for the quantum chaos in the model [185, 175, 176, 177, 186, 187, 188]. The further solutions are $h \approx 3.77, 5.68, 7.63, 9.60$ corresponding to the operators $\psi^{abc}(D_t^n \psi)^{abc}$ with $n = 3, 5, 7, 9$. In the limit of large n , $h_n \rightarrow n + \frac{1}{2}$. This is the expected limit $n + 2\Delta$, where $\Delta = \frac{1}{4}$ is the scaling dimension of the individual fermion.

4.3.1 Models with a Complex Fermion

Here we consider two quantum mechanical models of a complex 3-tensor ψ^{abc} . One of them is an $O(N)^3$ version of the quantum mechanical model recently studied by Gurau [168]:

$$S = \int dt \left(i\bar{\psi}^{abc} \partial_t \psi^{abc} + \frac{1}{4} g \psi^{a_1 b_1 c_1} \psi^{a_1 b_2 c_2} \psi^{a_2 b_1 c_2} \psi^{a_2 b_2 c_1} + \frac{1}{4} \bar{g} \bar{\psi}^{a_1 b_1 c_1} \bar{\psi}^{a_1 b_2 c_2} \bar{\psi}^{a_2 b_1 c_2} \bar{\psi}^{a_2 b_2 c_1} \right), \quad (4.35)$$

Another possibility is the model

$$S = \int dt \left(i\bar{\psi}^{abc} \partial_t \psi^{abc} + \frac{1}{2} g \psi^{a_1 b_1 c_1} \bar{\psi}^{a_1 b_2 c_2} \psi^{a_2 b_1 c_2} \bar{\psi}^{a_2 b_2 c_1} \right), \quad (4.36)$$

where the symmetry is enhanced to $U(N) \times O(N) \times U(N)$ because the transformations on the first and the third indices of the tensor are allowed to be $U(N)$. Models of this type have been studied in $d = 0$ [172, 173, 174]. Gauging this symmetry in the quantum mechanical model restricts the operators to the singlet sector, allowing for the existence of a gravity dual. The gauge invariant two-particle operators have the form

$$\mathcal{O}_2^n = \bar{\psi}^{abc} (D_t^n \psi)^{abc} \quad n = 0, 1, \dots, \quad (4.37)$$

which includes $\bar{\psi}^{abc} \psi^{abc}$. There is also a variety of operators made out of the higher powers of the fermionic fields similarly to the operators (4.18), (4.19), (4.20) in the $O(N)^3$ symmetric model of real fermions. As established in [172, 173, 174], the large N limit of the complex $U(N)^2 \times O(N)$ model (4.36) is once again given by the melon diagrams (the arguments are easier than in 4.2 since each index loop passes through an even number of vertices). The large N limit of this model appears to be related to

the variant of SYK model where the real fermions are replaced by the complex ones [179, 180].

Let us briefly discuss summing over melonic graphs in the model (4.36) at large N . The two-point function has the structure

$$\langle T(\bar{\psi}^{abc}(t)\psi^{a'b'c'}(0)) \rangle = \delta^{aa'}\delta^{bb'}\delta^{cc'}G(t), \quad (4.38)$$

and $G(t) = -G(-t)$. We find the same Schwinger-Dyson equation as (4.22); its solution is again (4.23) indicating that the fermion scaling dimension is $\Delta = 1/4$. Now we need to study the 4-point function $\langle \bar{\psi}^{a_1b_1c_1}(t_1)\psi^{a_1b_1c_1}(t_2)\bar{\psi}^{a_2b_2c_2}(t_3)\psi^{a_2b_2c_2}(t_4) \rangle$. It leads to the same integral eigenvalue equation as (4.30), but with kernel

$$K(t_1, t_2; t_3, t_4) = -g^2 N^3 (2G(t_{13})G(t_{24})G(t_{34})^2 - G(t_{14})G(t_{23})G(t_{34})^2). \quad (4.39)$$

Now it is possible to have not only the antisymmetric eigenfunctions as in (4.32), but also the symmetric ones

$$v(t_1, t_2) = \frac{1}{|t_1 - t_2|^{1/2-h}}. \quad (4.40)$$

This can be justified by noticing that the three point function now is $\langle \mathcal{O}_2^n(t_0)\psi^{abc}(t_1)\bar{\psi}^{abc}(t_2) \rangle$.

We see that for odd n it is antisymmetric under $t_1 \leftrightarrow t_2$, while for even n it is symmetric.

Substituting ansatz (4.40) into the integral equation, and using the integrals (4.33), we find

$$g_{\text{sym}}(h) = -\frac{1}{4\pi} l_{\frac{3}{2}-h, \frac{1}{2}}^- l_{1-h, \frac{1}{2}}^+ = -\frac{1}{2} \frac{\tan(\frac{\pi}{2}(h + \frac{1}{2}))}{h - 1/2}. \quad (4.41)$$

The scaling dimensions of the operators \mathcal{O}_2^n with even n are given by the solutions of $g_{\text{sym}}(h) = 1$. The first eigenvalue is $h = 1$, corresponding to the conserved $U(1)$ charge $\bar{\psi}^{abc}\psi^{abc}$. The additional values are $h \approx 2.65, 4.58, 6.55, 8.54$ corresponding to the operators with $n = 2, 4, 6, 8$ respectively. For large n the scaling dimensions approach $n + \frac{1}{2}$ as expected. The numerical results are in good agreement with the asymptotic formula [176]

$$h_n = n + \frac{1}{2} + \frac{1}{\pi n} + \mathcal{O}(n^{-3}) \quad (4.42)$$

for $n > 2$. For \mathcal{O}_2^n with odd n the spectrum is the same as for the two-particle operators (4.17) in the model with $O(N)^3$ symmetry.

4.4 $O(N)^3$ bosonic tensors

In this section we consider the d -dimensional field theory of a real commuting tensor field $\phi^{abc}(x)$ with distinguishable indices $a, b, c = 1, \dots, N$:

$$S = \int d^d x \left(\frac{1}{2} \partial_\mu \phi^{abc} \partial^\mu \phi^{abc} + \frac{1}{4} g \phi^{a_1 b_1 c_1} \phi^{a_1 b_2 c_2} \phi^{a_2 b_1 c_2} \phi^{a_2 b_2 c_1} \right), \quad (4.43)$$

This is the bosonic analogue of the $O(N)^3$ fermionic theory with interaction (4.3); it again has $O(N)^3$ symmetry. A feature of this theory is that the interaction potential is not bounded from below for $N > 2$. For $N = 2$ the potential may be written as a sum of squares, but for $N > 2$ we have explicitly checked that there is a negative direction. Nevertheless, we may consider formal perturbation theory in g .

The argument in section 4.2 that the melonic diagrams dominate in the large N limit applies both to the fermionic and bosonic version of the theory in any dimension d . We may therefore resum all such diagrams and derive the exact Schwinger-Dyson

equation similar to that in [154, 156, 155, 153, 189]. Let us explain this using a simple example of the two-point function in the theory (4.43).

We have for the bare propagator

$$\langle \phi^{abc}(p) \phi^{a'b'c'}(-p) \rangle_0 = G_0(p) \delta^{aa'} \delta^{bb'} \delta^{cc'} = \frac{1}{p^2} \delta^{aa'} \delta^{bb'} \delta^{cc'}. \quad (4.44)$$

In the large N limit one gets the same Schwinger-Dyson equation for the full two-point function as in (4.22), which we can write in the momentum space as

$$G(p) = G_0(p) + \lambda^2 G_0(p) \Sigma(p) G(p), \quad (4.45)$$

where we introduced the coupling $\lambda = gN^{3/2}$, which is held fixed in the large N limit and

$$\Sigma(p) = \int \frac{d^d k d^d q}{(2\pi)^{2d}} G(q) G(k) G(p + q + k). \quad (4.46)$$

One can rewrite (4.45) as

$$G^{-1}(p) = G_0^{-1}(p) - \lambda^2 \Sigma(p). \quad (4.47)$$

In the IR limit we can neglect the bare term $G_0(p)$ and get

$$G^{-1}(p) = -\lambda^2 \int \frac{d^d k d^d q}{(2\pi)^{2d}} G(q) G(k) G(p + q + k). \quad (4.48)$$

Using the integral

$$\int \frac{d^d k}{(2\pi)^d} \frac{1}{k^{2\alpha} (k+p)^{2\beta}} = \frac{1}{(4\pi)^{d/2}} \frac{\Gamma(d/2 - \alpha) \Gamma(d/2 - \beta) \Gamma(\alpha + \beta - d/2)}{\Gamma(\alpha) \Gamma(\beta) \Gamma(d - \alpha - \beta)} \frac{1}{(p^2)^{\alpha + \beta - d/2}} \quad (4.49)$$

it is not difficult to show that the solution to the equation (4.48) is

$$G(p) = \lambda^{-1/2} \left(\frac{(4\pi)^d d \Gamma(\frac{3d}{4})}{4\Gamma(1 - \frac{d}{4})} \right)^{1/4} \frac{1}{(p^2)^{\frac{d}{4}}}. \quad (4.50)$$

Alternatively, one can work in the coordinate representation and use the Fourier transform

$$\int d^d x \frac{e^{ikx}}{(x^2)^\alpha} = \frac{\pi^{d/2} \Gamma(d/2 - \alpha)}{2^{2\alpha - d} \Gamma(\alpha)} \frac{1}{(k^2)^{d/2 - \alpha}} \quad (4.51)$$

to find the solution of the equation $G^{-1}(x) = -\lambda^2 G^3(x)$:

$$G(x) = \lambda^{-1/2} \left(\frac{d \Gamma(\frac{3d}{4})}{4\pi^d \Gamma(1 - \frac{d}{4})} \right)^{1/4} \frac{1}{(x^2)^{\frac{d}{4}}}. \quad (4.52)$$

If one works with the cutoff regularization, then the UV divergence, which arises in the integrals can be absorbed into mass renormalization. Remarkably, the Schwinger-Dyson equation (4.48) was originally studied in 1964, and its $d = 3$ solution (4.50) was found [190].

4.4.1 Spectrum of two-particle operators

The $O(N)^3$ invariant two-particle operators of spin zero have the form $\phi^{abc}(\partial_\mu \partial^\mu)^n \phi^{abc}$, where $n = 0, 1, 2, \dots$. At the quantum level these operators mix with each other, although this mixing rapidly decreases as n increases, and the eigenvalues approach $2n + \frac{d}{2}$.

Let us denote the conformal three-point function of a general spin zero operator O_h with two scalar fields ϕ^{abc} by

$$v(x_1, x_2, x_3) = \langle O_h(x_1) \phi^{abc}(x_2) \phi^{abc}(x_3) \rangle = \frac{C_{O\phi\phi}}{(x_{12}^2 x_{13}^2)^{\frac{h}{2}} (x_{23}^2)^{\frac{1}{2}(d/2 - h)}}, \quad (4.53)$$

where h and $\Delta_\phi = d/4$ are the scaling dimensions.

In the large N limit one can write the Schwinger-Dyson equation for the three-point function [178]

$$v(x_0, x_1, x_2) = \int d^d x_3 d^d x_4 K(x_1, x_2, x_3, x_4) v(x_0, x_3, x_4), \quad (4.54)$$

where the kernel is given by the formula

$$K(x_1, x_2; x_3, x_4) = 3\lambda^2 G(x_{13})G(x_{24})G(x_{34})^2. \quad (4.55)$$

This equation determines the possible values of scaling dimension h of the operator O_h . Now using the general conformal integral [191]

$$\int d^d x_0 \frac{1}{(x_{01}^2)^{\alpha_1} (x_{02}^2)^{\alpha_2} (x_{03}^2)^{\alpha_3}} = \frac{L_d(\alpha_1, \alpha_2)}{(x_{12}^2)^{\frac{d}{2}-\alpha_3} (x_{13}^2)^{\frac{d}{2}-\alpha_2} (x_{23}^2)^{\frac{d}{2}-\alpha_1}}, \quad (4.56)$$

where $\alpha_1 + \alpha_2 + \alpha_3 = d$ and

$$L_d(\alpha_1, \alpha_2) = \pi^{\frac{d}{2}} \frac{\Gamma(\frac{d}{2} - \alpha_1) \Gamma(\frac{d}{2} - \alpha_2) \Gamma(\frac{d}{2} - \alpha_3)}{\Gamma(\alpha_1) \Gamma(\alpha_2) \Gamma(\alpha_3)} \quad (4.57)$$

one can find that [31]

$$\begin{aligned} \int d^d x_3 d^d x_4 K(x_1, x_2, x_3, x_4) v(x_0, x_3, x_4) &= g(h) v(x_0, x_1, x_2), \\ g(h) &= 3(C_\phi)^4 L_d\left(\frac{d}{4}, \frac{h}{2}\right) L_d\left(\frac{d-h}{2}, \frac{d}{4}\right) = -\frac{3\Gamma\left(\frac{3d}{4}\right) \Gamma\left(\frac{d}{4} - \frac{h}{2}\right) \Gamma\left(\frac{h}{2} - \frac{d}{4}\right)}{\Gamma\left(-\frac{d}{4}\right) \Gamma\left(\frac{3d}{4} - \frac{h}{2}\right) \Gamma\left(\frac{d}{4} + \frac{h}{2}\right)}. \end{aligned} \quad (4.58)$$

The dimensions of the spin zero operators in large N limit are determined by $g(h) = 1$. In $d = 4 - \epsilon$ this equation has solutions

$$\begin{aligned} h_0 &= 2 \pm i\sqrt{6\epsilon} - \frac{1}{2}\epsilon + \mathcal{O}(\epsilon^{3/2}), & h_1 &= 4 + \epsilon - \frac{15\epsilon^2}{4} + \mathcal{O}(\epsilon^3), \\ h_n &= 2(n+1) - \frac{\epsilon}{2} + \frac{3\epsilon^2}{2n^2(n^2-1)} + \mathcal{O}(\epsilon^3), & \text{for } n > 1. \end{aligned} \quad (4.59)$$

We note that the first scaling dimension, h_0 , is complex, which means that the critical point is unstable. From the $\text{AdS}_{5-\epsilon}$ side the relation between mass and scaling dimension

$$h = \frac{d}{2} \pm \sqrt{\frac{d^2}{4} + m^2} \quad (4.60)$$

gives

$$m^2 = -4 - 4\epsilon + 11\epsilon^2 + \mathcal{O}(\epsilon^3), \quad (4.61)$$

which is slightly below the Breitenlohner-Freedman [192] bound $m^2 > -d^2/4$.

More generally, for $d < 4$, the first solution of $g(h) = 1$ has the form

$$h_0 = \frac{d}{2} \pm i\alpha(d), \quad (4.62)$$

where $\alpha(d)$ is real. This is in agreement with (4.60) for $m^2 < -d^2/4$. On the other hand, for $4 < d < 4.155$, h_0 is real and the large N theory is free of this instability, at least formally.

4.4.2 Spectrum of higher-spin operators

Consider a higher-spin operator $J_s(x) = z^{\mu_1} \dots z^{\mu_s} J_{\mu_1 \dots \mu_s}$, where we introduced an auxiliary null vector z^μ , satisfying

$$z^2 = z^\mu z^\nu \delta_{\mu\nu} = 0. \quad (4.63)$$

The three-point function $\langle J_s \phi^{abc} \phi^{abc} \rangle$ is completely fixed by conformal invariance

$$\langle J_s(x_1) \phi^{abc}(x_2) \phi^{abc}(x_3) \rangle = C_{s00} \frac{\left(\frac{z \cdot x_{12}}{x_{12}^2} - \frac{z \cdot x_{13}}{x_{13}^2} \right)^s}{(x_{12}^2)^{\frac{\tau_s}{2}} (x_{23}^2)^{\Delta_\phi - \frac{\tau_s}{2}} (x_{31}^2)^{\frac{\tau_s}{2}}}, \quad (4.64)$$

where $\Delta_\phi = d/4$ and $\tau_s = \Delta_{J_s} - s$ and $\Delta_{J_s} = 2\Delta_\phi + s + \gamma_s$. If we set the J_s momentum to zero or equivalently, integrate over the position of J_s we get

$$v_s(x_2, x_3) = \int d^d x_1 \langle J_s(x_1) \phi^{abc}(x_2) \phi^{abc}(x_3) \rangle = \frac{(z \cdot x_{23})^s}{(x_{23}^2)^{\frac{\tau_s}{2} + s - \frac{d}{2} + \Delta_\phi}}. \quad (4.65)$$

In the large N limit one can again write the Schwinger-Dyson equation for the three-point function

$$v_s(x_1, x_2) = \int d^d x_3 d^d x_4 K(x_1, x_2, x_3, x_4) v_s(x_3, x_4). \quad (4.66)$$

To perform the integral in the r.h.s of (4.66) we use the well-known integral

$$\int d^d x \frac{(z \cdot x)^s}{x^{2\alpha} (x-y)^{2\beta}} = L_{d,s}(\alpha, \beta) \frac{(z \cdot y)^s}{(y^2)^{\alpha+\beta-d/2}},$$

$$L_{d,s}(\alpha, \beta) = \pi^{d/2} \frac{\Gamma\left(\frac{d}{2} - \alpha + s\right) \Gamma\left(\frac{d}{2} - \beta\right) \Gamma\left(\alpha + \beta - \frac{d}{2}\right)}{\Gamma(\alpha) \Gamma(\beta) \Gamma(d + s - \alpha - \beta)}. \quad (4.67)$$

Using (4.67) we find

$$\int d^d x_3 d^d x_4 K(x_1, x_2, x_3, x_4) v_s(x_3, x_4) = g(\tau_s, s) v_s(x_1, x_2),$$

$$g(\tau_s, s) = 3(C_\phi)^4 L_{d,s}\left(\frac{d}{4} + s + \frac{\tau_s}{2}, \frac{d}{4}\right) L_{d,s}\left(s + \frac{\tau_s}{2}, \frac{d}{4}\right) = -\frac{3\Gamma\left(\frac{3d}{4}\right)\Gamma\left(\frac{d-2\tau_s}{4}\right)\Gamma\left(\frac{4s+2\tau_s-d}{4}\right)}{\Gamma\left(-\frac{d}{4}\right)\Gamma\left(\frac{3d-2\tau_s}{4}\right)\Gamma\left(\frac{d+4s+2\tau_s}{4}\right)} \quad (4.68)$$

and to find the spectrum we have to solve the equation $g(\tau_s, s) = 1$. Note that for any d , there is a solution with $s = 2$ and $\tau_s = d - 2$. This corresponds to the conserved stress tensor, consistently with the conformal invariance.

For general fixed spin s , the dimensions should approach, at large n

$$\Delta_{J_s} = 2\Delta_\phi + s + 2n, \quad n = 0, 1, 2, \dots, \quad (4.69)$$

where n is interpreted as the number of contracted derivatives. Alternatively, one can also study the behavior for large spin s , and fixed n (say $n = 0$), where the dimensions should approach $\Delta_{J_s} \approx 2\Delta_\phi + s + c/s^{\tau_{\min}}$, where τ_{\min} is the lowest twist (excluding the identity) appearing in the OPE expansion of the ϕ 4-point function [193, 194, 195].

For $n = 0$ we have in $d = 4 - \epsilon$

$$\tau_s = d - 2 + \frac{(s-2)(s+3)}{2s(s+1)}\epsilon + \dots \quad (4.70)$$

Note that the correction to $d - 2$ vanishes for $s = 2$, as it should since the stress tensor is conserved. The fact that this correction for $s \neq 2$ is $\sim \epsilon$ also makes sense, because for nearly conserved currents the anomalous dimension starts at $\sim g^2$ on general grounds (like γ_ϕ). The spin dependence in the above result is the expected one for an almost conserved current near $d = 4$, see e.g. [196, 197].

In $d = 2$ the equation determining the dimensions becomes elementary and reads

$$\frac{3}{(1 - \tau_s)(2s + \tau_s - 1)} = 1 \quad (4.71)$$

with solutions

$$\tau_s = 1 - s \pm \sqrt{s^2 - 3} . \quad (4.72)$$

Surprisingly, this gives only one solution with $h > d/2$ for each spin, rather than the infinite number of solutions which are present in $d > 2$ (already in $d = 2 + \epsilon$ there are towers of real solutions). For $s = 0$ in $d = 2$ the solution (4.72) is complex

$$h \approx 1 + 1.5235i . \quad (4.73)$$

In $d = 2 + \epsilon$ there is also a tower of real solutions:⁵

$$\tau_s = 2n + \frac{d}{2} + \frac{3}{3 + 4n(n + s)}\epsilon + \mathcal{O}(\epsilon^2) . \quad (4.74)$$

In $d = 1$ the primary two-particle operators have the form $\phi^{abc} \partial_t^{2n} \phi^{abc}$, where $n = 0, 1, 2, \dots$. The graphical solution of the eigenvalue equation is shown in figure 4.16. The equation has a symmetry under $h \rightarrow 1 - h$. The first real solution greater than $1/2$ is the exact solution $h = 2$. It correspond to the $n = 1$ operator, which through the use of equations of motion is proportional to the potential $\phi^{a_1 b_1 c_1} \phi^{a_1 b_2 c_2} \phi^{a_2 b_1 c_2} \phi^{a_2 b_2 c_1}$. The first eigenvalue is complex, $h_0 = \frac{1}{2} + 1.525i$. Since it is of the form $\frac{1}{2} + is$, it is a normalizable mode which needs to be integrated over, similarly to the $h = 2$ mode.

⁵In the $\epsilon \rightarrow 0$ limit it appears to give additional states in $d = 2$ which are missed by the degenerate $d = 2$ equation (4.71).

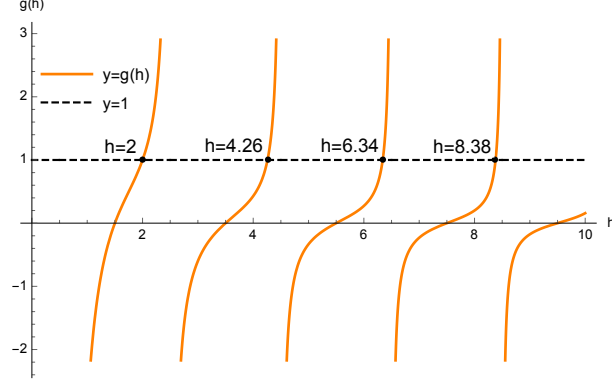


Figure 4.16: The graphical solution of the eigenvalue equation $g(h) = 1$ in $d = 1$.

4.4.3 Complex Large N Fixed Point in $d = 4 - \epsilon$

In this section we study the renormalizable theory in $4 - \epsilon$ dimensions with a 3-tensor degree of freedom and $O(N)^3$ symmetric quartic interactions:

$$S = \int d^d x \left(\frac{1}{2} \partial_\mu \phi^{abc} \partial^\mu \phi^{abc} + \frac{1}{4} (g_1 O_t(x) + g_2 O_p(x) + g_3 O_{ds}(x)) \right), \quad (4.75)$$

where g_1, g_2, g_3 are the bare couplings which correspond to the three possible invariant quartic interaction terms. The perturbative renormalizability of the theory requires that, in addition to the “tetrahedron” interaction term (4.5), we introduce the “pillow” and “double-sum” terms

$$\begin{aligned} O_p(x) &= \frac{1}{3} \left(\phi^{a_1 b_1 c_1} \phi^{a_1 b_1 c_2} \phi^{a_2 b_2 c_2} \phi^{a_2 b_2 c_1} + \phi^{a_1 b_1 c_1} \phi^{a_2 b_1 c_1} \phi^{a_2 b_2 c_2} \phi^{a_1 b_2 c_2} \right. \\ &\quad \left. + \phi^{a_1 b_1 c_1} \phi^{a_1 b_2 c_1} \phi^{a_2 b_1 c_2} \phi^{a_2 b_2 c_2} \right), \\ O_{ds}(x) &= \phi^{a_1 b_1 c_1} \phi^{a_1 b_1 c_1} \phi^{a_2 b_2 c_2} \phi^{a_2 b_2 c_2}. \end{aligned} \quad (4.76)$$

To find the beta functions we use a well-known result [59] for a general ϕ^4 -model with the interaction term $V = \frac{1}{4} g_{ijkl} \phi^i \phi^j \phi^k \phi^l$. In our case we can write interaction as

$$V = \frac{1}{4} g_{\kappa_1 \kappa_2 \kappa_3 \kappa_4} \phi^{\kappa_1} \phi^{\kappa_2} \phi^{\kappa_3} \phi^{\kappa_4}, \quad (4.77)$$

where $\kappa_i = (a_i b_i c_i)$ is a set of three indices and $g_{\kappa_1 \kappa_2 \kappa_3 \kappa_4}$ is a sum of three structures

$$g_{\kappa_1 \kappa_2 \kappa_3 \kappa_4} = g_1 T_{\kappa_1 \kappa_2 \kappa_3 \kappa_4}^t + g_2 T_{\kappa_1 \kappa_2 \kappa_3 \kappa_4}^p + g_3 T_{\kappa_1 \kappa_2 \kappa_3 \kappa_4}^{ds}. \quad (4.78)$$

Each structure is a sum of a product of Kronecker-delta terms, which after contraction with $\phi^{\kappa_1} \phi^{\kappa_2} \phi^{\kappa_3} \phi^{\kappa_4}$ reproduce (4.5) and (4.76). For example

$$T_{\kappa_1 \kappa_2 \kappa_3 \kappa_4}^t = \frac{1}{4!} \left(\delta_{a_1 a_2} \delta_{b_1 b_3} \delta_{c_1 c_4} \delta_{b_2 b_4} \delta_{c_2 c_3} \delta_{a_3 a_4} + \text{sym}(\kappa_1, \dots, \kappa_4) \right), \quad (4.79)$$

where the last term means that we have to add all terms corresponding to permutations of $\kappa_1, \dots, \kappa_4$. Using the explicit formulas in [59], we find the beta functions up to two loops

$$\begin{aligned} \beta_t = & -\epsilon g_1 + \frac{4}{3(4\pi)^2} \left(3g_1 g_2 (N+1) + 18g_1 g_3 + 2g_2^2 \right) \\ & + \frac{2}{9(4\pi)^4} \left(9(N^3 - 15N - 10)g_1^3 - 36g_1^2((N^2 + 4N + 13)g_2 + 15Ng_3) \right. \\ & - 3g_1((N^3 + 15N^2 + 93N + 101)g_2^2 + 12(5N^2 + 17N + 17)g_2 g_3 + 6(5N^3 + 82)g_3^2) \\ & \left. - 4g_2^2((2N^2 + 13N + 24)g_2 + 72g_3) \right), \end{aligned} \quad (4.80)$$

$$\begin{aligned} \beta_p = & -\epsilon g_2 + \frac{2}{3(4\pi)^2} \left(9g_1^2(N+2) + 12g_2 g_1(N+2) + g_2^2(N^2 + 5N + 12) + 36g_2 g_3 \right) \\ & - \frac{2}{9(4\pi)^4} \left(108(N^2 + N + 4)g_1^3 + 9g_1^2((N^3 + 12N^2 + 99N + 98)g_2 + 72(N+2)g_3) \right. \\ & + 36g_1 g_2((4N^2 + 18N + 29)g_2 + 3(13N + 16)g_3) + g_2((5N^3 + 45N^2 + 243N + 343)g_2^2 \\ & \left. + 36(7N^2 + 15N + 29)g_2 g_3 + 18(5N^3 + 82)g_3^2) \right), \end{aligned} \quad (4.81)$$

and

$$\begin{aligned}
\beta_{ds} = & -\epsilon g_3 + \frac{2}{3(4\pi)^2} \left(3g_3^2 (N^3 + 8) + 6g_3g_2 (N^2 + N + 1) + g_2^2(2N + 3) + 18g_1g_3N + 6g_1g_2 \right) \\
& - \frac{2}{9(4\pi)^4} \left(54Ng_1^3 + 9g_1^2(4(N^2 + N + 4)g_2 + 5(N^3 + 3N + 2)g_3) \right. \\
& + 36g_1(4(N + 1)g_2^2 + (5N^2 + 5N + 17)g_2g_3 + 33Ng_3^2) + 14(N^2 + 3N + 5)g_2^3 \\
& \left. + 3(5N^3 + 15N^2 + 93N + 97)g_2^2g_3 + 396(N^2 + N + 1)g_2g_3^2 + 54(3N^3 + 14)g_3^3 \right).
\end{aligned} \tag{4.82}$$

For the anomalous dimension we obtain

$$\begin{aligned}
\gamma_\phi = & \frac{1}{6(4\pi)^4} \left(3g_1^2(N^3 + 3N + 2) + 6g_3^2(N^3 + 2) + 12g_1(g_2(N^2 + N + 1) + 3g_3N) \right. \\
& \left. + 12g_2g_3(N^2 + N + 1) + g_2^2(N^3 + 3N^2 + 9N + 5) \right).
\end{aligned} \tag{4.83}$$

Now, using the large N scaling

$$g_1 = \frac{(4\pi)^2 \tilde{g}_1}{N^{3/2}}, \quad g_2 = \frac{(4\pi)^2 \tilde{g}_2}{N^2}, \quad g_3 = \frac{(4\pi)^2 \tilde{g}_3}{N^3}, \tag{4.84}$$

where \tilde{g}_i are held fixed, we find that the anomalous dimension

$$\gamma_\phi = \frac{\tilde{g}_1^2}{2} + \mathcal{O}(1/N) \tag{4.85}$$

and the beta functions

$$\begin{aligned}
\tilde{\beta}_t = & -\epsilon \tilde{g}_1 + 2\tilde{g}_1^3, \\
\tilde{\beta}_p = & -\epsilon \tilde{g}_2 + \left(6\tilde{g}_1^2 + \frac{2}{3}\tilde{g}_2^2 \right) - 2\tilde{g}_1^2 \tilde{g}_2, \\
\tilde{\beta}_{ds} = & -\epsilon \tilde{g}_3 + \left(\frac{4}{3}\tilde{g}_2^2 + 4\tilde{g}_2 \tilde{g}_3 + 2\tilde{g}_3^2 \right) - 2\tilde{g}_1^2(4\tilde{g}_2 + 5\tilde{g}_3).
\end{aligned} \tag{4.86}$$

We note that $\tilde{\beta}_t$ depends only on the tetrahedron coupling \tilde{g}_1 , while the beta functions for pillow and double-sum also contain \tilde{g}_1 . This is a feature of the large N limit. Similarly, in the large N limit of the quartic matrix theory, the double-trace coupling does not affect the beta function of the single-trace coupling (see the Appendix).

The large N critical point with a non-vanishing tetrahedron coupling is

$$\tilde{g}_1^* = (\epsilon/2)^{1/2}, \quad \tilde{g}_2^* = \pm 3i(\epsilon/2)^{1/2}, \quad \tilde{g}_3^* = \mp i(3 \pm \sqrt{3})(\epsilon/2)^{1/2}. \quad (4.87)$$

For the dimension of the $O = \phi^{abc}\phi^{abc}$ operator at large N we find

$$\Delta_O = d - 2 + 2(\tilde{g}_2^* + \tilde{g}_3^*) = 2 \pm i\sqrt{6\epsilon} + \mathcal{O}(\epsilon). \quad (4.88)$$

This exactly coincides with the large N solution (4.59), providing a nice perturbative check of the fact that the scaling dimension is complex. We note that the imaginary part originates from the complex pillow and double-sum couplings.

Now if we look for the dimension of the tetrahedron operator, then using the derivative of the beta function, we find

$$\Delta_{\text{tetra}} = d + \beta'_t(g_1^*) = 4 + \epsilon + \mathcal{O}(\epsilon^2), \quad (4.89)$$

which coincides with the scaling dimension h_1 of operator $\phi^{abc}\nabla^2\phi^{abc}$ found in (4.59).

4.4.4 Generalization to Higher q

The construction of theories for a single rank 3 tensor field with the quartic interaction (4.43) may be generalized to a single rank $q - 1$ tensor with the $O(N)^{q-1}$ symmetric interaction of order q . Since the indices of each $O(N)$ group must be contracted pairwise, q has to be even. The rank $q - 1$ tensor theories have a large N limit with $\lambda^2 = g^2 N^{(q-1)(q-2)/2}$ held fixed, which is dominated by the melonic diagrams (this

follows from the method of “forgetting” all but two colors in the graphs made out of $q - 1$ strands by analogy with the derivation [157, 30, 163, 31] for $q = 4$). For example, for $q = 6$ the explicit form of the interaction of a real rank 5 tensor is [31]

$$V_{\text{int}} = \frac{g}{6} \phi^{a_1 b_1 c_1 d_1 e_1} \phi^{a_1 b_2 c_2 d_2 e_2} \phi^{a_2 b_2 c_3 d_3 e_1} \phi^{a_2 b_3 c_2 d_1 e_3} \phi^{a_3 b_3 c_1 d_3 e_2} \phi^{a_3 b_1 c_3 d_2 e_3} . \quad (4.90)$$

Since every pair of fields have one index in common, this interaction may be represented by a 5-simplex.

The two-point Schwinger-Dyson equation has the form

$$G^{-1}(x) = -\lambda^2 G(x)^{q-1} . \quad (4.91)$$

The general d solution to this equation is

$$G(x) = \frac{C_\phi}{\lambda^{2/q}} \frac{1}{(x^2)^{\frac{d}{q}}} ,$$

$$C_\phi = \left(- \frac{\pi^{-d} \Gamma(\frac{d}{q}) \Gamma(\frac{d(q-1)}{q})}{\Gamma(\frac{d(2-q)}{2q}) \Gamma(\frac{d(q-2)}{2q})} \right)^{1/q} . \quad (4.92)$$

In analogy to Section (4.4.1) one can find a spectrum of spin zero operators by solving Schwinger-Dyson equation for the three-point function

$$v(x_0, x_1, x_2) = \int d^d x_3 d^d x_4 K(x_1, x_2, x_3, x_4) v(x_0, x_3, x_4) , \quad (4.93)$$

where the kernel is given by the formula

$$K(x_1, x_2; x_3, x_4) = (q - 1) \lambda^2 G(x_{13}) G(x_{24}) G(x_{34})^{q-2} . \quad (4.94)$$

Using the integral (4.56) and expression (4.92) we find

$$\begin{aligned}
g_q(h) &= (q-1)(C_\phi)^q L_d\left(\frac{d}{q}, \frac{h}{2}\right) L_d\left(\frac{d-h}{2}, \frac{d}{q}\right) \\
&= -\frac{(q-1)\Gamma\left(\frac{d(q-2)}{2q}\right)\Gamma\left(\frac{d(q-1)}{q}\right)\Gamma\left(\frac{h}{2} - \frac{d(q-2)}{2q}\right)\Gamma\left(\frac{d}{q} - \frac{h}{2}\right)}{\Gamma\left(\frac{d(2-q)}{2q}\right)\Gamma\left(\frac{d}{q}\right)\Gamma\left(\frac{h}{2} + \frac{d(q-2)}{2q}\right)\Gamma\left(\frac{d(q-1)}{q} - \frac{h}{2}\right)}, \tag{4.95}
\end{aligned}$$

where C_ϕ is given in (4.92).

By solving $g_q(h) = 1$ we find the spectrum of dimensions of spin zero two-particle operators. As we already noticed in (4.4.1), for $q = 4$ the lowest operator $O = \phi^2$ has complex dimension, which signals an instability of the theory. However, for d greater than the critical value d_{cr} , there exists q_{crit} such that for $q > q_{\text{crit}}$ the solutions of $g_q(h) = 1$ are real, and the two-particle operators do not cause instabilities. The d_{cr} is determined by

$$\frac{\Gamma(-d_{\text{cr}}/4)^2\Gamma(d_{\text{cr}}/2)\Gamma(d_{\text{cr}}+1)}{\Gamma(-d_{\text{cr}}/2)\Gamma(3d_{\text{cr}}/4)^2} = -1, \tag{4.96}$$

and we find $d_{\text{cr}} \approx 1.93427$. Interestingly, q_{crit} diverges at d_{cr} as $q_{\text{crit}} \approx \frac{4.092}{d-d_{\text{cr}}}$. The plot for q_{crit} as a function of d is shown in Figure 4.17.

In $d = 2$, the critical value of q is still large: $q_{\text{crit}} \approx 64.3$ [184], but it drops to ≈ 5.9 in $d = 3$. For $d < d_{\text{cr}}$ the lowest eigenvalue is complex for any q . In $d = 1$, in the large q limit

$$h_0 = \frac{1}{2} + i\frac{\sqrt{7}}{2} + \mathcal{O}(1/q). \tag{4.97}$$

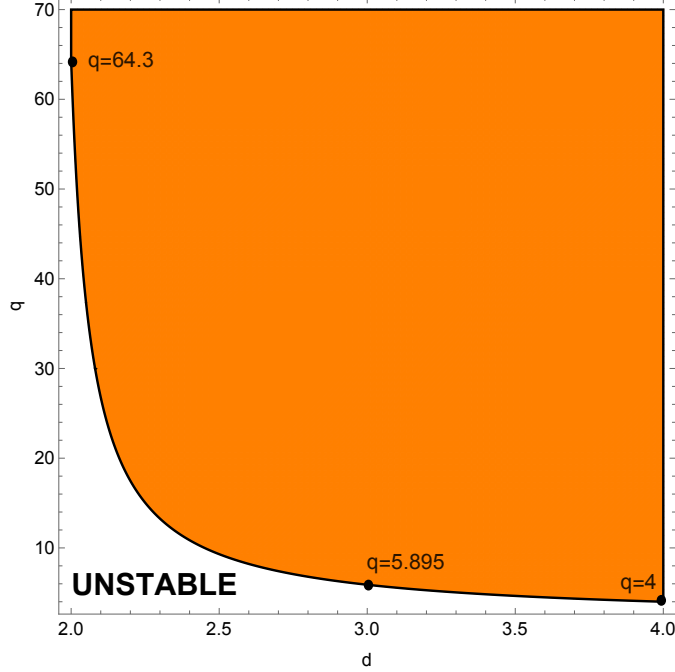


Figure 4.17: Plot of q_{crit} as a function of d . The orange region corresponds to $q > q_{\text{crit}}$, where Δ_{ϕ^2} is real and the theory is not obviously unstable. For integer dimensions we obtained $q_{\text{crit}}(2) \approx 64.3$, $q_{\text{crit}}(3) \approx 5.9$ and $q_{\text{crit}}(4) = 4$.

4.4.5 Higher spin operators

Similarly to the case $q = 4$, we may generalize the discussion of $q > 4$ to the higher spin operators. We find that ⁶

$$\begin{aligned}
g_q(\tau_s, s) &= (q-1)(C_\phi)^q L_{d,s}\left(\frac{d}{2} - \frac{d}{q} + s + \frac{\tau_s}{2}, \frac{d}{q}\right) L_{d,s}\left(s + \frac{\tau_s}{2}, \frac{d}{q}\right) \\
&= - \frac{(q-1)\Gamma\left(\frac{d(q-2)}{2q}\right)\Gamma\left(\frac{d(q-1)}{q}\right)\Gamma\left(\frac{d}{q} - \frac{\tau_s}{2}\right)\Gamma\left(s + \frac{\tau_s}{2} - \frac{d(q-2)}{2q}\right)}{\Gamma\left(\frac{d(2-q)}{2q}\right)\Gamma\left(\frac{d}{q}\right)\Gamma\left(\frac{d(q-1)}{q} - \frac{\tau_s}{2}\right)\Gamma\left(s + \frac{\tau_s}{2} + \frac{d(q-2)}{2q}\right)}. \quad (4.98)
\end{aligned}$$

As a check of this formula, we note that the equation $g_q(\tau_s, s) = 1$ for $s = 2$ has a solution $\tau_s = d - 2$ corresponding to the stress-energy tensor.

⁶For $d = 2$, this equation agrees with eq. (6.8) of [184] after the identifications $h = s + \frac{\tau}{2}$, $\tilde{h} = \frac{\tau}{2}$.

Similarly to the case $q = 4$, which degenerates for $d = 2$, we find a similar degeneration of (4.98) for $q = 8$ and $d = 4$,

$$g(\tau_s, s) = \frac{315}{(\tau_s - 5)(\tau_s - 3)(\tau_s - 1)(2s + \tau_s - 3)(2s + \tau_s - 1)(2s + \tau_s + 1)}, \quad (4.99)$$

and the equation $g = 1$ may be solved in terms of the square and cubic roots. The physically relevant solution for τ has the large s expansion

$$\tau_s = 1 + \frac{315}{64s^3} + \frac{315}{64s^5} + \dots \quad (4.100)$$

More generally, we have checked numerically that, in the large s limit, $\tau \rightarrow 2\Delta_\phi$, where $\Delta_\phi = d/q$. For example, for $q = 6$ and $d = 2$, we find

$$\tau_4 = 0.456, \quad \tau_6 = 0.547, \quad \tau_{1000} \approx 0.666. \quad (4.101)$$

4.4.6 A Melonic ϕ^6 Theory in 2.99 Dimensions

Using (4.95) for $q = 6$ we find that the spin zero spectrum is free of complex solutions in a small region of dimension below 3. Working in $d = 3 - \epsilon$, we find that the scaling dimensions are real for $\epsilon < 0.02819$. Expansions of the first three solutions of the equation $g_6(h) = 1$ are

$$\begin{aligned} h_- &= 1 + \frac{29\epsilon}{3} + \frac{400\epsilon^2}{9} + \frac{160}{27} (237 + 2\pi^2) \epsilon^3 + \mathcal{O}(\epsilon^4), \\ h_+ &= 2 - \frac{32\epsilon}{3} - \frac{400\epsilon^2}{9} - \frac{160}{27} (237 + 2\pi^2) \epsilon^3 + \mathcal{O}(\epsilon^4), \\ h_1 &= 3 + 3\epsilon - \frac{220\epsilon^2}{9} + \frac{40}{81} (503 + 3\pi^2) \epsilon^3 + \mathcal{O}(\epsilon^4), \end{aligned} \quad (4.102)$$

and the expansion coefficients grow rapidly. It appears that h_- corresponds to operator $\phi^{abcde}\phi^{abcde}$, h_+ to a quartic operator which mixes with it due to interactions, and h_1 to $\phi^{abcde}\partial_\mu\partial^\mu\phi^{abcde} \sim V_{\text{int}}$.

As ϵ increases, h_- approaches h_+ , and at $\epsilon_{\text{crit}} \approx 0.02819$ they merge and go off to complex plane (see Figure 4.18).

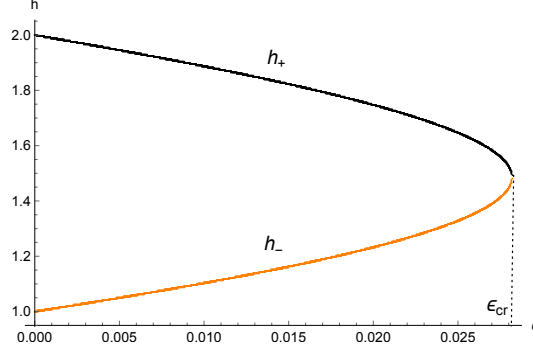


Figure 4.18: Plot of the two lowest operator dimensions h_- and h_+ as a function of ϵ . As ϵ increases, h_- approaches h_+ , and at $\epsilon_{\text{crit}} \approx 0.02819$ they merge and go off to complex plane.

The scaling dimension of operators $\phi^{abcde}(\partial_\mu\partial^\mu)^n\phi^{abcde}$ with $n > 1$ are found to be

$$h_n = 2n + 1 - \frac{\epsilon}{3} + \frac{20}{3(n-1)n(4n^2-1)}\epsilon^2 + \frac{80\left(H_{2n-3} - \frac{92n^4 - 128n^3 + 13n^2 + 23n - 45}{12n(n-1)(4n^2-1)}\right)}{9n(n-1)(4n^2-1)}\epsilon^3 + \mathcal{O}(\epsilon^4), \quad (4.103)$$

where H_n is the Harmonic number. For large n we get

$$h_n = 2n + 1 - \frac{\epsilon}{3} + \frac{5\epsilon^2}{3n^4} + \frac{5\epsilon^3(12\log(2ne^\gamma) - 23)}{27n^4} + \mathcal{O}(\epsilon^4). \quad (4.104)$$

This agrees with the fact that the dimension of operators $\phi^{abcde}(\partial_\mu\partial^\mu)^n\phi^{abcde}$ should approach $2n + \frac{d}{3}$ for large n .

For operators of $s > 0$, we may use (4.98) to obtain for $n = 0$

$$\begin{aligned}
h(s) = d - 2 + s + \frac{8(s^2 - 4)}{3(4s^2 - 1)}\epsilon \\
- \frac{20}{3(4s^2 - 1)} \left(\psi\left(s - \frac{1}{2}\right) - \psi\left(\frac{3}{2}\right) - \frac{2(s-2)(20s^3 + 4s^2 + 43s + 5)}{3(4s^2 - 1)^2} \right) \epsilon^2 + \mathcal{O}(\epsilon^3) .
\end{aligned} \tag{4.105}$$

The first term is the dimension of the operator in free field theory, while the additional terms appear due to the ϕ^6 interactions.

It would be interesting to reproduce the $3 - \epsilon$ expansions found in this section using perturbative calculations in the $O(N)^5$ invariant renormalizable ϕ^6 theory. This is technically more complicated than the similar calculation we carried out in $4 - \epsilon$ dimensions, because there are several invariant ϕ^6 terms. An obvious danger is that the coupling constants for some of the sextic operators will be complex in $d = 3 - \epsilon$. We hope to return to these issues in the future.

4.5 Appendix A. Matrix model in $d = 4 - \epsilon$ dimension

In this appendix we consider renormalizable theory in $4 - \epsilon$ dimensions with a matrix degree of freedom and $O(N)^2$ symmetric quartic interactions:

$$S = \int d^d x \left(\frac{1}{2} \partial_\mu \phi^{ab} \partial^\mu \phi^{ab} + \frac{1}{4} g_1 O_{st}(x) + \frac{1}{4} g_2 O_{dt}(x) \right), \tag{4.106}$$

where g_1, g_2 are the bare couplings which correspond to the two possible invariant quartic interaction terms. The perturbative renormalizability of the theory requires that, in addition to the single-trace term

$$O_{st}(x) = \phi^{ab} \phi^{cb} \phi^{cd} \phi^{ad} = \text{Tr} \phi \phi^T \phi \phi^T, \tag{4.107}$$

we introduce the double-trace term

$$O_{dt}(x) = \phi^{ab}\phi^{ab}\phi^{cd}\phi^{cd} = \text{Tr}\phi\phi^T\text{Tr}\phi\phi^T. \quad (4.108)$$

In analogy with the section 4.4.3 we find the beta functions using a well-known result [59] for a general ϕ^4 -model with the interaction vertex $V = \frac{1}{4}g_{ijkl}\phi^i\phi^j\phi^k\phi^l$. The beta functions up to two loops are

$$\begin{aligned} \beta_{st} &= -\epsilon g_1 + \frac{g_1(g_1(N+2) + 6g_2)}{4\pi^2} \\ &\quad - \frac{g_1(3g_1^2(N(N+6) + 17) + 4g_1g_2(22N+29) + 2g_2^2(5N^2+82))}{128\pi^4}, \\ \beta_{dt} &= -\epsilon g_2 + \frac{3g_1^2 + 2g_1g_2(2N+1) + g_2^2(N^2+8)}{8\pi^2} \\ &\quad - \frac{6g_1^3(2N+3) + g_1^2g_2(5N(N+2) + 87) + 44g_1g_2^2(2N+1) + 6g_2^3(3N^2+14)}{128\pi^4}. \end{aligned} \quad (4.109)$$

Now, using the large N scaling

$$g_1 = \frac{(4\pi)^2\tilde{g}_1}{N}, \quad g_2 = \frac{(4\pi)^2\tilde{g}_2}{N^2}, \quad (4.110)$$

where \tilde{g}_i are held fixed, we find the beta functions

$$\begin{aligned} \tilde{\beta}_{st} &= -\epsilon\tilde{g}_1 + 4\tilde{g}_1^2 - 6\tilde{g}_1^3, \\ \tilde{\beta}_{dt} &= -\epsilon\tilde{g}_2 + (6\tilde{g}_1^2 + 2\tilde{g}_2^2 + 8\tilde{g}_1\tilde{g}_2) - 2\tilde{g}_1^2(12\tilde{g}_1 + 5\tilde{g}_2). \end{aligned} \quad (4.111)$$

We note that $\tilde{\beta}_{st}$ depends only on the single-trace coupling \tilde{g}_1 , while the double-trace beta function depends on both couplings. This is a familiar phenomenon for beta functions in large N matrix theories [198]. Comparing with the beta functions (4.80–4.82) of the large N 3-tensor theory, we observe that the tetrahedron coupling in the tensor model is analogous to the single-trace coupling in the matrix model,

while the pillow and double-sum couplings in the tensor model are analogous to the double-trace coupling in the matrix model.

The large N critical point with a non-vanishing single-trace coupling is

$$\tilde{g}_1^* = \frac{\epsilon}{4} + \frac{3\epsilon^2}{32}, \quad \tilde{g}_2^* = -\frac{1}{4} \left(1 \pm i\sqrt{2}\right) \epsilon - \frac{1}{32} \left(1 \mp 2i\sqrt{2}\right) \epsilon^2. \quad (4.112)$$

For the dimension of the $O = \phi^{ab}\phi^{ab}$ operator at large N we find

$$\Delta_O = d - 2 + 4\tilde{g}_1^* + 2\tilde{g}_2^* = 2 - \frac{1}{2} \left(1 \pm i\sqrt{2}\right) \epsilon + \mathcal{O}(\epsilon^2). \quad (4.113)$$

The imaginary part originates from the double-trace coupling. So, in spite of the positivity of the interaction term O_{st} , this large N critical point is unstable due to an operator dimension being complex. The form of the dimension, $\frac{d}{2} + i\alpha$, corresponds to a field violating the Breitenlohner-Freedman bound in the dual AdS space.

Bibliography

- [1] J. C. Le Guillou and J. Zinn-Justin, “Critical Exponents from Field Theory,” *Phys. Rev.*, vol. B21, pp. 3976–3998, 1980.
- [2] L. D. Landau, “On the theory of phase transitions,” *Zh. Eksp. Teor. Fiz.*, vol. 7, pp. 19–32, 1937.
- [3] K. G. Wilson and M. E. Fisher, “Critical exponents in 3.99 dimensions,” *Phys.Rev.Lett.*, vol. 28, pp. 240–243, 1972.
- [4] S. El-Showk, M. F. Paulos, D. Poland, S. Rychkov, D. Simmons-Duffin, and A. Vichi, “Solving the 3d Ising Model with the Conformal Bootstrap II. c-Minimization and Precise Critical Exponents,” *J. Stat. Phys.*, vol. 157, p. 869, 2014.
- [5] R. Guida and J. Zinn-Justin, “Critical exponents of the N vector model,” *J.Phys.*, vol. A31, pp. 8103–8121, 1998.
- [6] K. G. Wilson and J. B. Kogut, “The Renormalization group and the epsilon expansion,” *Phys. Rept.*, vol. 12, pp. 75–200, 1974.
- [7] A. M. Polyakov, “Nonhamiltonian approach to conformal quantum field theory,” *Zh. Eksp. Teor. Fiz.*, vol. 66, pp. 23–42, 1974. [Sov. Phys. JETP39,9(1974)].

- [8] S. Ferrara, A. F. Grillo, and R. Gatto, “Tensor representations of conformal algebra and conformally covariant operator product expansion,” *Annals Phys.*, vol. 76, pp. 161–188, 1973.
- [9] S. Ferrara, R. Gatto, and A. F. Grillo, “Positivity Restrictions on Anomalous Dimensions,” *Phys. Rev.*, vol. D9, p. 3564, 1974.
- [10] S. El-Showk, M. F. Paulos, D. Poland, S. Rychkov, D. Simmons-Duffin, and A. Vichi, “Solving the 3D Ising Model with the Conformal Bootstrap,” *Phys. Rev.*, vol. D86, p. 025022, 2012.
- [11] S. El-Showk, Y. Nakayama, and S. Rychkov, “What Maxwell Theory in $D \neq 4$ teaches us about scale and conformal invariance,” *Nucl. Phys.*, vol. B848, pp. 578–593, 2011.
- [12] J. S. Schwinger, “Gauge Invariance and Mass. 2.,” *Phys. Rev.*, vol. 128, pp. 2425–2429, 1962.
- [13] T. Appelquist and R. D. Pisarski, “High-Temperature Yang-Mills Theories and Three-Dimensional Quantum Chromodynamics,” *Phys. Rev.*, vol. D23, p. 2305, 1981.
- [14] T. Appelquist, D. Nash, and L. C. R. Wijewardhana, “Critical Behavior in (2+1)-Dimensional QED,” *Phys. Rev. Lett.*, vol. 60, p. 2575, 1988.
- [15] M. Moshe and J. Zinn-Justin, “Quantum field theory in the large N limit: A Review,” *Phys. Rept.*, vol. 385, pp. 69–228, 2003.
- [16] M. Beneke and V. A. Smirnov, “Ultraviolet renormalons in Abelian gauge theories,” *Nucl. Phys.*, vol. B472, pp. 529–590, 1996.
- [17] L. Di Pietro, Z. Komargodski, I. Shamir, and E. Stamou, “Quantum Electrodynamics in $d=3$ from the epsilon-expansion,” 2015.

- [18] J. B. Marston and I. Affleck, “Large- n limit of the Hubbard-Heisenberg model,” *Phys. Rev.*, vol. B39, pp. 11538–11558, 1989.
- [19] M. Franz, Z. Tesanovic, and O. Vafek, “QED(3) theory of pairing pseudogap in cuprates. 1. From D wave superconductor to antiferromagnet via ‘algebraic’ Fermi liquid,” *Phys. Rev.*, vol. B66, p. 054535, 2002.
- [20] I. F. Herbut, “QED(3) theory of underdoped high temperature superconductors,” *Phys. Rev.*, vol. B66, p. 094504, 2002.
- [21] R. D. Pisarski, “Chiral Symmetry Breaking in Three-Dimensional Electrodynamics,” *Phys. Rev.*, vol. D29, p. 2423, 1984.
- [22] T. W. Appelquist, M. J. Bowick, D. Karabali, and L. C. R. Wijewardhana, “Spontaneous Chiral Symmetry Breaking in Three-Dimensional QED,” *Phys. Rev.*, vol. D33, p. 3704, 1986.
- [23] C. Vafa and E. Witten, “Eigenvalue Inequalities for Fermions in Gauge Theories,” *Commun. Math. Phys.*, vol. 95, p. 257, 1984.
- [24] G. ’t Hooft, “A Planar Diagram Theory for Strong Interactions,” *Nucl. Phys.*, vol. B72, p. 461, 1974.
- [25] E. Brezin, C. Itzykson, G. Parisi, and J. B. Zuber, “Planar Diagrams,” *Commun. Math. Phys.*, vol. 59, p. 35, 1978.
- [26] J. Ambjorn, B. Durhuus, and T. Jonsson, “Three-dimensional simplicial quantum gravity and generalized matrix models,” *Mod. Phys. Lett.*, vol. A6, pp. 1133–1146, 1991.
- [27] N. Sasakura, “Tensor model for gravity and orientability of manifold,” *Mod. Phys. Lett.*, vol. A6, pp. 2613–2624, 1991.

- [28] M. Gross, “Tensor models and simplicial quantum gravity in > 2 -D,” *Nucl. Phys. Proc. Suppl.*, vol. 25A, pp. 144–149, 1992.
- [29] V. Bonzom, R. Gurau, and V. Rivasseau, “Random tensor models in the large N limit: Uncoloring the colored tensor models,” *Phys. Rev.*, vol. D85, p. 084037, 2012.
- [30] S. Carrozza and A. Tanasa, “ $O(N)$ Random Tensor Models,” *Lett. Math. Phys.*, vol. 106, no. 11, pp. 1531–1559, 2016.
- [31] I. R. Klebanov and G. Tarnopolsky, “Uncolored random tensors, melon diagrams, and the Sachdev-Ye-Kitaev models,” *Phys. Rev.*, vol. D95, no. 4, p. 046004, 2017.
- [32] S. Giombi, G. Tarnopolsky, and I. R. Klebanov, “On C_J and C_T in Conformal QED,” *JHEP*, vol. 08, p. 156, 2016.
- [33] S. Giombi, I. R. Klebanov, and G. Tarnopolsky, “Conformal QED_d, F -Theorem and the ϵ Expansion,” 2015.
- [34] D. L. Jafferis, I. R. Klebanov, S. S. Pufu, and B. R. Safdi, “Towards the F -Theorem: $\mathcal{N} = 2$ Field Theories on the Three- Sphere,” *JHEP*, vol. 06, p. 102, 2011.
- [35] I. R. Klebanov, S. S. Pufu, and B. R. Safdi, “ F -Theorem without Supersymmetry,” *JHEP*, vol. 1110, p. 038, 2011.
- [36] R. C. Myers and A. Sinha, “Seeing a C-Theorem with Holography,” *Phys. Rev.*, vol. D82, p. 046006, 2010.
- [37] H. Casini, M. Huerta, and R. C. Myers, “Towards a Derivation of Holographic Entanglement Entropy,” *JHEP*, vol. 05, p. 036, 2011.

- [38] T. Grover, “Entanglement Monotonicity and the Stability of Gauge Theories in Three Spacetime Dimensions,” *Phys. Rev. Lett.*, vol. 112, no. 15, p. 151601, 2014.
- [39] E. Dyer, M. Mezei, and S. S. Pufu, “Monopole Taxonomy in Three-Dimensional Conformal Field Theories,” 2013.
- [40] I. R. Klebanov, S. S. Pufu, S. Sachdev, and B. R. Safdi, “Entanglement Entropy of 3-d Conformal Gauge Theories with Many Flavors,” *JHEP*, vol. 05, p. 036, 2012.
- [41] J. A. Gracey, “Computation of critical exponent η at $O(1/N(f)^{**2})$ in quantum electrodynamics in arbitrary dimensions,” *Nucl. Phys.*, vol. B414, pp. 614–648, 1994.
- [42] R. K. Kaul and S. Sachdev, “Quantum criticality of $u(1)$ gauge theories with fermionic and bosonic matter in two spatial dimensions,” *Phys. Rev. B*, vol. 77, p. 155105, Apr 2008.
- [43] C. Xu, “Renormalization group studies on four-fermion interaction instabilities on algebraic spin liquids,” *Phys. Rev. B*, vol. 78, p. 054432, Aug. 2008.
- [44] K. Kaveh and I. F. Herbut, “Chiral symmetry breaking in QED(3) in presence of irrelevant interactions: A Renormalization group study,” *Phys. Rev.*, vol. B71, p. 184519, 2005.
- [45] C. S. Fischer, R. Alkofer, T. Dahm, and P. Maris, “Dynamical chiral symmetry breaking in unquenched QED(3),” *Phys. Rev.*, vol. D70, p. 073007, 2004.
- [46] J. Braun, H. Gies, L. Janssen, and D. Roscher, “Phase structure of many-flavor QED_3,” *Phys. Rev.*, vol. D90, no. 3, p. 036002, 2014.

- [47] S. S. Pufu, “Anomalous dimensions of monopole operators in three-dimensional quantum electrodynamics,” *Phys. Rev.*, vol. D89, no. 6, p. 065016, 2014.
- [48] H. Gies and J. Jaeckel, “Chiral phase structure of QCD with many flavors,” *Eur. Phys. J.*, vol. C46, pp. 433–438, 2006.
- [49] D. B. Kaplan, J.-W. Lee, D. T. Son, and M. A. Stephanov, “Conformality Lost,” *Phys. Rev.*, vol. D80, p. 125005, 2009.
- [50] N. Seiberg, “Electric - magnetic duality in supersymmetric nonAbelian gauge theories,” *Nucl.Phys.*, vol. B435, pp. 129–146, 1995.
- [51] H. Casini and M. Huerta, “On the RG running of the entanglement entropy of a circle,” *Phys.Rev.*, vol. D85, p. 125016, 2012.
- [52] H. Liu and M. Mezei, “A Refinement of entanglement entropy and the number of degrees of freedom,” *JHEP*, vol. 1304, p. 162, 2013.
- [53] S. Giombi and I. R. Klebanov, “Interpolating between a and F ,” *JHEP*, vol. 1503, p. 117, 2015.
- [54] L. Fei, S. Giombi, I. R. Klebanov, and G. Tarnopolsky, “Generalized F -Theorem and the ϵ Expansion,” 2015.
- [55] I. Drummond and G. Shore, “Conformal Anomalies for Interacting Scalar Fields in Curved Space-Time,” *Phys.Rev.*, vol. D19, p. 1134, 1979.
- [56] L. S. Brown and J. C. Collins, “Dimensional Renormalization of Scalar Field Theory in Curved Space-time,” *Annals Phys.*, vol. 130, p. 215, 1980.
- [57] S. Hathrell, “Trace Anomalies and $\lambda\phi^4$ Theory in Curved Space,” *Annals Phys.*, vol. 139, p. 136, 1982.

- [58] I. Jack and H. Osborn, “Background Field Calculations in Curved Space-time. 1. General Formalism and Application to Scalar Fields,” *Nucl.Phys.*, vol. B234, p. 331, 1984.
- [59] I. Jack and H. Osborn, “Analogues for the c Theorem for Four-dimensional Renormalizable Field Theories,” *Nucl.Phys.*, vol. B343, pp. 647–688, 1990.
- [60] I. T. Drummond and G. M. Shore, “Dimensional Regularization of Massless Quantum Electrodynamics in Spherical Space-Time. 1.,” *Annals Phys.*, vol. 117, p. 89, 1979.
- [61] S. J. Hathrell, “Trace Anomalies and QED in Curved Space,” *Annals Phys.*, vol. 142, p. 34, 1982.
- [62] G. M. Shore, “Conformal Anomaly for Massless Quantum Electrodynamics in Spherical Space-time,” *Phys. Rev.*, vol. D21, p. 2226, 1980.
- [63] B. A. Harris and G. C. Joshi, “Matrix element and complex l plane evaluation of two loop vacuum amplitudes in QED on $S(4)$,” *Int. J. Mod. Phys.*, vol. A10, pp. 1281–1328, 1995.
- [64] C. Strouthos and J. B. Kogut, “The Phases of Non-Compact QED(3),” *PoS*, vol. LAT2007, p. 278, 2007.
- [65] O. Raviv, Y. Shamir, and B. Svetitsky, “Nonperturbative beta function in three-dimensional electrodynamics,” *Phys. Rev.*, vol. D90, no. 1, p. 014512, 2014.
- [66] H. Osborn and A. Petkou, “Implications of conformal invariance in field theories for general dimensions,” *Annals Phys.*, vol. 231, pp. 311–362, 1994.
- [67] A. C. Petkou, “ $C(T)$ and $C(J)$ up to next-to-leading order in $1/N$ in the conformally invariant $O(N)$ vector model for $2 < d < 4$,” *Phys.Lett.*, vol. B359, pp. 101–107, 1995.

- [68] K. Diab, L. Fei, S. Giombi, I. R. Klebanov, and G. Tarnopolsky, “On C_J and C_T in the Gross-Neveu and $O(N)$ Models,” 2016.
- [69] A. N. Vasiliev and M. Yu. Nalimov, “Analog of Dimensional Regularization for Calculation of the Renormalization Group Functions in the $1/n$ Expansion for Arbitrary Dimension of Space,” *Theor. Math. Phys.*, vol. 55, pp. 423–431, 1983. [Teor. Mat. Fiz.55,163(1983)].
- [70] A. Vasiliev, M. Pismak, Yu, and Y. Khonkonen, “Simple Method of Calculating the Critical Indices in the $1/N$ Expansion,” *Theor.Math.Phys.*, vol. 46, pp. 104–113, 1981.
- [71] A. Vasiliev, Y. Pismak, and Y. Khonkonen, “ $1/N$ Expansion: Calculation of the Exponents η and ν in the Order $1/N^2$ for Arbitrary Number of Dimensions,” *Theor.Math.Phys.*, vol. 47, pp. 465–475, 1981.
- [72] S. E. Derkachov and A. N. Manashov, “The Simple scheme for the calculation of the anomalous dimensions of composite operators in the $1/N$ expansion,” *Nucl. Phys.*, vol. B522, pp. 301–320, 1998.
- [73] M. Ciuchini, S. E. Derkachov, J. A. Gracey, and A. N. Manashov, “Quark mass anomalous dimension at $O(1/N(f)**2)$ in QCD,” *Phys. Lett.*, vol. B458, pp. 117–126, 1999.
- [74] J. A. Gracey, “Electron mass anomalous dimension at $O(1/(N_f^2))$ in quantum electrodynamics,” *Phys. Lett.*, vol. B317, pp. 415–420, 1993.
- [75] Y. Huh, P. Strack, and S. Sachdev, “Conserved current correlators of conformal field theories in 2+1 dimensions,” *Phys. Rev.*, vol. B88, p. 155109, 2013. [Erratum: *Phys. Rev.*B90,no.19,199902(2014)].
- [76] S. M. Chester and S. S. Pufu, “Towards Bootstrapping QED₃,” 2016.

- [77] T. Nishioka and K. Yonekura, “On RG Flow of τ_{RR} for Supersymmetric Field Theories in Three-Dimensions,” *JHEP*, vol. 1305, p. 165, 2013.
- [78] M. A. Rubin and C. R. Ordonez, “Symmetric Tensor Eigen Spectrum of the Laplacian on n Spheres,” *J. Math. Phys.*, vol. 26, p. 65, 1985.
- [79] R. Camporesi and A. Higuchi, “Spectral functions and zeta functions in hyperbolic spaces,” *J.Math.Phys.*, vol. 35, pp. 4217–4246, 1994.
- [80] M. Beccaria and A. A. Tseytlin, “Conformal a-anomaly of some non-unitary 6d superconformal theories,” 2015.
- [81] C. A. Agon, M. Headrick, D. L. Jafferis, and S. Kasko, “Disk entanglement entropy for a Maxwell field,” *Phys. Rev.*, vol. D89, no. 2, p. 025018, 2014.
- [82] S. S. Gubser and I. R. Klebanov, “A Universal result on central charges in the presence of double trace deformations,” *Nucl.Phys.*, vol. B656, pp. 23–36, 2003.
- [83] S. Giombi, I. R. Klebanov, S. S. Pufu, B. R. Safdi, and G. Tarnopolsky, “AdS Description of Induced Higher-Spin Gauge Theory,” *JHEP*, vol. 1310, p. 016, 2013.
- [84] D. E. Diaz and H. Dorn, “Partition functions and double-trace deformations in AdS/CFT,” *JHEP*, vol. 0705, p. 046, 2007.
- [85] E. Witten, “Nonabelian Bosonization in Two-Dimensions,” *Commun. Math. Phys.*, vol. 92, pp. 455–472, 1984.
- [86] D. Gepner, “Nonabelian Bosonization and Multiflavor QED and QCD in Two-dimensions,” *Nucl. Phys.*, vol. B252, p. 481, 1985.
- [87] I. Affleck, “On the Realization of Chiral Symmetry in (1+1)-dimensions,” *Nucl. Phys.*, vol. B265, p. 448, 1986.

- [88] E. Fradkin and A. A. Tseytlin, “Conformal Supergravity,” *Phys.Rept.*, vol. 119, pp. 233–362, 1985.
- [89] A. Tseytlin, “Weyl anomaly of conformal higher spins on six-sphere,” *Nucl.Phys.*, vol. B877, pp. 632–646, 2013.
- [90] S. Giombi, I. R. Klebanov, and B. R. Safdi, “Higher Spin $\text{AdS}_{d+1}/\text{CFT}_d$ at One Loop,” *Phys.Rev.*, vol. D89, p. 084004, 2014.
- [91] C. Cordova, T. T. Dumitrescu, and K. Intriligator, “Anomalies, Renormalization Group Flows, and the a-Theorem in Six-Dimensional (1,0) Theories,” 2015.
- [92] S. L. Adler, “Massless, Euclidean quantum electrodynamics on the five-dimensional unit hypersphere,” *Phys. Rev.*, vol. D6, pp. 3445–3461, 1972. [Erratum: *Phys. Rev.*D7,3821(1973)].
- [93] S. L. Adler, “Massless Electrodynamics on the five-dimensional unit hypersphere: an amplitude - integral formulation,” *Phys. Rev.*, vol. D8, pp. 2400–2418, 1973. [Erratum: *Phys. Rev.*D15,1803(1977)].
- [94] G. M. Shore, “Dimensional Regularization of Gauge Theories in Spherical Space-Time: Free Field Trace Anomalies,” *Annals Phys.*, vol. 117, p. 121, 1979.
- [95] A. M. Polyakov, “Compact Gauge Fields and the Infrared Catastrophe,” *Phys. Lett.*, vol. B59, pp. 82–84, 1975.
- [96] N. K. Nielsen, “The Energy Momentum Tensor in a Nonabelian Quark Gluon Theory,” *Nucl. Phys.*, vol. B120, pp. 212–220, 1977.
- [97] M. F. Zoller and K. G. Chetyrkin, “OPE of the energy-momentum tensor correlator in massless QCD,” *JHEP*, vol. 12, p. 119, 2012.
- [98] E. A. Ivanov, A. V. Smilga, and B. M. Zupnik, “Renormalizable supersymmetric gauge theory in six dimensions,” *Nucl. Phys.*, vol. B726, pp. 131–148, 2005.

- [99] E. A. Ivanov and A. V. Smilga, “Conformal properties of hypermultiplet actions in six dimensions,” *Phys. Lett.*, vol. B637, pp. 374–381, 2006.
- [100] A. V. Smilga, “6D superconformal theory as the theory of everything,” in *Proceedings of Advanced Studies Institute and Workshop on Symmetries and Spin (PRAHA SPIN 2005)*, pp. 443–459, 2005. [,443(2005)].
- [101] A. V. Smilga, “Chiral anomalies in higher-derivative supersymmetric 6D theories,” *Phys. Lett.*, vol. B647, pp. 298–304, 2007.
- [102] J. A. Gracey, “Six dimensional QCD at two loops,” 2015.
- [103] M. Ciuchini, S. E. Derkachov, J. A. Gracey, and A. N. Manashov, “Computation of quark mass anomalous dimension at $O(1 / N^{*2}(f))$ in quantum chromodynamics,” *Nucl. Phys.*, vol. B579, pp. 56–100, 2000.
- [104] E. Witten, “ $SL(2,Z)$ action on three-dimensional conformal field theories with Abelian symmetry,” 2003.
- [105] R. G. Leigh and A. C. Petkou, “ $SL(2,Z)$ action on three-dimensional CFTs and holography,” *JHEP*, vol. 0312, p. 020, 2003.
- [106] A. Cappelli, D. Friedan, and J. I. Latorre, “C theorem and spectral representation,” *Nucl. Phys.*, vol. B352, pp. 616–670, 1991.
- [107] A. Petkou, “Conserved currents, consistency relations and operator product expansions in the conformally invariant $O(N)$ vector model,” *Annals Phys.*, vol. 249, pp. 180–221, 1996.
- [108] N. Karthik and R. Narayanan, “No evidence for bilinear condensate in parity-invariant three-dimensional QED with massless fermions,” 2015.
- [109] T. Appelquist, A. G. Cohen, and M. Schmaltz, “A New constraint on strongly coupled gauge theories,” *Phys. Rev.*, vol. D60, p. 045003, 1999.

- [110] A. Hasenfratz and P. Hasenfratz, “The Equivalence of the SU(N) Yang-Mills theory with a purely fermionic model,” *Phys. Lett.*, vol. B297, pp. 166–170, 1992.
- [111] J. A. Gracey, “Quark, gluon and ghost anomalous dimensions at $O(1/N(f))$ in quantum chromodynamics,” *Phys. Lett.*, vol. B318, pp. 177–183, 1993.
- [112] D. I. Kazakov and G. S. Vartanov, “Renormalizable $1/N(f)$ Expansion for Field Theories in Extra Dimensions,” *JHEP*, vol. 06, p. 081, 2007.
- [113] D. B. Ali and J. A. Gracey, “Anomalous dimension of nonsinglet quark currents at $O(1/N(f)^{**2})$ in QCD,” *Phys. Lett.*, vol. B518, pp. 188–194, 2001.
- [114] D. Dudal, J. A. Gracey, V. E. R. Lemes, R. F. Sobreiro, S. P. Sorella, and H. Verschelde, “Renormalization properties of the mass operator $A(a)(\mu) A(a)(\mu)$ in three dimensional Yang-Mills theories in the Landau gauge,” *Annals Phys.*, vol. 317, pp. 203–219, 2005.
- [115] J. F. Bennett and J. A. Gracey, “Three loop renormalization of the SU(N(c)) nonAbelian Thirring model,” *Nucl. Phys.*, vol. B563, pp. 390–436, 1999.
- [116] G. Bhanot, K. Demeterfi, and I. R. Klebanov, “(1+1)-dimensional large N QCD coupled to adjoint fermions,” *Phys. Rev.*, vol. D48, pp. 4980–4990, 1993.
- [117] H. Osborn and A. Stergiou, “ C_T for non-unitary CFTs in higher dimensions,” *JHEP*, vol. 06, p. 079, 2016.
- [118] I. Gradshteyn and I. Ryzhik, “Table of Integrals, Series, and Products,” *3rd Edition Press, Inc.*, 1965.
- [119] I. R. Klebanov, S. S. Pufu, S. Sachdev, and B. R. Safdi, “Renyi Entropies for Free Field Theories,” *JHEP*, vol. 1204, p. 074, 2012.

- [120] J. J. Friess, S. S. Gubser, G. Michalogiorgakis, and S. S. Pufu, “Expanding plasmas and quasinormal modes of anti-de Sitter black holes,” *JHEP*, vol. 04, p. 080, 2007.
- [121] A. Higuchi, “Symmetric Tensor Spherical Harmonics on the N Sphere and Their Application to the De Sitter Group $SO(N,1)$,” *J. Math. Phys.*, vol. 28, p. 1553, 1987. [Erratum: *J. Math. Phys.*43,6385(2002)].
- [122] M. A. Rubin and C. R. Ordonez, “Eigenvalues and degeneracies for n -dimensional tensor spherical harmonics,” *J. Math. Phys.*, vol. 25, p. 2888, 1984.
- [123] A. Chodos and E. Myers, “Gravitational Contribution to the Casimir Energy in Kaluza-Klein Theories,” *Annals Phys.*, vol. 156, p. 412, 1984.
- [124] M. Czakon, “Automatized analytic continuation of Mellin-Barnes integrals,” *Comput.Phys.Commun.*, vol. 175, pp. 559–571, 2006.
- [125] A. Smirnov and V. Smirnov, “On the Resolution of Singularities of Multiple Mellin-Barnes Integrals,” *Eur.Phys.J.*, vol. C62, pp. 445–449, 2009.
- [126] V. A. Smirnov, “Analytic tools for Feynman integrals,” *Springer Tracts Mod.Phys.*, vol. 250, pp. 1–296, 2012.
- [127] D. H. Bailey, “A Fortran 90-based multiprecision system,” *ACM Trans. Math. Softw.*, vol. 21, pp. 379–387, 1995.
- [128] G. L. Pimentel, A. M. Polyakov, and G. M. Tarnopolsky, “Vacuum decay in CFT and the Riemann-Hilbert problem,” *Nucl. Phys.*, vol. B907, pp. 617–632, 2016.
- [129] J. S. Schwinger, “On gauge invariance and vacuum polarization,” *Phys.Rev.*, vol. 82, pp. 664–679, 1951.

- [130] T. Tomaras, N. Tsamis, and R. Woodard, “Back reaction in light cone QED,” *Phys.Rev.*, vol. D62, p. 125005, 2000.
- [131] T. Tomaras, N. Tsamis, and R. Woodard, “Pair creation and axial anomaly in light cone QED(2),” *JHEP*, vol. 0111, p. 008, 2001.
- [132] A. M. Polyakov and P. Wiegmann, “Goldstone Fields in Two-Dimensions with Multivalued Actions,” *Phys.Lett.*, vol. B141, pp. 223–228, 1984.
- [133] J. Wess and B. Zumino, “Consequences of anomalous Ward identities,” *Phys.Lett.*, vol. B37, p. 95, 1971.
- [134] S. Novikov, “The Hamiltonian formalism and a many valued analog of Morse theory,” *Usp.Mat.Nauk*, vol. 37N5, pp. 3–49, 1982.
- [135] E. Witten, “Global Aspects of Current Algebra,” *Nucl.Phys.*, vol. B223, pp. 422–432, 1983.
- [136] A. O. Caldeira and A. J. Leggett, “Influence of dissipation on quantum tunneling in macroscopic systems,” *Phys. Rev. Lett.*, vol. 46, p. 211, 1981.
- [137] A. O. Caldeira and A. J. Leggett, “Quantum tunneling in a dissipative system,” *Annals Phys.*, vol. 149, pp. 374–456, 1983.
- [138] A. Alekseev and S. L. Shatashvili, “Path Integral Quantization of the Coadjoint Orbits of the Virasoro Group and 2D Gravity,” *Nucl.Phys.*, vol. B323, p. 719, 1989.
- [139] M. Bershadsky and H. Ooguri, “Hidden $SL(n)$ Symmetry in Conformal Field Theories,” *Commun.Math.Phys.*, vol. 126, p. 49, 1989.
- [140] A. M. Polyakov, “Gauge Transformations and Diffeomorphisms,” *Int.J.Mod.Phys.*, vol. A5, p. 833, 1990.

- [141] A. M. Polyakov, “Quantum Gravity in Two-Dimensions,” *Mod.Phys.Lett.*, vol. A2, p. 893, 1987.
- [142] A. M. Polyakov and P. Wiegmann, “Theory of Nonabelian Goldstone Bosons,” *Phys.Lett.*, vol. B131, pp. 121–126, 1983.
- [143] I. Gohberg, M. A. Kaashoek, and I. M. Spitkovsky, “An overview of matrix factorization theory and operator applications,” in *Factorization and integrable systems*, pp. 1–102, Springer, 2003.
- [144] M. Baumgartl, I. Sachs, and S. L. Shatashvili, “Factorization conjecture and the open/closed string correspondence,” *JHEP*, vol. 05, p. 040, 2005.
- [145] M. Baumgartl and I. Sachs, “Open-closed string correspondence: D-brane decay in curved space,” *JHEP*, vol. 03, p. 024, 2007.
- [146] M. F. Atiyah, V. K. Patodi, and I. M. Singer, “Spectral asymmetry and Riemannian Geometry 1,” *Math. Proc. Cambridge Phil. Soc.*, vol. 77, p. 43, 1975.
- [147] M. F. Atiyah, V. K. Patodi, and I. M. Singer, “Spectral asymmetry and Riemannian geometry 2,” *Math. Proc. Cambridge Phil. Soc.*, vol. 78, p. 405, 1976.
- [148] M. F. Atiyah, V. K. Patodi, and I. M. Singer, “Spectral asymmetry and Riemannian geometry. III,” *Math. Proc. Cambridge Phil. Soc.*, vol. 79, pp. 71–99, 1976.
- [149] V. Knizhnik, A. M. Polyakov, and A. Zamolodchikov, “Fractal Structure of 2D Quantum Gravity,” *Mod.Phys.Lett.*, vol. A3, p. 819, 1988.
- [150] T. D. Chung and H. L. Verlinde, “Dynamical moving mirrors and black holes,” *Nucl. Phys.*, vol. B418, pp. 305–336, 1994.
- [151] C. G. Callan, Jr., S. B. Giddings, J. A. Harvey, and A. Strominger, “Evanescent black holes,” *Phys. Rev.*, vol. D45, pp. 1005–1009, 1992.

- [152] S. Giombi, I. R. Klebanov, and G. Tarnopolsky, “Bosonic Tensor Models at Large N and Small ϵ ,” arXiv:1707.03866, 2017, submitted to journal.
- [153] R. Gurau, “Colored Group Field Theory,” *Commun. Math. Phys.*, vol. 304, pp. 69–93, 2011.
- [154] R. Gurau and J. P. Ryan, “Colored Tensor Models - a review,” *SIGMA*, vol. 8, p. 020, 2012.
- [155] R. Gurau and V. Rivasseau, “The $1/N$ expansion of colored tensor models in arbitrary dimension,” *Europhys. Lett.*, vol. 95, p. 50004, 2011.
- [156] R. Gurau, “The complete $1/N$ expansion of colored tensor models in arbitrary dimension,” *Annales Henri Poincare*, vol. 13, pp. 399–423, 2012.
- [157] V. Bonzom, R. Gurau, A. Riello, and V. Rivasseau, “Critical behavior of colored tensor models in the large N limit,” *Nucl. Phys.*, vol. B853, pp. 174–195, 2011.
- [158] I. R. Klebanov and A. A. Tseytlin, “Entropy of near extremal black p-branes,” *Nucl. Phys.*, vol. B475, pp. 164–178, 1996.
- [159] J. A. Harvey, R. Minasian, and G. W. Moore, “NonAbelian tensor multiplet anomalies,” *JHEP*, vol. 09, p. 004, 1998.
- [160] I. R. Klebanov and A. A. Tseytlin, “Intersecting M-branes as four-dimensional black holes,” *Nucl. Phys.*, vol. B475, pp. 179–192, 1996.
- [161] T. Banks and W. Fischler, “Holographic Space-time and Newton’s Law,” 2013.
- [162] T. Banks and W. Fischler, “Holographic Space-time, Newton’s Law and the Dynamics of Black Holes,” 2016.
- [163] E. Witten, “An SYK-Like Model Without Disorder,” 2016.

- [164] S. Sachdev and J. Ye, “Gapless spin fluid ground state in a random, quantum Heisenberg magnet,” *Phys. Rev. Lett.*, vol. 70, p. 3339, 1993.
- [165] O. Parcollet and A. Georges, “Non-Fermi-liquid regime of a doped Mott insulator,” *Physical Review B*, vol. 59, pp. 5341–5360, Feb. 1999.
- [166] A. Georges, O. Parcollet, and S. Sachdev, “Mean Field Theory of a Quantum Heisenberg Spin Glass,” *Physical Review Letters*, vol. 85, pp. 840–843, July 2000.
- [167] A. Kitaev, “A simple model of quantum holography,” <http://online.kitp.ucsb.edu/online/entangled15/kitaev/>, <http://online.kitp.ucsb.edu/online/entangled15/kitaev2/>. Talks at KITP, April 7, 2015 and May 27, 2015.
- [168] R. Gurau, “The complete $1/N$ expansion of a SYK-like tensor model,” 2016.
- [169] J. M. Maldacena, “The Large N limit of superconformal field theories and supergravity,” *Int. J. Theor. Phys.*, vol. 38, pp. 1113–1133, 1999. [Adv. Theor. Math. Phys.2,231(1998)].
- [170] S. S. Gubser, I. R. Klebanov, and A. M. Polyakov, “Gauge theory correlators from noncritical string theory,” *Phys. Lett.*, vol. B428, pp. 105–114, 1998.
- [171] E. Witten, “Anti-de Sitter space and holography,” *Adv. Theor. Math. Phys.*, vol. 2, pp. 253–291, 1998.
- [172] A. Tanasa, “Multi-orientable Group Field Theory,” *J. Phys.*, vol. A45, p. 165401, 2012.
- [173] S. Dartois, V. Rivasseau, and A. Tanasa, “The $1/N$ expansion of multi-orientable random tensor models,” *Annales Henri Poincare*, vol. 15, pp. 965–984, 2014.

- [174] A. Tanasa, “The Multi-Orientable Random Tensor Model, a Review,” *SIGMA*, vol. 12, p. 056, 2016.
- [175] J. Polchinski and V. Rosenhaus, “The Spectrum in the Sachdev-Ye-Kitaev Model,” *JHEP*, vol. 04, p. 001, 2016.
- [176] J. Maldacena and D. Stanford, “Comments on the Sachdev-Ye-Kitaev model,” *Phys. Rev.*, vol. D94, no. 10, p. 106002, 2016.
- [177] A. Jevicki, K. Suzuki, and J. Yoon, “Bi-Local Holography in the SYK Model,” *JHEP*, vol. 07, p. 007, 2016.
- [178] D. J. Gross and V. Rosenhaus, “A Generalization of Sachdev-Ye-Kitaev,” 2016.
- [179] S. Sachdev, “Bekenstein-Hawking Entropy and Strange Metals,” *Phys. Rev.*, vol. X5, no. 4, p. 041025, 2015.
- [180] W. Fu, D. Gaiotto, J. Maldacena, and S. Sachdev, “Supersymmetric SYK models,” 2016.
- [181] Y. Gu, X.-L. Qi, and D. Stanford, “Local criticality, diffusion and chaos in generalized Sachdev-Ye-Kitaev models,” *JHEP*, vol. 05, p. 125, 2017.
- [182] G. Turiaci and H. Verlinde, “Towards a 2d QFT Analog of the SYK Model,” 2017.
- [183] P. Narayan and J. Yoon, “SYK-like Tensor Models on the Lattice,” 2017.
- [184] J. Murugan, D. Stanford, and E. Witten, “More on Supersymmetric and 2d Analogs of the SYK Model,” 2017.
- [185] A. Almheiri and J. Polchinski, “Models of AdS₂ backreaction and holography,” *JHEP*, vol. 11, p. 014, 2015.

- [186] J. Maldacena, D. Stanford, and Z. Yang, “Conformal symmetry and its breaking in two dimensional Nearly Anti-de-Sitter space,” 2016.
- [187] J. Engelsoy, T. G. Mertens, and H. Verlinde, “An investigation of AdS₂ back-reaction and holography,” *JHEP*, vol. 07, p. 139, 2016.
- [188] K. Jensen, “Chaos in AdS₂ Holography,” *Phys. Rev. Lett.*, vol. 117, no. 11, p. 111601, 2016.
- [189] R. Gurau, “The Schwinger Dyson equations and the algebra of constraints of random tensor models at all orders,” *Nucl. Phys.*, vol. B865, pp. 133–147, 2012.
- [190] A. Z. Patashinskii and V. L. Pokrovskii, “Second Order Phase Transitions in a Bose Fluid,” *JETP*, vol. 19, p. 677, 1964.
- [191] K. Symanzik, “On Calculations in conformal invariant field theories,” *Lett. Nuovo Cim.*, vol. 3, pp. 734–738, 1972.
- [192] P. Breitenlohner and D. Z. Freedman, “Stability in Gauged Extended Supergravity,” *Annals Phys.*, vol. 144, p. 249, 1982.
- [193] L. F. Alday and J. M. Maldacena, “Comments on operators with large spin,” *JHEP*, vol. 11, p. 019, 2007.
- [194] A. L. Fitzpatrick, J. Kaplan, D. Poland, and D. Simmons-Duffin, “The Analytic Bootstrap and AdS Superhorizon Locality,” *JHEP*, vol. 1312, p. 004, 2013.
- [195] Z. Komargodski and A. Zhiboedov, “Convexity and Liberation at Large Spin,” *JHEP*, vol. 11, p. 140, 2013.
- [196] E. D. Skvortsov, “On (Un)Broken Higher-Spin Symmetry in Vector Models,” 2015.

- [197] S. Giombi and V. Kirilin, “Anomalous Dimensions in CFT with Weakly Broken Higher Spin Symmetry,” 2016.
- [198] A. Dymarsky, I. R. Klebanov, and R. Roiban, “Perturbative search for fixed lines in large N gauge theories,” *JHEP*, vol. 08, p. 011, 2005.